OULU 2008
D 980

ACTA UNIVERSITATIS OULUENSIS

Kari Palosaari

QUANTITATIVE AND SEMIQUANTITATIVE IMAGING TECHNIQUES IN DETECTING JOINT INFLAMMATION IN PATIENTS WITH RHEUMATOID ARTHRITIS

PHASE-SHIFT WATER-FAT MRI METHOD FOR FAT SUPPRESSION AT 0.23 T, CONTRAST-ENHANCED DYNAMIC AND STATIC MRI, AND QUANTITATIVE ^{99M}TC-NANOCOLLOID SCINTIGRAPHY

FACULTY OF MEDICINE,
INSTITUTE OF DIAGNOSTICS, DEPARTMENT OF DIAGNOSTIC RADIOLOGY,
INSTITUTE OF CLINICAL MEDICINE, DEPARTMENT OF INTERNAL MEDICINE,
UNIVERSITY OF OULU;
RHEUMATISM FOUNDATION HOSPITAL;
DEPARTMENT OF MUSCULOSKELETAL MEDICINE AND REHABILITATION, MEDICAL SCHOOL,
UNIVERSITY OF TAMPERE

ACTA UNIVERSITATIS OULUENSIS
D Medica 980

KARI PALOSAARI

QUANTITATIVE AND SEMIQUANTITATIVE IMAGING TECHNIQUES IN DETECTING JOINT INFLAMMATION IN PATIENTS WITH RHEUMATOID ARTHRITIS

Phase-shift water-fat MRI method for fat suppression at 0.23 T, contrast-enhanced dynamic and static MRI, and quantitative ^{99m}Tc-nanocolloid scintigraphy

Academic Dissertation to be presented, with the assent of the Faculty of Medicine of the University of Oulu, for public defence in Auditorium 7 of Oulu University Hospital, on September 26th, 2008, at 12 noon

OULUN YLIOPISTO, OULU 2008

Acta Univ. Oul. D 980, 2008

Supervised by
Professor Osmo Tervonen
Professor Markku Hakala

Reviewed by
Docent Kimmo Mattila
Professor Timo Möttönen

ISBN 978-951-42-8861-6 (Paperback)
ISBN 978-951-42-8862-3 (PDF)
http://herkules.oulu.fi/isbn978951428862 3/
ISSN 0355-3221 (Printed)
ISSN 1796-2234 (Online)
http://herkules.oulu.fi/issn03553221/

Cover design
Raimo Ahonen

OULU UNIVERSITY PRESS
OULU 2008

Palosaari, Kari, Quantitative and semiquantitative imaging techniques in detecting joint inflammation in patients with rheumatoid arthritis. Phase-shift water-fat MRI method for fat suppression at 0.23 T, contrast-enhanced dynamic and static MRI, and quantitative ^{99m}Tc-nanocolloid scintigraphy

Faculty of Medicine, Institute of Diagnostics, Department of Diagnostic Radiology, Institute of Clinical Medicine, Department of Internal Medicine, University of Oulu, P.O.Box 5000, FI-90014 University of Oulu, Finland; Rheumatism Foundation Hospital, Pikijärventie 1, FI-18120 Heinola, Finland; Department of Musculoskeletal Medicine and Rehabilitation, Medical School, University of Tampere, FI-33014 University of Tampere, Finland

Abstract

The purpose of this study was to evaluate the value of 0.23T low-field magnetic resonance imaging (MRI) and nanocolloid (NC) scintigraphy in assessing joint pathology associated with rheumatoid arthritis (RA).

Fat suppression methods combined with contrast media enhancement aid in distinguishing enhancing inflamed tissue from the surrounding fat, especially in the imaging of arthritic joints. The feasibility and image quality of a phase-shift water-fat MRI method for fat suppression at low-field 0.23T open configuration MR scanner was evaluated. The technique was combined with contrast-enhanced imaging to assess the conspicuity of synovial hypertrophy in the joints of 30 RA patients. Improved conspicuity and delineation of synovitis was detected with this method. However, because of a great amount of manual post processing, future development is needed to make this method more feasible.

Contrast-enhanced MRI and NC scintigraphy may provide objective and quantitative information about the inflammatory activity in arthritic joints. The value of quantitative and semiquantitative measures of inflammation derived from NC scintigraphy and low-field MRI of the wrist joint of 28 early RA patients was evaluated. Furthermore, it was investigated whether these parameters have predictive value of further erosive development during two years of follow-up.

Strong correlations were detected between the NC scintigraphy and MRI measures, and these parameters were associated with laboratory markers of inflammation. During the two-year follow-up, the initial MRI and NC scintigraphy measures were closely related with the progression of wrist joint erosions.

Small erosive-like bone defects can occasionally be found in wrist MRI of patients without clinically overt arthritis. The prevalence of these lesions was studied in bilateral wrist MRI examinations of 31 healthy persons. Small lesions resembling erosions were detected in 14 out of 31 subjects. Altogether 24 of the 930 wrist bones evaluated showed such lesions (3%). Thus small changes resembling erosions can be found in the wrist MRI of healthy subjects; the significance of these findings must always be interpreted with reference to the clinical picture.

In conclusion, early RA patients with high local inflammatory activity, as detected by NC scintigraphy and MRI are at risk of developing further bone damage. Furthermore, in the follow-up of early RA patients, if clinically sustained response is not achieved, these methods help to identify patients who need more intensive drug treatment.

Keywords: contrast-enhanced MRI, fat suppression, low-field MRI, magnetic resonance imaging, rheumatoid arthritis, scintigraphy

Acknowledgements

This study was carried out at the Department of Diagnostic Radiology, University of Oulu, during the years 2000–2006, and the Rheumatism Foundation Hospital, Heinola, during 2003 and 2004.

I owe my deepest gratitude to my supervisor, Professor Osmo Tervonen, M.D., Head of the Department of Diagnostic Radiology. He created the opportunity, facilities and optimal conditions for my research. His support and unfailing optimism have been invaluable for this study.

I am deeply grateful to my other supervisor, Professor Markku Hakala, M.D., Department of Musculoskeletal Medicine and Rehabilitation, Medical School, University of Tampere. This work would have been impossible to accomplish without his advice and expertise on rheumatic diseases and research.

I am deeply grateful to Professor (emeritus) Ilkka Suramo, M.D. Former Head of the Department of Diagnostic Radiology, University of Oulu. His advice and encouragement have been important throughout this study.

I am sincerely grateful to my closest co-workers Reijo Takalo, M.D., Head of the Department of Nuclear Medicine, University of Oulu, Jorma Vuotila, M.D., specialist in rheumatic diseases and internal medicine, and Irma Soini, M.D., Head of the Department of Radiology, Rheumatism Foundation Hospital, Heinola. They gave numerous hours of their time for this study.

I wish to express my gratitude to my other co-authors: Raija Niemelä, M.D., and Anna Karjalainen, M.D., both from the Department of Internal Medicine, University of Oulu; Airi Jartti, Deparment of Diagnostic Radiology, University of Oulu; Kalevi Kaarela, M.D., Docent from the Rheumatism Foudation Hospital, Heinola, and Hannu Kautianen, M.Sc, Medcare Foudation, Äänekoski. Their input has been essential for this study.

I owe my sincere thanks to Marianne Haapea, M.Sc., for her invaluable work in statistical analysis.

I am grateful to Professor Timo Möttönen, M.D., and Docent Kimmo Mattila, M.D., for their constructive criticism and encouraging comments as the reviewers of this thesis.

I wish to extend my warm thanks to Anna Vuolteenaho M.A., for the skilful revision of this summary.

I thank the personnel of the 0.23T MRI unit of Oulu University Hospital: Salme Meriläinen, Kyösti Palomaa, Raija Ylävaara and Anu Kauppila for excellent co-operation during this study.

My warm thanks to Jari Erkkilä, M.Sc., and Jukka Tanttu, Ph.D., for valuable information about MR physics. I also wish to thank Mrs. Kaisa Punakivi, Mrs. Leila Salo and Mrs. Marja-Liisa Raipola for their kind assistance in practical matters.

I wish to thank all my colleagues at the Radiology Deparments of Oulu University Hospital. I thank especially Professor Seppo Lähde, Professor Juhani Pyhtinen, Docent Sami Leinonen, Docent Peter Lanning and Docent Eija Pääkkö for excellent teaching. Thanks to Docent Eero Ilkko and Docent Jukka Perälä for arranging me to have time for this research.

I want to thank all my friends at the infamous Bothnia Penguins hockey club; our games and tournaments have brought me many memorable moments.

Last but not least, sincere thanks to my mother Terttu for raising me with love and patience, rest in peace, and to my father Aaro. Thanks to my brother Jussi and sister Leena. Finally, most loving thanks to my wife Päivi, and to our daughters Saana, Venla and Pinja, for all the love and understanding they have given me during these years; you are my everything.

Abbreviations

2D	Two-dimensional
3D	Three-dimensional
ACR	American College of Rheumatology
CI	Confidence interval
CNR	Contrast-to-noise ratio
CR	Conventional radiography
CRP	C-reactive protein
CT	Computed tomography
DAS	Disease activity score
DEMRI	Dynamic contrast-enhanced magnetic resonance imaging
DMARD	Disease-modifying antirheumatic drug
E-rate	Enhancement rate
ESR	Erythrocyte sedimentation rate
EULAR	The European League Against Rheumatism
fAb	Fragment of monoclonal antibody
FDG	Fluorodeoxyglucose
FE	Field echo
FFE	Fast field echo
FOW	Field of view
FSE	Fast spin echo
Gd-DTPA	Gadolinium diethylene triamine pentaacetic acid
GM-CSF	Granulocyte macrophage cell stimulating factor
GRE	Gradient echo
HAQ	Health Assessment Questionnaire score
HIG	Human non-specific immunoglobulin
HMPAO	Hexamethylenepropylene amine oxime
Hz	Hertz
ICC	Intraclass correlation coefficient
IgG	Immunoglobulin G
IgM	Immunoglobulin M
IL	Interleukin
In	Indicium
IQR	Interquartile range
IR	Inversion recovery
mAb	Monoclonal antibody

MCP	Metacarpophalangeal
MDCT	Multidetector computed tomography
MDP	Methylene diphosphonate
MRI	Magnetic resonance imaging
NC	Nanocolloid
NAC-90	Non-specific cross-reacting antigen 90
NFκB	Nuclear factor kappa B
OMERACT	Outcome Measures in Rheumatology
OR	Odds ratio
PET	Positron emission tomography
RA	Rheumatoid arthritis
RAMRIS	Rheumatoid Arthritis Magnetic Resonance Scoring System
RF	Rheumatoid factor
ROI	Region of interest
SD	Standard deviation
SE	Spin echo
SI	Signal intensity
SNR	Signal-to-noise ratio
SSEA-1	Anti-stage specific embryonic antigen-1
STIR	Short tau inversion recovery
T	Tesla
T1	Longitudinal relaxation time
T1w	T1 weighted
T2	Transverse relaxation time
Tc	Technetium
TE	Echo time
TI	Time for inversion
TNF-α	Tumour necrosis factor alpha
TR	Repetition time
US	Ultrasonography

List of original publications

This thesis is based on the following articles, which are referred to in the text by their Roman numerals.

I Palosaari K & Tervonen O (2002) Post-processing water-fat imaging technique for fat suppression in a low-field MR imaging system, evaluation in patients with rheumatoid arthritis. MAGMA 15: 1–9.

II Palosaari K, Vuotila J, Takalo R, Jartti A, Niemelä R, Haapea M, Tervonen O & Hakala M (2004) Contrast-enhanced dynamic and static MRI correlates with quantitative 99Tcm-labelled nanocolloid scintigraphy. Study of early rheumatoid arthritis patients. Rheumatology 43: 1364–1373.

III Palosaari K, Vuotila J, Takalo R, Jartti A, Niemelä RK, Karjalainen A, Haapea M, Soini I, Tervonen O & Hakala M (2006) Bone edema predicts erosive progression on wrist MRI in early RA. A two-year observational MRI and NC scintigraphy study. Rheumatology 45: 1542–1548.

IV Palosaari K, Vuotila J, Soini I, Kaarela K, Kautiainen H & Hakala M (2008) Changes resembling erosions in bilateral wrist MRI of healthy subjects. Manuscript.

Contents

1 Introduction

Rheumatoid arthritis (RA) is an autoimmune disorder of unknown aetiology characterized by inflammation of the joints, periarticular bone resorption and cartilage destruction. The clinical course of the disease is variable, ranging from mild, self-limiting arthritis to rapidly progressive multisystem inflammation with profound morbidity and mortality. RA affects about 1% of the adult population, in a female/male ratio of 2.5/1 (Lee & Weinblatt 2001, Firestein 2003). The modern treatment strategy with highly effective therapies aims to complete suppression of joint inflammation to prevent damage and functional disability as early as possible during the course of the disease (American College of Rheumatology Subcommittee on Rheumatoid Arthritis Guidelines 2002). However, in the early disease, clinical examination, biochemical assessments and conventional radiography are not alone sensitive and specific enough to discriminate RA from other inflammatory polyarthritis and to discriminate between self-limiting disease and persistent erosive arthritis (Brower 1990, McQueen *et al.* 1998, Backhaus *et al.* 1999, Dixon & Symmons 2005).

In recent years, advancement in newer imaging methods such as magnetic resonance imaging (MRI), computed tomography (CT), ultrasonography (US) and scintigraphy have shown enormous potential in early diagnosis and in monitoring disease activity, therapy response and joint damage. In particular, MRI, being a superior imaging modality in its ability to visualize both destructive and inflammatory disease manifestations, offers an excellent tool to explore all aspects of joint disease. However, the means for quantitative documentation of the degree of synovial inflammation and bone damage need to be explored in order to monitor disease activity and therapy response as accurately as possible. Methods for quantifying the "inflammatory load" of synovial joint by MRI include volume estimation of the hypertrophied pannus tissue and the measurement of the speed and intensity of contrast media enhancement of the pannus, described as dynamic contrast-enhanced MRI (DEMRI) (König *et al.* 1990). Enhancement rates derived from dynamic MRI and synovial tissue volume estimation from static MRI have been shown to correlate with histopathology and subsequent bone damage, underlining the importance of these methods in producing predictive and useful information about the severity of the disease (Konig *et al.* 1990, Ostergaard *et al.* 1997, Gaffney *et al.* 1998, Ostergaard *et al.* 1999, McQueen *et al.* 1999, Huang *et al.* 2000, McQueen *et al.* 2003, Conaghan

et al. 2003b). However, the reproducibility and accuracy of these methods needs further evaluation.

Most of the MRI work in RA has been done with high field scanners, which offer better spatial and contrast resolution than low field scanners. Technical limitations due to low field strength have prevented the development of certain optimal techniques for imaging joint pathology with low field scanners, such as spectral fat suppression. However, low-field-strength scanners are generally less expensive and more comfortable for the patient (especially those of open configuration design) than standard cylindrical closed bore high field scanners (Savnik *et al.* 2001). Few studies have compared high field and low field scanners in hand arthritis, but similar performances in terms of synovitis and erosion detection have been shown (Savnik *et al.* 2001, Taouli *et al.* 2004, Ejbjerg *et al.* 2005a).

The purpose of this study was to look for optimal imaging methods for assessing joint inflammation associated with RA in a low field 0.23T open configuration MRI and in nanocolloid (NC) scintigraphy. The feasibility and image quality of a phase-difference based fat suppression method in the visualisation of contrast-enhanced synovial hypertrophy in RA joints was evaluated. Furthermore, the value of quantitative and semiquantitative measures of inflammation derived from NC scintigraphy and low-field MRI of the wrist joint in early RA patients was evaluated. It was investigated whether these measures can produce reliable information about local disease activity at the onset of the disease, and whether these imaging parameters have predictive value of further erosive development during two years of follow-up. Finally, the presence of changes resembling findings typical to RA in healthy individuals on low field MRI was explored.

2 Review of the literature

2.1 The synovial joint

The articular capsule surrounding a synovial joint consists of a thick outer layer, the fibrous capsule, and a thinner inner layer, the synovial membrane. The synovium serves as an important source of nutrients for cartilage since cartilage itself is avascular. In addition, synovial cells synthesize joint lubricants such as hyaluronic acid, as well as collagens and fibronectin that constitute the structural framework of the synovial interstitium.

The synovial membrane lines the non-articular portions of a synovial joint. It is attached to the bones at the osteochondral junction. The normal synovium has two layers, the superficial "intimal" cellular layer, which is only 1-3 cells thick (approximately 20 μm), and the "subintimal layer", which consists of connective tissue, blood vessels, fat cells and fibroblasts (Edwards 1994).

In RA, the intimal layer is greatly hypertrophied (8–10 cells thick), and the subintimal area is heavily infiltrated with inflammatory cells, including T and B lymphocytes, macrophages and mast cells. The intense cellular infiltrate is accompanied by new blood vessel growth (angiogenesis). A characteristic feature in RA is the formation of destructive hypertrophied synovial tissue, often called pannus tissue. It is locally invasive and may cause bone erosions in sites where the synovium is directly connected to the adjacent bone (Figure 1). The pannus is a fibrovascular granulation tissue, primarily comprised of invasive lining cells with very little sublining mononuclear infiltration. Histological evaluation of the synovial membrane is of limited diagnostic and prognostic value in RA, due to high variability in the synovial histology between patients as well within a single joint. Furthermore, there is overlap with other diseases, since virtually any chronic inflammatory arthritis may have the same histological picture. (Firestein GS 1994).

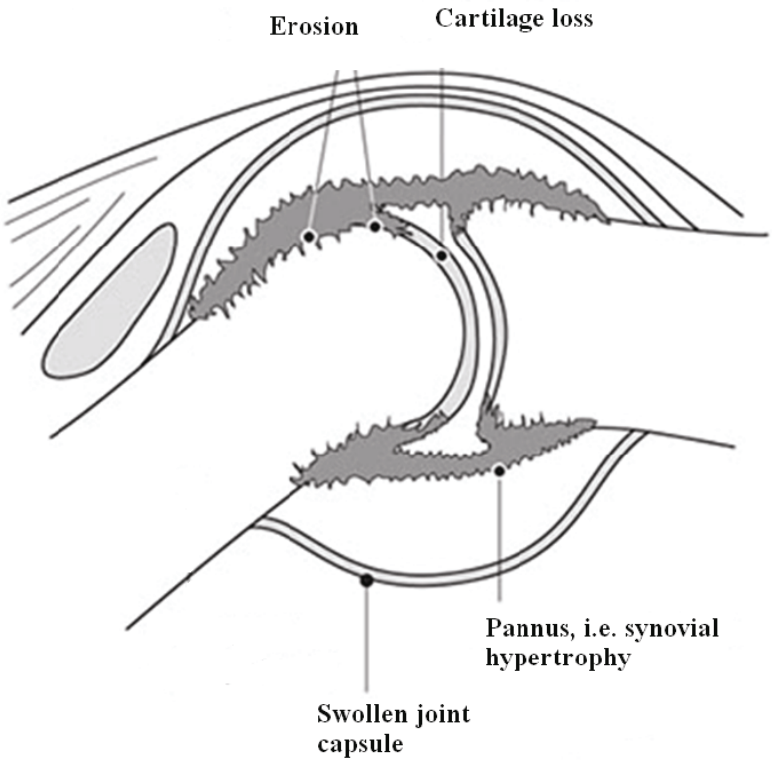

Fig. 1. Hypothesis of erosion development in RA: inflamed and hypertrophied synovium invades and damages the cartilage and adjacent bone surface.

2.2 Rheumatoid arthritis

2.2.1 Aetiology, epidemiology and clinical features of RA

RA is a multifactor disease of unknown origin, resulting from the interaction of genetic and environmental factors. Presentation of an as yet unknown antigen or antigens to T-cells is believed to trigger an autoimmune response. Subsequent proliferation of T and B cells as well as synovial angiogenesis occurs. Synovial hypertrophy begins and neutrophils accumulate within the joint in response to chemotactic factors produced by the fixing of complement and the production of

cytokines by macrophages and synoviocytes such as tumour necrosis factor alpha (TNF-α), interleukin 1 and 6 (IL-1, IL-6), and granulocyte macrophage cell stimulating factor (GM-CSF) follows. Finally, through release of matrix degenerating enzymes in conjunction with osteoclast activation, the destruction of cartilage and bone occurs (Firestein GS 1994).

Palaeopathological studies of skeleton specimens dating back several thousand years have shown evidence of RA in Native American tribes in North America. However, evidence of RA in Europe first appeared in early 17th century Dutch art, and the first case report was published in 1676 (Firestein 2003). Recent studies on the epidemiology of rheumatoid arthritis (RA) have obtained a prevalence of between 0.5 and 1.0%, and an annual incidence of around 25–50 new cases per 100,000 inhabitants in Northern European and North American areas (Hakala *et al.* 1993, Kaipiainen-Seppänen *et al.* 1996, Alamanos & Drosos 2005). A relatively lower prevalence has been reported in southern European countries and in developing countries (Carmona *et al.* 2002, Senna *et al.* 2004, Alamanos *et al.* 2004).

The female:male ratio varies from about 2:1 to 3:1. There is a low incidence of RA in men under 45, the peak age of onset in women is at the age of 65–74, and in those aged over 75, there is a higher incidence in men than in women. A shift towards older age in the incidence of RA has been reported in Finland during 1975–1990 (Kaipiainen-Seppänen *et al.* 1996). Mortality rates are higher among RA patients compared to general population. The life expectancy is likely to decrease 3–10 years according to the severity of the disease and the age at disease onset. Cardiovascular disease morbidity and mortality are increased in patients with rheumatoid arthritis (Myllykangas-Luosujärvi *et al.* 1995, Goodson *et al.* 2002, Alamanos & Drosos 2005, Gerli & Goodson 2005).

RA is characterized by usually symmetric inflammation of the peripheral joints, potentially resulting in progressive destruction of articular and periarticular structures; generalized manifestations may also be present. The onset of the disease is highly variable, ranging from abrupt and acute to gradual and insidious. The patterns of the disease range from mild and self-limiting (20%) to severe, destructing and mutilative (10%). Most patients present a chronic fluctuating course of the disease that may result in progressive joint destruction, deformity and disability (American College of Rheumatology Subcommittee on Rheumatoid Arthritis Guidelines 2002, Gordon DA & Hastings DE 2006).

2.2.2 Early RA: diagnostics and the prediction of the course of the disease

Increasing joint destruction has been shown to lead to increasing disability (Scott *et al.* 2000, Drossaers-Bakker *et al.* 2002). Bone erosions typically occur within the first years of the disease (Möttönen 1988, van der Heijde 1995), and even patients with less than 3 to 4 months duration of symptoms may already have evidence of bone destruction (McQueen *et al.* 1998, Machold *et al.* 2002). Several clinical trials have shown that therapeutic intervention with disease-modifying antirheumatic drugs (DMARDs) and oral steroids early in the course of the disease reduces functional and structural deterioration (Egsmose *et al.* 1995, Stenger *et al.* 1998, Möttönen *et al.* 1999, Lard *et al.* 2001, Landewe *et al.* 2002, Korpela *et al.* 2004). Furthermore, treatment with newer biological agents seems to offer more benefit to early RA patients at high risk of erosive progression than conventional DMARDs (Bathon *et al.* 2000, Genovese *et al.* 2002, Breedveld *et al.* 2004). Since spontaneous remission of synovitis is frequently seen in patients with less than three months of symptoms, not all patients need to be treated with these potentially toxic therapies (Raza *et al.* 2006). Therefore, there is a growing need for powerful and sensitive methods that can accurately diagnose and indicate the prognosis of patients with RA and monitor the efficacy of treatment (Landewe 2007).

Early diagnosis has been challenging due to the non-specific signs and symptoms associated with many polyarthropathies and the lack of accurate definitive diagnostic tests that can accurately classify RA at presentation. The currently widely used 1987 classification criteria of the American College of Rheumatology (ACR) criteria of RA (Arnett *et al.* 1988) performs poorly in the early months of RA (Harrison *et al.* 1998, Saraux *et al.* 2001, Machold *et al.* 2002, Symmons *et al.* 2003), since the criteria were developed using patients with established RA (mean disease duration close to 8 years).

In the early disease, prediction models based on risk factors for the development of erosive changes instead of classification of the disease have been developed, but they require more validation (Visser *et al.* 2002). Symptom duration over 12 weeks, arthritis in three or more joints, and presence of IgM rheumatoid factor (RF) are established initial risk factors for persistent erosive disease (Harrison *et al.* 1998). Older age, female sex, presence of erosions on radiography at presentation, erythrocyte sedimentation rate (ESR) and C-reactive protein (CRP) may also be indicative of poor outcome in early RA (Green *et al.*

1999, Kroot *et al.* 2000, Goronzy *et al.* 2004). In a six-year follow-up study of 142 patients with early RA, high clinical disease activity (including morning stiffness, pain scale, grip strength, Ritchie's articular index, haemoglobin and erythrocyte sedimentation rate) and rheumatoid factor positivity were found to be the best predictors of poor prognosis in early RA (Möttönen *et al.* 1998).

Recent studies have highlighted the importance of MRI in the detection of early signs of joint inflammation and bone damage as well as in the monitoring of therapy response and in the prognostication of the severity of the disease (Ostergaard *et al.* 1999, McQueen *et al.* 2003, Conaghan *et al.* 2003b, Benton *et al.* 2004, Conaghan *et al.* 2005).

2.3 Imaging modalities in RA

The optimal imaging modality in RA would provide the following features: early diagnosis, sensitive monitoring of joint inflammation and joint destruction, prediction of the course of the disease, and high reliability and reproducibility of evaluation methods (Ostergaard & Szkudlarek 2003, McQueen & Ostergaard 2007). At present, MRI is the only imaging method that may contribute to all the aspects mentioned before, but more data are still needed, particularly on validation of different MRI scanners and parameters and the ability of these parameters to predict structural and functional outcome. The current imaging methods available for assessing inflammation and joint destruction in RA are reviewed below.

2.3.1 Conventional radiography

Radiography of the hands and feet is the traditional imaging method used for the diagnosis, staging and follow-up of patients with established RA (Brower 1990, American College of Rheumatology Subcommittee on Rheumatoid Arthritis Guidelines 2002). Late signs of RA, such as erosions, joint space narrowing, juxta-articular osteoporosis, bone cysts, joint subluxations, malalignment or ankylosis, can be demonstrated (Watt 1997).

Conventional radiography (CR) is a well-established tool for the evaluation of disease progression and outcome measurement in RA clinical trials; several scoring systems have been developed and validated for this purpose (Larsen *et al.* 1977, Sharp *et al.* 1985, van der Heijde *et al.* 1995). Radiographic damage is strongly correlated with disease duration, CRP, ESR and RF (Wolfe & Sharp 1998,

Bukhari *et al.* 2002). However, radiographs are only weakly correlated with pain, joint tenderness and function (Sokka *et al.* 2000).

The advantages of CR include low cost and wide availability. Furthermore, radiography can help in differentiation of RA from other joint diseases such as osteoarthritis, psoriatic arthritis and neoplasms (Watt 1997). The disadvantages include the superimposition of structures due to two-dimensional representation of 3D pathology, the use of ionizing radiation, insufficiency for assessment of soft tissue changes including synovitis and inferior sensitivity to detect bone damage when compared to MRI or multidetector computed tomography (MDCT) (McQueen *et al.* 1998, Backhaus *et al.* 1999, Backhaus *et al.* 2002, Ostergaard *et al.* 2003a, Dohn *et al.* 2006, Dohn *et al.* 2007).

In early RA, erosions visible on radiography have been reported to occur in 10–26% of patients within 3 months of disease onset (McQueen *et al.* 1998, van der Horst-Bruinsma IE *et al.* 1998, Machold *et al.* 2002). Within two years, 75% of patients with RA have shown erosive joint damage (van der Heijde 1995). Patients with no erosions by two years are unlikely to show subsequent erosive damage (Scott 2002). Erosions visible on radiography early in the disease have been shown to have high specificity but low sensitivity for discriminating between self-limiting and persistent disease and for discriminating between RA and non-RA according to clinical diagnosis (Visser *et al.* 2002, Devauchelle, V *et al.* 2004). Therefore, there has been an increasing interest in other imaging methods that provide more sensitive data and better predictive value. In early disease, radiographic damage is not related to functional outcome, while after 5 to 10 years, a significant association is detected (Scott *et al.* 2000).

2.3.2 Computed tomography

Computed tomography of the wrist joint offers high resolution imaging of bone erosions with possibility to multiplanar reformats and quantitative bone erosion volume estimations (Goldbach-Mansky *et al.* 2003, Perry *et al.* 2005). Although few reports exist as yet, modern MDCT seems to be more sensitive than MR in erosion detection, due to better definition of cortical bone and more favourable spatial resolution (Perry *et al.* 2005, Dohn *et al.* 2006, Dohn *et al.* 2007). In an older study, less RA-associated humeral head erosions were depicted with CT when compared to MRI or US (Alasaarela *et al.* 1998). However, the CT examinations in that study were done with a conventional single slice scanner, which had poorer spatial resolution, compared to modern MDCT.

The benefits of CT compared to MRI are lower price and faster imaging. CT has had better availability, but in recent years, the number of MRI units has increased rapidly. Disadvantages include the use of ionizing radiation and incapability to evaluate bone marrow oedema and soft tissue pathology (Perry *et al.* 2005).

2.3.3 Ultrasonography

Previous studies have shown that US offers accurate information on inflammatory and destructive changes in the joints of RA patients (Alasaarela *et al.* 1998, Backhaus *et al.* 1999, Wakefield *et al.* 2000, Szkudlarek *et al.* 2004, Szkudlarek *et al.* 2006). Joint effusion as well as fluid in bursae and tendon sheaths can be detected. Tendons and ligaments, including inflammation at their insertions (enthesitis), can be evaluated (Swen *et al.* 2000, Grassi *et al.* 2000). US allows assessment of synovial inflammation by direct visualization of the hypertrophied synovial membrane, and by the possibility to detect the increased synovial blood flow with power Doppler techniques (Newman *et al.* 1996). In the knee joint, power Doppler signal has been found to correlate with the histological assessment of synovial membrane microvascular density (Walther *et al.* 2001) When compared to MRI, US performance is good in easily accessible joints such as MCP joints and interphalangeal joints (Backhaus *et al.* 1999, Szkudlarek *et al.* 2006), but poorer in anatomically more complicated joints, such as the wrist (Wakefield *et al.* 2000).

Technical advances such as three-dimensional power Doppler ultrasound offers new possibilities for the precise description of morphological vascular patterns in inflammatory arthritis (Strunk *et al.* 2006). Recent studies have also shown US to be a useful tool in the monitoring of biologic therapy in RA (Iagnocco *et al.* 2007a, Iagnocco *et al.* 2007b).

The advantages of US include low cost, non-invasiveness, lack of ionizing radiation, easy repeatability, and the possibility to image guided interventions, such as punctures and injections of joints, bursae and tendon sheaths. The disadvantages include inaccessibility to all parts of the joint due to inability of ultrasound to penetrate bone, dependency on a skilled investigator, and variation between investigators (Ostergaard & Szkudlarek 2003, Koski *et al.* 2006). More data on the standardization, reproducibility, follow-up and prognostic value of US in RA are needed (Ostergaard *et al.* 2005c, Joshua *et al.* 2007).

2.4 Magnetic resonance imaging

2.4.1 MRI physics

In MRI, the nuclei of protons are aligned in a strong, uniform magnetic field, absorb energy from tuned radiofrequency pulses, and emit radiofrequency signals as their excitation decays. These signals, which vary in intensity according to nuclear abundance and molecular chemical environment, are converted into sets of tomographic (selected planes) images by using field gradients in the magnetic field, which permits 3-dimensional localization of the point sources of the signals. Images with excellent soft tissue contrast are produced, without the use of ionizing radiation (Reimer *et al.* 2003).

2.4.2 Low-field MRI

MRI of the peripheral joints can be performed by using standard cylindrical closed bore MR-units, which work on high magnetic field or by using low-field scanners (usually extremity-only or open configuration type). A closed bore MRI unit has limited space, which excludes claustrophobic and unusually large patients from the examination. The open MRI magnet is more comfortable to these patients. Furthermore, open configuration allows access to image-guided procedures (Ojala 2002).

The main disadvantage of low-field MR imaging is the lower signal-to-noise ratio (SNR), which is usually compensated for by increasing section thickness, reducing in-plane resolution and increasing the number of acquisitions, which leads to longer acquisition times. In addition, the number of possible imaging techniques is reduced due to low field strength. In particular, frequency selective presaturation pulse techniques that are routine and effective fat suppression sequences on standard up-to-date high-field scanners, cannot be acquired in low-field strength scanners (Peterfy *et al.* 1998). However, improvements in magnet homogeneity and receiving coil technology with dedicated pulse sequences may compensate some of these difficulties of low-field-strength MRI (Bredella *et al.* 2001).

Due to poorer SNR and image quality, lower sensitivity in detecting joint pathology would be expected at low-field scanners when compared to high-field units. Few studies have compared high-field and low-field scanners in hand arthritis, but similar performances in terms of synovitis and erosion detection

have been shown in three previous studies (Savnik *et al.* 2001, Taouli *et al.* 2004, Ejbjerg *et al.* 2005a). One study explored intermachine and interreader variability between 1.0T high-field and 0.2T extremity-only low-field scanner in scoring synovitis, erosions and bone oedema. In this study, 15 MCP and wrist joints of RA patients were imaged according to the OMERACT criteria on two subsequent days. MRI images were evaluated by three experienced MRI readers. Similar performance and good agreement was reached regarding assessment of bone erosions. However, for scoring synovitis and bone oedema, considerable intermachine and interreader variability was found. According to this one study, extremity-only low-field scanner seems to have lower sensitivity in assessing joint inflammation, but more studies are needed to confirm this finding (Bird *et al.* 2007).

2.4.3 Fat suppression methods at low field

Fat suppression methods are important for musculoskeletal applications to aid in visualizing abnormal signal intensities. Suppression of signal from fat improves the conspicuity of fluid content such as bone marrow oedema, fluid filling tendon defects and joint effusions (Harned *et al.* 1990, Quinn *et al.* 1995, Disler *et al.* 1996). In addition, when combined with contrast media enhancement, areas of accumulated contrast agent are more easily depicted without the high signal presence of surrounding fat (Rominger *et al.* 1993, Klarlund *et al.* 1999). Various methods have been presented to suppress the fat signal or to separate the fat and water components, including chemical shift-based techniques, such as selective saturation or excitation, the Dixon method and its modifications and longitudinal magnetization (T1)-based methods, such as inversion-recovery (IR) imaging.

Chemical shift-based presaturation pulse sequences (fat saturation, e.g. CHESS, FatSat, ChemSat) (Haase *et al.* 1985, Joseph 1985) are frequently used in fat suppression techniques in high-field MRI scanners. This method is difficult to employ in low-field scanners because of the lower resonance frequency and smaller frequency shift between fat and water (34 HZ at 0.23T vs. 223 HZ at 1.5T). To our knowledge, no applications utilizing this technique exist in low-field scanners. However, one study demonstrated binominal pulse sequences-based chemical-shift fat saturation at low field strength (Baudouin *et al.* 1992). The major problem of this technique is the sensitivity to magnetic field inhomogeneities which often produces uneven saturation in areas with irregular

space and air-bone-soft tissue boundaries (Smith *et al.* 1991, Yoshimitsu *et al.* 1995).

A frequently used method for fat suppression that can also be employed at low field strengths is the short tau inversion time inversion-recovery (STIR) sequence (Tsai & Zlatkin 1990). STIR is based on the rapid T1 recovery of fat and is therefore not affected by magnetic field inhomogeneities (Bydder & Young 1985, Atlas *et al.* 1988). However, the major disadvantage of this method is that the fat suppression is non-specific. Signal from tissues or fluid with similar T1 to that of fat (e.g. mucous tissue, haemorrhage, proteinaceous fluid and gadolinium) will also be suppressed (Krinsky *et al.* 1996). Therefore, this technique cannot be combined with gadolinium-DTPA-enhanced imaging, which is often essential in assessing synovial inflammation of the RA joints. This method also suffers from long acquisition times and low signal-to-noise ratios.

An alternative method for fat suppression that is independent of field strength is the phase-contrast method, first described by Dixon (Dixon 1984), and further developed by many investigators (Glover & Schneider 1991, Szumowski *et al.* 1994, Wang *et al.* 1998). In his original work, Dixon used shifted 180 radiofrequency pulses or time of echoes to place the magnetization vectors of water and fat parallelly and antiparallelly, respectively, in a pair of images. Separated fat or water images can be produced by adding and subtracting these images (two-point Dixon technique). Shortly after Dixon published his work, a related alternative method that uses only a single-scan spin echo sequence was described (Paltiel 1985, Patrick *et al.* 1985, Ahn *et al.* 1986, Pohjonen 1993). The fat suppression method that is available in the low-field open scanner of the University Hospital of Oulu is based on this technique. The method requires adjustment of TE to show a detectable phase difference between fat and water. Phase images along with magnitude images are collected, and phase error corrections and fat suppression are done at a workstation (Pohjonen 1993). The method is capable of correcting field errors larger than the chemical shift between fat and water and does not require a 90^0 phase shift between fat and water. Scanning does not take longer, as the selection of fat or water reference regions and fat or water suppression operations takes place during image post-processing at a workstation.

The method has many advantages when compared to the presaturation chemical shift selective techniques. It can be applied at any field strength, it does not require an additional radio-frequency saturation pulse, no special field shimming is required, and along with fat-suppressed images, non-fat-suppressed

and water-suppressed images are also available in the image data information. Furthermore, this technique is not as sensitive to field inhomogeneities as the conventional presaturation chemical shift selective methods, but it is critically important to ensure that each image shows consistent behaviour of fat and water within each voxel of the section. However, compared to Dixon's original technique, the imaging time is considerably shorter and imaging sequence parameters are more widely selectable in the single-scan phase-contrast method. The pulse sequence demonstrating a single-scan gradient echo technique for water-fat separation is presented in Figure 2.

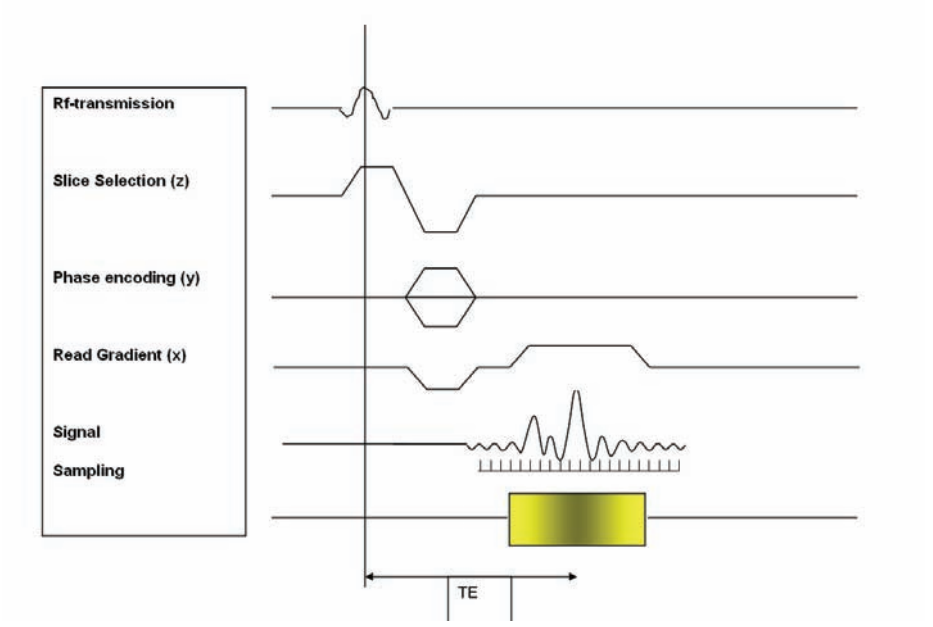

Fig. 2. The pulse sequence demonstrating a single-scan gradient echo technique for water-fat separation. The gradient echo pulse sequence of the used scanner functions at 9.8 MHz, and the frequency difference between fat and water is 35 Hz. When a standard gradient echo sequence is used this difference is not inherently compensated in the echo and thus is detected in the sampling of the signal. Immediately after the excitation the transverse magnetization vectors of fat and water start to lose phase coherence in the different speeds due the 35 Hz frequency difference. This accumulates phase shift. A 180-degree difference occurs or opposite phase happens after 15 ms. If the images are reconstructed by maintaining phase information, it is possible to differentiate fat and water signals. The correction of spatial errors caused by magnet and rf-receiving coil and fat suppression procedures is done in the post-processing session.

Another fat suppression method that utilizes the phase difference between water and fat is the modified three-point Dixon technique (Zhang *et al.* 1996). This method combines three acquisitions in a single scan. With this technique, by adding a third acquisition, off-resonance phase accumulations can be achieved on a pixel-by-pixel basis, providing the possibility to calculate a B0 map. This map is used to compensate for phase shifts caused by B0 inhomogeneities in each pixel and therefore allows a more accurate decomposition into water-specific and fat-specific images. This technique is fully automatic, which is a clear advantage when compared to the modification available in the 0.23T scanner at Oulu University Hospital. The scan time is probably longer due to multiple acquisitions, increasing the risk of movement artefacts. However, one group has demonstrated this technique to produce reliable and homogenous fat suppression at 0.35T in the evaluation of knee cartilage and in contrast enhanced spine examinations (Bredella *et al.* 2001, Huegli *et al.* 2004).

2.5 Value of MRI in detecting joint inflammation and bone damage in RA

Early bone damage (erosions), bone marrow oedema and inflammatory soft tissue changes (synovitis) that are not detectable by conventional clinical, biochemical or radiographic methods, can be directly visualized and evaluated in detail by MRI (Peterfy 2001, Ostergaard *et al.* 2004). These three key lesions of RA are now clearly defined by OMERACT (Outcome Measures in RA Clinical Trials)(Ostergaard *et al.* 2003b) (Table 1).

Table 1. OMERACT definitions of RA lesions detected by MRI.

Synovitis	An area in the synovial compartment that shows above-normal post-gadolinium enhancement of a thickness greater than the normal synovium
Bone oedema	A lesion within the trabecular bone with ill-defined margins and signal characteristics consistent with increased water content
Erosion	A sharply marginated bone lesion, with correct juxtaarticular localization and typical signal characteristics, visible in 2 planes with a cortical break in at least 1 plane

Furthermore, the lack of ionizing radiation, possibility of standardization and allowance of blinded readings make MRI a potentially valuable tool for assessing diagnosis, classification, prognosis, and long-term evaluation of treatment outcome (Peterfy 2004, Ostergaard *et al.* 2005c).

MRI is a more sensitive method than clinical examination and radiography in detecting joint inflammation and bone erosions (Jorgensen *et al.* 1993, McQueen *et al.* 1998, Backhaus *et al.* 1999, Ostergaard *et al.* 1999, Klarlund *et al.* 1999, McGonagle *et al.* 1999a). Furthermore, MRI is more sensitive for monitoring erosive progression (Ostergaard *et al.* 1999, McQueen *et al.* 1999, Backhaus *et al.* 2002). Erosions on MRI have been demonstrated to correspond to and precede erosions detectable on radiography by a median of two years (Ostergaard *et al.* 2003a). These results have encouraged researchers to use MRI-detectable damage as an outcome measure in RA clinical trials (Conaghan *et al.* 2003b, Conaghan *et al.* 2005, Quinn *et al.* 2005).

The disadvantages of MRI include higher cost and lower availability compared to radiography, long examination times with ensuing patient discomfort, and restriction to evaluation of only one or few joints per session. However, there are some preliminary case reports on whole-body MRI showing promising results in the detection of inflammatory lesions (bone oedema and joint effusions) in patients with spondyloarthritis (Althoff *et al.* 2007, Appel *et al.* 2007). Much further study is needed, but in the near future, whole-body MRI will offer a novel tool in assessing disease activity of multiple joints in the same imaging session.

The issues of standardization and reliability have been approached by international initiatives under the EULAR and OMERACT workgroups (Conaghan *et al.* 2001, McQueen *et al.* 2003, Ostergaard *et al.* 2005d). Based on data from interactive multicentre studies (Ostergaard *et al.* 2001, Lassere *et al.* 2003) an semiquantitative OMERACT RA MRI Scoring System (RAMRIS) has been developed (Ostergaard *et al.* 2003b). The method has been proven to be valid, reliable and sensitive to change in various further studies (Conaghan *et al.* 2003a, Haavardsholm *et al.* 2005, Ejbjerg *et al.* 2005b). Based on this scoring system, an reference image atlas of the wrist and MCP joints has been devised to help in assessing RA joint pathology (Ostergaard *et al.* 2005b).

There are several pitfalls in assessing joint pathology based on MR images. Well-established MRI artefacts such as susceptibility, chemical shift, partial volume averaging, truncation, wraparound and movement can lead to misinterpretations (Nitz 2003, McQueen *et al.* 2005). In addition, normal features can cause false positive or false negative findings. Intraosseous ganglion cysts,

degenerative changes, nutrient foramina and small bony notches can be mistaken for erosions and need to be distinguished from these (Schrank *et al.* 2003, Ejbjerg *et al.* 2004, McQueen *et al.* 2005, Robertson *et al.* 2006). Imaging in two opposite planes and using thin slice thickness to avoid misinterpretations is recommended in the scoring of RA damage in the carpal area (Ostergaard *et al.* 2003b, McQueen *et al.* 2005).

Due to superior sensitivity to detect early inflammatory and erosive changes and high sensitivity to detect response to treatment, MRI will gain major significance in clinical trials and practice of RA in the near future. Reduction in trial size and length may be possible due to more sensitive separation of responders from non-responders, compared to conventional radiography and clinical evaluation. In clinical practice, treating physicians who use MRI may potentially make quicker, more optimal decisions thanks to the availability of more accurate information (Ostergaard & Szkudlarek 2003).

2.5.1 Methods of assessing synovial inflammation

In RA the hypertrophied synovium of inflamed joints shows a large number of capillaries, enhanced capillary perfusion and permeability (Firestein 1999). Furthermore, the presence of angiogenetic factors (e.g. vascular endothelial growth factor) has been shown to associate with bone damage (Ballara *et al.* 2001).

Synovitis, i.e., inflammation and hypertrophy of the synovial membrane, is a prominent feature and predictor of consecutive erosive development in RA (Ostergaard *et al.* 1999, Conaghan *et al.* 2003b, Tanaka *et al.* 2005). Synovitis, which is reversible and potentially rapidly fluctuating, is considered as a measure of current disease activity (Ostergaard & Szkudlarek 2001). Bone erosions are seldom detected without synovitis and effective suppression of synovitis can decrease the development of new erosions (Conaghan *et al.* 2003b). Thus, MRI-detectable synovitis as a measure of local disease activity has become frequently used in monitoring treatment response (Ostergaard *et al.* 1999, Backhaus *et al.* 2002, Reece *et al.* 2002, Conaghan *et al.* 2003b, Argyropoulou *et al.* 2005, Ostergaard *et al.* 2005a).

Synovitis can be evaluated by two approaches: synovial membrane volume estimations from standard post-contrast T1w MR images (Ostergaard *et al.* 1997, Bird *et al.* 2003), and measurement of the synovial enhancement rates from

dynamic MRI scans (Ostergaard *et al.* 1998, Gaffney *et al.* 1998). Both methods require the use of contrast media, i.e., Gd-DTPA.

After intravenous injection, Gd-DTPA is transported unlinked in the plasma and diffuses rapidly through the damaged basement membrane into the extracellular spaces of highly vascularized tissues, such as the inflamed synovial membrane and tumours (Reiser & Naegele 1993). Gd-DTPA is a paramagnetic inert substance which shortens the T1 relaxation time, increasing the signal intensity in T1 sequences, thus allowing the differentiation of enhancing tissue (such as synovitis) from the non-enhancing tissues (e.g. ligaments, fat, muscle) (Balzer 2003).

Quantitative and semiquantitative synovial volume estimations

Synovial membrane volume measurements from post-contrast MR images have been shown to correlate to the macroscopic and microscopic signs of synovitis and to the progression of erosions (Ostergaard *et al.* 1997, Ostergaard *et al.* 1999). The method utilizes a combination of manual outlining of the synovial area and computer processing of the data. The investigator manually outlines the synovial area from each of multiple image slices. Computer software can then be used to calculate the synovial tissue volume based on the image slice thickness.

This approach can be refined further by using segmentation algorithms in which enhancing tissue is differentiated from non-enhancing tissue based on signal intensity (Ostergaard *et al.* 1999, Huh *et al.* 1999, Argyropoulou *et al.* 2005).

Quantitative measurements of hypertrophied synovial membrane volume are time-consuming and difficult to apply in clinical practise. Therefore, more feasible semiquantitative scoring systems to assess RA inflammation (synovitis and bone oedema) and damage (erosions) in wrist and metacarpophalangeal (MCP) joints have been developed (McQueen *et al.* 1998, Ostergaard *et al.* 2003b, Haavardsholm *et al.* 2005).

Multiple different qualitative and semiquantitative scoring systems have been used to evaluate the amount of synovial hypertrophy of the hand (Jorgensen *et al.* 1993, Rominger *et al.* 1993, Ostergaard *et al.* 1995, Tonolli-Serabian *et al.* 1996, Jevtic *et al.* 1997, McQueen *et al.* 1998, Backhaus *et al.* 1999, Goupille *et al.* 2001). However, the validity, reliability and responsiveness to change using rigorous scientific measurement principles are seldom reported (Lassere & Bird 2001). At present, a standardized simple scoring system (RAMRIS) developed by

the international OMERACT group is the most widely accepted one in clinical trials (McQueen & Ostergaard 2007). Reliability of a global MRI synovitis scoring of the wrist has been demonstrated by the OMERACT group with intraclass correlation of 0.60–0.90 (Lassere *et al.* 2003, Haavardsholm *et al.* 2005, Conaghan *et al.* 2007). Sensitivity to detect change with this method in a clinical trial setting has also been reported (Conaghan *et al.* 2003b, Quinn *et al.* 2005).

Dynamic MRI

Dynamic Gd-DTPA-enhanced MRI (DEMRI) is a method to quantitatively estimate increased vascularity of synovial inflammation. The method requires fast and repeated scanning of the same area of interest where the contrast media-induced signal intensity increase over time is detected (Reiser *et al.* 1989, König *et al.* 1990).

Contrast media enhancement is a complex function of blood flow, capillary permeability and the size of the extracellular space. Enhancement rates indicating the speed and intensity of the diffusion of a contrast agent in inflamed tissue can be calculated with this method. A curve plotting signal intensity in the region of interest over time can be obtained.

The enhancement of inflamed synovium is usually rapid during the first 1–2 minutes after contrast injection, followed by a flat uniform enhancement during following minutes. After about 10–15 minutes, the contrast medium diffuses into the synovial fluid, making the differentiation of synovial tissue from fluid in the joint cavity difficult (Ostergaard & Klarlund 2001). Enhancement rates (increase in signal intensity of enhancing synovium over time) calculated from the rapid, early enhancement phase (i.e. 1–2 minutes after intravenous injection of Gd-DTPA) have been shown to correlate to the histological grade and microscopic features consisted with inflammation as well as to the volume of the synovial membrane (König *et al.* 1990, Tamai *et al.* 1994, Gaffney *et al.* 1995, Ostergaard *et al.* 1998, Gaffney *et al.* 1998).

DEMRI has been shown to be sensitive in detecting inflammatory changes in active RA. It can differentiate patients with active RA from those in remission and from controls (Ostergaard *et al.* 1998, Cimmino *et al.* 2003). The method has also been reported to be sensitive for assessing treatment response (Ostergaard *et al.* 1996b, Reece *et al.* 2002). However, DEMRI cannot be used in differentiating patients with rheumatoid arthritis from early unclassified polyarthritis or psoriatic arthritis (Klarlund *et al.* 2000b, Cimmino *et al.* 2005).

DEMRI is difficult to apply into clinical practice since it has many potential pitfalls for false estimation. The method requires accurate timing of contrast injection and imaging and careful manual delineation of enhancing tissue from other tissues (i.e. bone, cartilage, ligaments and vessels) that differ in contrast enhancement. Furthermore, the enhancement rates of inflamed synovium calculated from different regions of the joint can vary, which may be due to technical problems (patient movement, partial volume artefacts etc.) or intra-articular inflammatory heterogeneity (Ostergaard *et al.* 1998, Klarlund *et al.* 2000b). However, the inter-, and intraobserver variations of the method have been reported to vary from 9% to 15%, indicating sufficient reproducibility of the method (Ostergaard *et al.* 1996a, Huang *et al.* 2000).

2.5.2 Bone marrow oedema/osteitis in MRI

The presence of an increased portion of water in the bone marrow, generally referred to as "bone oedema" or "osteitis", is a non-specific MRI finding frequently detected in trauma, tumours, osteoarthritis and RA. Bone oedema has been defined as "a lesion within the trabecular bone, with ill-defined margins and signal characteristics consistent with increased water content". Bone oedema is detected as increased signal intensity within the bone marrow in T2w fat-suppressed or STIR images and as low signal intensity in T1w images (Ostergaard *et al.* 2003b). It cannot be visualized by any other imaging methods, such as radiography, CT or US. Bone marrow oedema can be detected, but not differentiated from other inflammatory changes (synovitis or erosions) by scintigraphy.

Bone oedema is a common finding in RA (McGonagle *et al.* 1999b, Savnik *et al.* 2002). A cohort study of 42 early RA patients (McQueen *et al.* 1998) revealed bone oedema to be present at the wrist joint in 64% of patients within 6 months of disease onset and in 45% after 6 years (McQueen *et al.* 2003). The presence of bone oedema in wrist and finger bones in early RA patients has been found to associate with the severity of the disease status as measured by clinical disease activity score (DAS), serologic variables (interleukin-6, matrix metalloproteinase 3, CRP) and MRI scores of synovitis and erosions (Tamai *et al.* 2007). Bone oedema has also been shown to predict subsequent erosive bone damage and functional outcome (Savnik *et al.* 2002, McQueen *et al.* 2003, Benton *et al.* 2004). In the cohort described by McQueen et al, the bone oedema score at presentation was a stronger individual predictor of radiographic and functional outcome at 6

years than any other MRI parameter, including synovitis and erosion scores (McQueen *et al.* 2003).

A recent histopathology study of late-stage RA patients (3 patients, 12 joints) undergoing joint replacement surgery demonstrated replacement of bone marrow fat by inflammatory infiltrates at the sites of bone oedema on MRI, thus indicating findings similar to sterile "osteitis" or "osteomyelitis", rather than true oedema (Jimenez-Boj *et al.* 2007). McQueen *et al.* also found frequent high-grade bone oedema at the site of intended surgery in RA patients awaiting joint replacement or fusion (McQueen *et al.* 2007). These data suggest that bone marrow oedema may especially be associated with aggressive disease.

New work is now emerging, linking bone marrow pathology to current theories of the immunopathologies of RA. Hirohata *et al.* described a study of bone marrow cells aspirated from the iliac crest of RA patients. CD34+ stem cells that were abnormally sensitive to tumour necrosis factor alpha (TNF-α) were found to express high levels of the nuclear factor kappa B (NFκB) transcription factor, contrasting with cells from osteoarthritis patients where NFκB expression was normal and TNF-α sensitivity not observed. The authors suggested that a bone marrow stem cell abnormality could underlie RA, and proposed a disease model where such cells could, under the influence of TNF- α, differentiate into fibroblast-like cells, and travel to the synovial membrane where they might appear as type B synoviocytes and promote synovitis (Hirohata *et al.* 2001, Hirohata *et al.* 2006). However, the histopathologic equivalent of bone oedema, frequently seen and often reversible in the MRI of early RA patients, remains unknown.

The reliability of scoring bone oedema with the RAMRIS system has been poorer than for erosions, with reported ICC ranging from 0.5 to 0.86, probably due to difficulty in defining the borders of involved bone as well as technical challenges with failed suppression of fat content in trabecular bone (McQueen *et al.* 2003, Lassere *et al.* 2003, Ejbjerg *et al.* 2005a, McQueen *et al.* 2007).

2.5.3 Bone erosions in MRI

The OMERACT consensus group has defined MRI erosion as "a sharply marginated bone lesion with correct juxtaarticular localization and typical signal characteristics visible in two opposite imaging planes with a cortical break seen in at least one plane" (Ostergaard *et al.* 2003b). Typical signal characteristics include focal loss of the normal low signal intensity of cortical bone and loss of normal

high signal intensity of trabecular bone on T1-weighted images. GdDTPA-enhancement within erosions is frequently detected, suggesting the presence of active, hypervascularized tissue in the erosion (Ostergaard *et al.* 2005b). Histopathologically, MRI bone erosions have been shown to be composed of dense infiltrates consisting of synovial inflammatory tissue invading the bone marrow, lymphocytic infiltrates emerging at the interface between synovial tissue and bone marrow fat, and blood vessels close to inflammatory infiltrates (Jimenez-Boj *et al.* 2007).

Little data exist on the accuracy of MRI to detect erosions. Surface bone defects seen arthroscopically at metacarpophalangeal (MCP) joints have been shown to match up with erosions scored in MRI (Ostendorf *et al.* 2001). At present, modern MDCT offers best spatial resolution on calcified tissue, and can thus be considered a standard imaging reference for detecting bony erosions (Perry *et al.* 2005, Dohn *et al.* 2006, Dohn *et al.* 2007). In a recent study using MDCT as a reference method, the sensitivity, specificity and accuracy of 0.6 T open MRI scanner in detecting subtle (radiographically invisible) erosions in metacarpophalangeal joints of RA patients was reported to be 65%, 96%, and 90%, respectively (Dohn *et al.* 2006).

The quantification of erosions may involve simple numeric counting or estimation of erosion volume. Computer-aided volume measurements have been shown to correlate to more easily obtainable semiquantitative estimations of erosion volumes (scorings) (Bird *et al.* 2003, Dohn *et al.* 2007). The levels of reliability in scoring bone destruction by the most widely used semiquantitative OMERACT RAMRIS system have been shown equivalent to those published for radiographic erosion scoring methods (intraclass correlation coefficients 0.75–0.95) (McQueen *et al.* 2003).

2.6 Findings resembling erosions, synovitis and bone oedema in wrist MRI of asymptomatic subjects

A few MRI studies of the wrist joint in RA have included normal controls in their protocol (Beltran *et al.* 1987, Jorgensen *et al.* 1993, Nakahara *et al.* 1996, Tonolli-Serabian *et al.* 1996, Pierre-Jerome *et al.* 1996, Lindegaard *et al.* 2001). In the study with the largest number of controls (n = 42), erosive-like changes were detected in six subjects (14%) (Pierre-Jerome *et al.* 1996). No marrow infiltration (bone marrow oedema) was seen in the controls, while 35% of the patients had marrow infiltration. The major weakness of this study was the image acquisition

by only one sequence (axial T2 FFE), which reduces the sensitivity of detecting erosions, marrow oedema and synovitis, and increases the risk of misinterpretations, caused by partial volume artefacts.

Three papers have focused on describing changes resembling synovitis or erosions in the wrist region of healthy persons (Partik *et al.* 2002, Ejbjerg *et al.* 2004, Robertson *et al.* 2006).

In a study of 28 healthy individuals, MRI depicted erosion-like changes in 7 of the evaluated 420 wrist bones (1.7%) and mild synovitis-like changes in 6 subjects (21%) (Ejbjerg *et al.* 2004). Bone marrow oedema was not found. In this study, the imaging was performed in two planes and with additional contrast media-enhanced sequences to achieve the best sensitivity to detect synovitis-like changes.

In another study of 18 healthy subjects, eight individuals (44.4%) had contrast enhancement in the radiocarpal joints, located especially in the region of the prestyloid process. In this study, bone lesions were not studied (Partik *et al.* 2002).

In a recently published paper on 30 asymptomatic volunteers, 24 osseous lesions were identified in 14 subjects (47%, 95% CI 29–65%) by two musculoskeletal radiologists (Robertson *et al.* 2006). Among the osseous lesions, erosions, intraosseous ganglia, subchondral cysts, and contrary to the study of Ejbjerg *et al.*, also bone marrow oedema was identified. The authors postulated that asymptomatic bone oedema may represent early lesions soon to become symptomatic, or reflect increased exercise or other activities, since their volunteers were younger than the ones in the study of Ejbjerg *et al.* (mean age 31 vs. 47 years).

These published studies indicate that small erosive-like bone lesions, mild synovitis-like changes, and occasionally also bone marrow oedema, can occur in wrist MRI of asymptomatic people, thus addressing the importance of interpreting MRI findings together with clinical data.

The data on the role of anatomic and biomechanical factors in the distribution of bone erosions in wrist or finger joints are scarce (Pierre-Jerome *et al.* 1996, Tan *et al.* 2003). In the study by Pierre-Jerome *et al.*, most erosions seen on the wrist MRI of 31 RA patients were located at the force-bearing column of the wrist (Pierre-Jerome *et al.* 1996). Tan *et al.* reported that in early RA patients, most MRI-detectable bone erosions of the MCP joints were located adjacent to the radial collateral ligaments (Tan *et al.* 2003). The study also included 28 healthy controls, 9 of whom had altogether 20 erosive lesions. Even in these healthy

subjects, the occurrence of bone damage was mostly detected on the radial side of the MCP joints. Thus, according to these series, there does not seem to be much difference between the location of the true erosions seen in the wrist MRI of RA patients and the erosive-like defects seen in asymptomatic individuals.

2.7 Nuclear imaging in RA

2.7.1 Background

Nuclear imaging with different pharmaceuticals has been used as an investigative tools for the detection and treatment of arthritis activity in RA since the 1950s (de Bois *et al.* 1995a). The development of radiopharmaceuticals is targeted against different features in RA pathogenesis. Both non-specific and specific radiopharmaceuticals are used to image inflammation in RA. Increased blood flow, enhanced vascular permeability and influx of white blood cells are processes that result in the accumulation of radiopharmaceuticals in the inflammatory foci.

The non-specific tracers (e.g. radiolabelled disphosphonates, nanocolloids, leucocytes, liposomes and non-specific immunoglobulins) accumulate due to increased vascular permeability. Accumulation of specific radiolabelled compounds (such as radiolabelled antibodies, granulocytes, cytokines and fluorodeoxyglucose) results from multiple different mechanisms, such as enhanced influx of leukocytes, binding to the activated endothelium or enhanced glucose-uptake by activated leukocytes). However, to some extent, all radiopharmaceuticals accumulate in a non-specific way at the site of inflammation (Rennen *et al.* 2001, Bleeker-Rovers *et al.* 2004).

All these methods are non-specific, i.e. different types of arthritis cannot be differentiated. In addition, nuclear imaging lacks the spatial resolution achieved with other imaging methods, but offers greater anatomical coverage compared to MRI, making whole-body assessments possible.

Nuclear imaging of inflammation in RA is traditionally performed with non-specific tracers (^{99m}Tc-NC or ^{99m}Tc-HIG) in everyday clinical practice. Imaging with specific radiolabelled proinflammatory molecules (TNF-α, ilterleukin-1) and functional molecular imaging (PET) may give more specific information about the disease. However, a great deal of further work is needed to assess the clinical feasibility and reproducibility of these newer methods.

2.7.2 Bone scintigraphy

Bone scintigraphy with radiophosphates (usually ^{99}Tc-labelled MDP) is widely used in the imaging of bone metabolism (Imhof *et al.* 2002, Love *et al.* 2003). In normal bone, the uptake of radiophosphate is uniform. In the case of bone formation and resorption the osteoblastic activity is increased, which can be detected as increased uptake of the tracer. Imaging is typically performed 2 to 6 hours after intravenous administration of the radionuclide. The method is non-specific, but sensitive in the detection of bone metastases, trauma, osteoarthritis, inflammatory arthritis and periprosthetic changes (loosening and infection) (Gnanasegaran *et al.* 2005).

Three-phase bone scintigraphy is a method modified from bone scintigraphy. In addition to bone imaging, also soft tissue inflammation and infection can be evaluated with this method (Love *et al.* 2003). The technique allows dynamic imaging of the accumulation of the tracer. Images are acquired at three time-points: at arterial phase using an acquisition time of 5 to 6 seconds per frame up to 1 to 2 minutes after the injection of the tracer; at soft tissue phase from 2 to 8 minutes post-injection, and at bone-metabolic phase 3 hours after the injection. While the first two phases represent blood flow and blood pooling within soft tissues, the third phase provides information about bony abnormalities (Love *et al.* 2003). Only images from one specific area of interest (e.g. the palmar area or one large joint) can be acquired with the first two phases, while whole-body bone metabolic images can be obtained in the third phase.

Three-phase bone scintigraphy is the most common scintigraphic procedure performed in patients with arthralgia. The reports regarding the utility of three-phase bone scintigraphy in the diagnosis of arthritis are controversial. Warchol *et al.* (Warchol *et al.* 1998) did not find it equally suitable as ^{99m}Tc-NC and ^{99m}Tc-HIG in the differential diagnosis of painful small joints, while another study (Klett *et al.* 2000) showed an excellent agreement in the visualization of synovitis by ^{99m}Tc-HIG and the blood pool phase of bone scintigraphy. Klett *et al.* proposed that the mechanism of tracer accumulation in the blood pool phase of bone is mainly based on increased vascular permeability similar to the accumulation mechanism of ^{99m}Tc-NC and ^{99m}Tc-HIG. Accordingly, similar performances in detecting the efficacy of radionuclide synovectomy of RA knees were found between three-phase bone scintigraphy and ^{99m}Tc-HIG (Arzu *et al.* 2003).

In a comparative study of finger joints of 60 patients with various forms of arthritis, abnormal uptake of tracer in three-phase scintigraphy was detected with

high sensitivity but poor specificity (Backhaus *et al.* 1999). Significant correlations were found between pathologic findings on scintigraphy and those on physical examination and ultrasound, but not on MRI and conventional radiography. The authors concluded that three-phase scintigraphy is a potentially useful screening method in a subset of patients with early arthritis, but that the method is not specific enough for the detection of erosions (Backhaus *et al.* 1999).

Bone scintigraphy may have value in predicting erosive development. In a longitudinal study of 13 patients with early RA, high radiophosphate uptake was found to relate to the development of erosions in hand and feet radiographs after 24 months. Clinical activity correlated well with high uptake and predicted erosions in hand joints, whereas in foot joints, scintigraphy correlated better than clinical evaluation with the development of erosions. Interestingly, in this study, the joints with no uptake of radiophosphate never eroded (Möttönen *et al.* 1988).

However, conventional bone scintigraphy (i.e. bone phase only) is not regarded as useful as ^{99m}Tc-HIG in detecting active joint inflammation in RA, since bone scintigraphy cannot discriminate accurately between actively inflamed and chronically affected joints (Berna *et al.* 1992, de Bois *et al.* 1994, Sahin *et al.* 1999).

2.7.3 Radiolabelled non-specific human immunoglobulin (HIG)

The mechanism of immunoglobulin accumulation at the site of inflammation has not been completely elucidated. Initially it was hypothesized that human polyclonal immunoglobulin (HIG) was retained in inflammatory processes by specific interaction with Fc-receptors as expressed on infiltrating leukocytes (Fischman *et al.* 1990). Later it was shown that radiolabelled HIG accumulates primarily by non-specific extravasation due to locally enhanced vascular permeability (Fischman *et al.* 1992, Juweid *et al.* 1992).

Several studies with radiolabelled HIG have shown this method to have good correlation with clinical disease activity in RA (Liberatore *et al.* 1992, de Bois *et al.* 1992, Jamar *et al.* 1995, Pons *et al.* 1996, Cindas *et al.* 2001). HIG accumulation has also been shown to correlate with the degree of histologically detected knee synovitis more sensitively than clinical examination (de Bois *et al.* 1995b). De Bois *et al.* showed that ^{99m}Tc-HIG scintigraphy can also be used to predict RA in patients with arthralgia and that it detects accurately treatment response in those patients (de Bois *et al.* 1993, de Bois *et al.* 1994, de Bois *et al.* 1996). These studies suggest that ^{99m}Tc-HIG scintigraphy reflects the activity of

local inflammation, but not other aspects of destructive arthritis (de Bois *et al.* 1995a, Chianelli *et al.* 2006).

Labelling of HIG is usually performed with technetium, which offers easy usability, low radiation exposure and short half-life (Buscombe *et al.* 1990). No toxic or allergic side-effects have been observed (Chianelli *et al.* 2006). The general limitation of this method is the relatively long time span of 4–48 hours between injection and imaging (Boerman *et al.* 2001).

Until recently, ^{99m}Tc-HIG has been the most frequently used commercially available radiopharmaceutical method for the imaging of synovial inflammation in RA (Chianelli *et al.* 2006), but at the moment, this radiopharmaceutical is no longer commercially available.

2.7.4 ^{99m}Tc-labelled nanocolloids (NC)

In 1987, ^{99m}Tc-labelled nanocolloids were proposed as a suitable radiopharmaceutical to detect inflammatory processes (De Schrijver M. *et al.* 1987). Nanocolloids are small inert 30-nanometer particles produced from albumin. Radiolabelled nanocolloids are actively taken up by the cells of the reticuloendothelial system, after which they are lysosomally degraded and about 50% renally excreted after 24 hours. Owing to increased vascular permeability, they leak non-specifically into inflamed tissues and accumulate following phagocytosis by macrophages (De Schrijver M. *et al.* 1987).

The technique is easy and safe to perform. Furthermore, the radiopharmaceutical is relatively inexpensive when compared to other commercially available tracers. ^{99m}Tc-NC is injected intravenously and the uptake of the tracer can be detected after one hour because of its rapid clearance from blood. This is much quicker than with other radiopharmaceuticals.

^{99m}Tc-NC scintigraphy has been shown to be reliable in detecting bone and joint inflammation and infections (Vorne *et al.* 1989, Liberatore *et al.* 1992, Adams *et al.* 2001). However, the method does not seem to be suitable for the detection of inflammatory bowel diseases, prosthetic vascular graft infections or soft tissue abscesses (Vorne *et al.* 1989, Wheeler *et al.* 1990). Some reports have found this method to have inferior sensitivity to detect clinically noted synovitis when compared to disphosphonate scintigraphy (Ruther *et al.* 1989, 1990).

The clinical information concerning the sensitivity between different scintigraphy methods is scarce, but ^{99m}Tc-NC scintigraphy has been shown to

have similar sensitivity in the detection of joint inflammation in established RA as ^{99m}Tc-HIG (Liberatore *et al.* 1992).

2.7.5 Radiolabelled leukocytes

Inflammatory activity in joints can be assessed by using ^{99m}Tc-hexamethyl-propylene amine oxime labelled leukocytes (^{99m}Tc-HMPAO); however, the technique is laborious. A blood sample is collected from the patient and leukocytes are separated *in vitro*. The leukocytes are then labelled with radioactive isotope, after which they are reinjected. The preparation procedures take a trained technician approximately 3 hours (Bleeker-Rovers *et al.* 2004). In addition, the need to handle potentially contaminated blood can result in transmission of pathogens such as hepatitis or human immunodeficiency virus to technicians or patients (Lange *et al.* 1990, Fleury *et al.* 2003).

The principal clinical indications for radiolabelled leukocytes include inflammatory bowel disease, osteomyelitis, the follow-up of patients with infections of vascular or orthopaedic prostheses and soft tissue infections (Peters 1994, Liberatore *et al.* 1998, Larikka *et al.* 2001).

There are conflicting results concerning the utility of ^{99m}Tc-HMPAO in synovitis. Jorgensen *et al.* and Gaal *et al.* showed a significant correlation between ^{99m}Tc-HMPAO accumulation and clinically assessed disease activity (Jorgensen *et al.* 1995, Gaal *et al.* 2002). Vorne *et al.* (Vorne *et al.* 1989) reported that ^{99m}Tc-HMPAO gave equal information to ^{99m}Tc-NC, but Liberatore *et al.* (Liberatore *et al.* 1992) found it to have less potential than ^{99m}Tc-NC or ^{99m}Tc-HIG in detecting inflammatory activity in joints. However, Vorne *et al.* regarded ^{99m}Tc-NC as the preferred method, because it is simpler, faster and cheaper than the ^{99m}Tc-HMPAO (Vorne *et al.* 1989).

Consequently, because of the complexity of the method, labelled leukocyte imaging is no longer used in RA patients (Chianelli *et al.* 2006).

2.7.6 Radiolabelled antibodies

Radioimmunoscintigraphy was first developed to identify malignant tissue (DeLand *et al.* 1979, Kim *et al.* 1980). The main purpose of the development of monoclonal antibodies (mAb) against surface antigens present on activated leukocytes is the advantage that labelling procedures are easier than with

radiolabelled leukocytes and do not require handling of potentially contaminated blood (Bleeker-Rovers *et al.* 2004).

In particular, E-selectin is a surface adhesion molecule specifically expressed on activated endothelium and not expressed on non-inflamed tissues. One study demonstrated higher diagnostic accuracy with ^{111m}In-labelled anti-E-selectin mAb when compared to ^{99m}Tc-HIG in the evaluation of RA patients (Jamar *et al.* 1997). The disadvantages of the use of mAb, however, include high molecular weight, resulting in slow diffusion into sites of inflammation, a long plasma half-life and uptake in the liver due to clearance by the reticuloendothelial system. The use of mAb of murine origin can induce production of human anti-mouse antibodies, which can lead to allergic reactions if repeated injections are given (Bleeker-Rovers *et al.* 2004).

Theoretically, the use of antibody fragments (fAb) provides the advantage of lower immunogenicity, faster blood clearance and higher accumulation in inflammatory foci than with mAb. ^{99m}Tc- and ^{111m}In-labelled fAb fragments against E-selectin have showed better diagnostic accuracy than ^{99m}Tc-HIG (Chapman *et al.* 1996) and bone scintigraphy (Jamar *et al.* 2002) in RA patients.

Other antibodies against activated granulocytes, such as anti-NCA-95 IgG, anti-stage specific embryogenic antigen-1 (anti-SSEA-1) IgM and anti-NCA-90 fAb, have also been successfully used for the imaging of various inflammatory and infectious processes, such as osteomyelitis, septic loosening of hip and knee prostheses, diabetic foot infections and endocarditis. However, there are no studies assessing the accuracy of these methods in the evaluation of disease activity in RA patients (Bleeker-Rovers *et al.* 2004).

Monoclonal antibodies and antibody fragments against lymphocytes have also been applied to assess RA inflammation. ^{99m}Tc-anti CD4 antibody has showed accurate uptake in inflamed RA joints when compared to clinical signs and early phase of three-phase scintigraphy (Becker *et al.* 1990) and when compared to ^{99m}Tc-HIG (Kinne *et al.* 1993). In addition, a recent study of ^{99m}Tc-anti-CD3 showed good clinical correlation in the evaluation of affected joints in 38 RA patients (Martins *et al.* 2008). However, side effects reflecting biological activity (shaking chills and neck pain) have been reported with this method (Marcus *et al.* 1994).

2.7.7 Radiolabelled anti-TNF-α antagonists

Progress in understanding the biological mechanism of RA has led to therapies that are better targeted than traditional DMARDs. In particular, biological drugs that are capable of modifying biological response have evolved rapidly and are frequently used, especially in aggressive forms of inflammatory arthritis. The current drugs approved for use in RA include TNF-α antagonists and IL-1 inhibitors.

Most RA patients respond to anti-TNF-α therapy. However, some do not, probably due to large inter- and intraindividual variation in the level of TNF-α expression or the involvement of other proinflammatory cytokines in the disease (Chianelli *et al.* 2006). Evidence of the formation of human anti-chimeric antibodies against TNF-α agonist (infliximab) has also been found in some non-responders (van der Laken *et al.* 2007). Knowing whether TNF-α is expressed in the affected joints would be useful in selecting suitable patients for anti-TNF-α therapy. The use of radiolabelled anti-TNF-α antibodies for specific targeting of membrane-bound or soluble form of TNF-α can provide accurate information about TNF-α expression, disease activity and localization. Only a few preliminary studies have so far utilized radiolabelled biological drugs for imaging joint inflammation in humans (Barrera *et al.* 2003, Chianelli *et al.* 2006, van der Laken *et al.* 2007)

Radiolabelled adalimumab, a fully human anti-TNF-α monoclonal antibody, has been successfully used in the detection of inflamed joints in a pilot study of 10 patients with active RA. Additionally, the method detected decreased uptake of the tracer after treatment with steroids or therapeutic dose of adalimumab, which correlated with clinical disease activity (Barrera *et al.* 2003)

Infliximab, a chimeric mouse/human anti-TNF-α antibody, has also been successfully radiolabelled with technetium and used in the detection of articular TNF-a mediated inflammation in RA patients before and after intra-articular treatment with infliximab (Chianelli *et al.* 2006). The authors suggest that anti-TNF-a scintigraphy may be useful in the selection of patients for anti-TNF-α therapy.

2.7.8 Imaging of enhanced glucose uptake

Another approach using nuclear imaging is to use markers that can identify increased metabolic function and cellular turnover in synovial tissue. ^{18}F-FDG

PET (fluorodeoxyglucose positron emission tomography) offers unique information on glucose metabolism that cannot be supplied by other imaging techniques. ^{18}F-FDG accumulates in tissues with a high rate of glucolysis, such as tumours and inflammatory processes. FDG-uptake is present in all activated leukocytes. Phosphorylated FDG passes the cell membrane and remains trapped inside the cell. Increased ^{18}F-FDG-uptake can be further detected by using a dedicated PET scanner. Besides the imaging of neoplasms, ^{18}F-FDG PET scanning has been used in the imaging of conditions such as osteomyelitis, spondylodiscitis, prosthetic joint infections, vascular graft infections, vasculitis, inflammatory bowel disease and rheumatoid arthritis (Bleeker-Rovers *et al.* 2004).

^{18}F-FDG PET studies on RA patients are few. In a study of 9 RA patients and 3 psoriatic arthritis patients, quantitative ^{18}F-FDG PET uptake of the wrist joint correlated well with the volume of enhanced synovial hypertrophy measured from contrast-enhanced MRI images before and after treatment with DMARDs, but these measures were not associated with clinical measures of global disease activity. However, the measures correlated significantly with clinical symptoms of the imaged wrist (wrist pain and swelling) (Palmer *et al.* 1995).

Another study of 10 patients with inflammatory arthritis showed that ^{18}F-FDG PET and methyl-^{11}C-choline PET correlate with MRI measures of synovial proliferation in the knee joint (Roivainen *et al.* 2003).

Beckers *et al.* imaged multiple joints of 21 RA patients with clinically active disease by ^{18}F-FDG PET and US. The number of ^{18}F-FDG PET-positive joints correlated significantly with the number of affected joints evaluated clinically or with US. Furthermore, quantitative measurements of ^{18}F-FDG PET uptake correlated with increased vascularity, as evaluated by power Doppler signal in US, and with multiple clinical and laboratory measures of inflammation (Beckers *et al.* 2004). The same group reported significant associations between ^{18}F-FDG PET, DEMRI and US in the evaluation of synovial inflammation of 16 knees of clinically active RA patients. Four weeks after treatment with anti-TNF-α therapy, changes in ^{18}F-FDG PET uptake were further significantly correlated with the changes in MRI parameters and with the changes in laboratory measures of inflammation (CRP and MMP-3 values) (Beckers *et al.* 2006).

The obvious limitations of this method are its limited accessibility and expensiveness. In addition, much further research must be done to assess the validity of this method. However, ^{18}F-FDG PET offers unique metabolic information that can be used to evaluate disease activity and therapy response in RA.

3 Purpose of the study

The purpose of this study was to evaluate the value of 0.23T low-field MRI and NC scintigraphy in assessing joint pathology associated with rheumatoid arthritis. In particular:

1. To explore the feasibility and image quality of a phase difference-based fat suppression method at low field in the imaging of contrast-enhanced synovial hypertrophy of arthritic joints.
2. To explore the value of quantitative ^{99m}technetium-labelled nanocolloid (NC) scintigraphy with reference to dynamic and static MRI in assessing wrist joint inflammation in early RA patients.
3. To evaluate whether MRI and NC scintigraphy can predict progression of wrist joint damage during two-year follow-up in early RA patients.
4. To document the presence of lesions resembling erosions and synovitis on wrist MRI in asymptomatic population.

4 Materials and methods

4.1 Study population

The present study was performed in Oulu University Hospital during 2000 – 2006 (I–III) and the Rheumatism Foundation Hospital, Heinola during 2003–2004 (IV). The study population in studies I, II and III consisted of rheumatoid arthritis patients recruited by rheumatologists and orthopaedic surgeons specializing in rheumatic diseases at Oulu University Hospital. The total number of patients with RA included in the study was 48 (32 women). These patients fulfilled the revised American College of Rheumatology (ACR) criteria for rheumatoid arthritis (Arnett *et al.* 1988).

The subjects in study IV were recruited from among the staff members of the Rheumatism Foundation Hospital, Heinola. They consisted of 31 healthy volunteers (18 women) without any history of joint pain or joint disorders.

Study I consisted of 30 consecutive symptomatic RA patients referred to MRI examination (30 patients; 10 knees, 10 elbows and 10 wrists). The 10 patients who had wrist MRI were also included in studies II and III.

Study II consisted of 28 early RA patients (mean duration of symptoms 5 months, range 1 to 12 months) who were followed for one year and two years in study III (27 patients for one year and 24 patients for two years). At one year, one patient had dropped out because of refusal to undergo MRI and NC scintigraphy examinations. At two years, an additional three patients had dropped out because two patients could not be reached and one was pregnant.

The number of subjects, their sex and age and the number of imaging and clinical examinations performed are presented in Table 2.

All subjects of these studies gave their informed consent to the protocol, which had been approved by local ethics committees in Oulu (I–III) and Heinola (IV).

Table 2. Description of the subjects and examinations in studies I–IV.

Study	N (male/female)	Age, years mean (range)	MRI examinations	NC scintigraphy	Clinical assessments[1]
I	30 (13/17)	49 (21–71)	30		
II	28 (7/21)	51 (21–71)	28	28	28
III	27* (7/20), 24**(7/17)	52*(22–72), 53**(23–73)	27*, 24**	27*, 24**	27*, 24**
IV	31 (13/18)	49 (32–64)	62***		

[1]i.e. swollen/tender joint count, HAQ, laboratory tests.*at one-year follow-up, **at two-year follow-up, ***bilateral wrist MRI.

4.2 Clinical evaluation of the subjects

The clinical assessments the patients in studies II and III were made by senior rheumatologists working at Oulu University Hospital. Swollen joint count, tender joint count (52 joints/patient examined) and Health Assessment Questionnaire score (HAQ) (Fries *et al.* 1980) were recorded. In addition, ESR, CRP and IgM RF levels were measured at baseline and during follow-up. The clinical assessments at baseline (study II) were performed a few days or weeks before (range 0–11 weeks, median 4 weeks) MRI and NC scintigraphy, which were performed on the same day. Altogether 24 patients were taking disease-modifying anti-rheumatic drugs (DMARDs) before imaging, as the patients were usually started on medication immediately after the clinical assessment.

During follow-up, drug treatment was not standardized, and was modified freely by the treating rheumatologists based on clinical judgement. Response to the treatment at follow-up was defined as $\geq$ 50% improvement in the tender and swollen joint scores and HAQ, and normal CRP or ESR. At one-year follow-up, all but one patient were taking one or more DMARDs. At two years, two patients were not on DMARD medication. TNF-α antagonists were not used by any of the patients.

All of the volunteers participating in study IV were interviewed and examined by a clinical rheumatologist. Anyone with current or past symptoms of inflammatory joint diseases, history of wrist injury or surgery, pregnancy, renal insufficiency, allergy to contrast media or other contraindications to MRI were excluded from the study.

4.3 Imaging of the subjects

All subjects in this study were imaged with an open-configuration 0.23T MR scanner (Philips Outlook Proview, Philips Medical Systems MR-technologies Finland, Vantaa, Finland) located at Oulu University Hospital (studies I, II and III) and Rheumatism Foundation Hospital, Heinola (study IV)).

NC scintigraphy was performed in Oulu University Hospital with an Elscint 409 ECT camera (Haifa, Israel) equipped with a low-energy general-purpose collimator (studies II and III).

In study IV, conventional radiography of both hands was obtained in the posterior-anterior projections. All radiographs were evaluated blindly by two readers who were unaware of the MRI findings. In the case of diverging opinions, a consensus reading was done. Radiographic bone erosions were evaluated separately in each wrist bone.

4.3.1 MRI parameters

The imaging parameters for the wrist images in the study I were: 1) STIR SE coronal sequence [1800/25/80 msec (TR/TE/TI), 18 x 18 cm field of view, 216 x 256 matrix, one excitation, slice thickness 3mm, imaging time 9 min 43 sec]. 2) T1w 3D GRE coronal sequence [30/10 msec (TR/TE), flip angle 40 degrees, 16 x 16 cm field of view (FOV), 256 x 256 matrix, one excitation, slice thickness 2mm, imaging time 6 min 9 sec] with an intravenous Gd-DTPA bolus (Magnevist 469mg/ml, 15ml, Schering AG, Berlin, Germany). The parameters for the evaluated elbow images were: 3) STIR SE coronal sequence [1800/25/80 msec (TR/TE/TI), 18 x 18 FOV, 216 x 256 matrix, one excitation, slice thickness 4mm, imaging time 9 min 43 sec.]. 4) T1w 3D GRE sagittal sequence [30/10 msec (TR/TE), flip angle 40 degrees, 16 x 16 FOV, 256 x 256 matrix, one excitation, slice thickness 3 mm, imaging time 4 min 36 sec. The parameters for the evaluated knee images were: 5) STIR fast SE coronal sequence [4800/70/80 msec (TR/TE/TI), 22 x 22 FOV, 256 x 256 matrix, 2 excitations, slice thickness 5 mm, imaging time 6 min 43 sec]. 6) T1w GRE 3D sagittal sequence [26/9.5 msec (TR/TE), flip angle 30 degrees, 20 x 20 FOV, 256 x 256 matrix, one excitation, slice thickness 5mm, imaging time 4 min 41 sec].

The fat suppression images were obtained from sequences 2, 4 and 6. For the procedure, time of echo was adjusted to show a detectable phase difference between fat and water (At 0.23 T, TE 5 – 28 msec). Magnitude images with phase

images were acquired. The processing regions and the fat reference regions were selected manually for each image slice, and phase image correction was applied to remove phase errors. Finally, the fat-suppressed images were calculated (Philips VIA 2.0 software, Philips Medical Systems MR-technologies Finland, Vantaa, Finland). In order to get as homogeneous fat saturation as possible, the reference area was defined in each selected slice. The work was done by a specially trained radiographer at a workstation and it took approximately 3–4 minutes.

The imaging parameters in studies II and III were: Dynamic T1w 3D GRE coronal sequence; [30/10 msec (TR/TE), flip angle 40 degrees, 16 x 16 cm FOV, 128 x 256 matrix, slice thickness 2mm]. Each acquisition consisted of 12 slices and was obtained in 69 seconds. A pre-contrast scan was performed and a 15 ml Gd-DTPA bolus (Magnevist 469mg/ml, Schering AG) was then injected intravenously through a cannula in the opposite forearm. This injection was given manually over a period of 15–25 seconds, with a subsequent flush of 10 ml of normal saline, followed by the first post-contrast sequence. Four post-contrast sequences were obtained. The duration of each was 69 sec, with a delay of one second between the sequences. The imaging time of the dynamic scan was 5 min 50 s. Before contrast-enhanced dynamic imaging, the following sequences were obtained: STIR SE coronal sequence [1800/25/80 msec (TR/TE/TI), 18 x 18 FOV, 216 x 256 matrix, one excitation, slice thickness 3mm, imaging time 9 min 43 sec], T2 FSE axial sequence [4000/100 msec (TR/TE), 15 x 15 FOV, 240 x 256 matrix, slice thickness 3mm, 0.5mm gap, imaging time 6 min] and T1w 3D GRE coronal sequence [30/10 msec (TR/TE), flip angle 40 degrees, 16 x 16 FOV, 256 x 256 matrix, one excitation, slice thickness 2mm, imaging time 6 min 9 sec]. After dynamic imaging, post-contrast coronal T1w 3D GRE images were obtained. Total imaging time was about 40 minutes. At the one-year and two-year follow-up examinations (study III), the axial T2 FSE sequence was replaced by a post-contrast axial T1w 3D sequence because of its better delineation of synovial hypertrophy and bone erosions.

The parameters in study IV were: T1w 3D FFE coronal sequence [30/10 msec (TR/TE), flip angle 30 degrees, 16 x 16 FOV, 384 x 384 matrix, one excitation, slice thickness 1.5mm, imaging time 3 min 36 sec], T1w 3D FFE axial sequence [28/10 msec (TR/TE), flip angle 30 degrees, 12 x 12 FOV, 384 x 384 matrix, two excitations, slice thickness 3 mm, imaging time 5 min 15 sec], T2*w 3D FFE coronal sequence [70/16 msec (TR/TE), flip angle 12 degrees, 16 x 16 FOV, 320 x 320 matrix, slice thickness 2 mm, imaging time 7 min 0 sec], T2*w 3D FFE

axial sequence [72/20 msec (TR/TE), flip angle 12 degrees, 12 x 12 cm FOV, 384 x 384 matrix, slice thickness 3 mm, imaging time 5 min 51 sec]. Both wrists were imaged. Intravenous administration of 0.2ml/kg Gd-DTPA contrast medium (Omniscan, GE Healthcare) was used in the first 10 subjects (post-contrast T1w 3D FFE images in axial and coronal plane). In the following 21 subjects, no contrast medium was used, and post-contrast T1-w sequences were replaced by T2*-weighted field echo sequences. When contrast medium was used, the image series were obtained in the following order: 1. non-dominant wrist, 2. dominant wrist, 3. post-contrast dominant wrist, and 4. post-contrast non-dominant wrist. The post-contrast imaging of non-dominant wrist began about 12 minutes after contrast medium injection.

4.3.2 Imaging and assessment of nanocolloid scintigraphy (II and III)

In studies II and III, all patients received an intravenous injection of 555 MBq of ^{99m}Tc-labelled nanocolloid (Nanocoll®, Nycomed Amersham Sorin, Saluggia, Italy), and anterior spot views of their hands were acquired 1 hour later using an Elscint 409 ECT camera (Haifa, Israel) equipped with a low-energy general-purpose collimator. Matrix size was 128 x 128 mm and acquisition time of the wrist joints was 10 min. The image data were transferred into a Hermes processing system (Nuclear Diagnostics, Hagerstad, Sweden) and filtered using a low-pass filter (Starck & Carlsson 1997). Starck and Carlsson used a transmission phantom to find the type of filter most suitable for static images at various count levels. They used a cobalt-57 flood source, and images containing 100, 350, and 1000 kcounts were acquired in a 256 × 256 matrix. Only minor differences between the different filter types were found. For a low-pass filter, the cut-off frequency of 0.32 cycles per centimetre was the best at all count levels. Therefore, it was a logical choice for our purposes. The rescaling and measurements were chosen so that they were as objective as possible. In the rescaling operation, all the pixel values were multiplied with a constant, determined by the count level in a normal radius. The data were normalized by rescaling the images so that the mean counts/pixel in the normal radius was 100. The quantification was focused on the more painful or dominant wrist. The accumulation of the radiolabelled nanocolloid varied considerably within the wrist region of most patients. Therefore, maximum uptake in three different regions of interest (ROIs) of the wrist was measured. The area of the most intense uptake of the ^{99m}Tc-NC was always included in one of the ROIs. For comparison with the clinical data and the

static MRI scores, the average uptake of the whole wrist region was also measured. The filtering, rescaling and measurements of ^{99m}Tc-NC uptake were done by a nuclear medicine specialist (R.T.), who was blinded to the clinical evaluation, laboratory results and MR imaging. The NC measurements of each wrist joint took 10 to 15 minutes per patient on a workstation. ^{99m}Tc-NC images of all the major joints were acquired in eight-image data collection, total imaging time being thus about 90 minutes.

4.3.3 MRI assessments

In study I, the following image sets were evaluated by two radiologists (K.P. and O.T.): a) STIR images, b) contrast-enhanced T1-weighted 3D gradient echo images (non-fat-suppressed images). c) contrast-enhanced post-processed fat-suppressed T1-weighted 3D gradient echo images (fat-suppressed images).

The image sets were retrospectively reviewed at a workstation (RadWorks 5.1 Software, Applicare Medical Imaging B.V.) in a random order. A five-point visual rating scale was used, with 1 as the lowest and 5 as the highest score as follows: The conspicuity of enhancing synovial hypertrophy was evaluated for the non-fat-suppressed and fat-suppressed images: 1, not seen; 2, poor; 3, moderate; 4 good; and 5, excellent; the delineation of enhancing synovial hypertrophy was analysed for the non-fat-suppressed and fat-suppressed images: 1, blurry; 2, poor; 3, moderate; 4 good; and 5, sharp; the uniformity of fat suppression was analysed for the fat-suppressed and STIR images: 1, inadvertent fat suppression; 2, poor; 3, fair; 4, good; and 5, excellent; and general image quality was scored for all the image data: 1, unsatisfactory; 2, poor; 3, moderate; 4, good; and 5, excellent.

For quantitative analysis, the signal intensities of the enhancing synovial hypertrophy tissue, the adjacent bone marrow and subcutaneous fat, and the background noise were obtained with measurements by one radiologist (K.P.). Regions of interest (ROIs) of identical size and location on the non-fat-suppressed and fat-suppressed images were measured. The CNR values for contrast-enhanced synovium-to-bone marrow and subcutaneous fat were calculated by dividing the difference between enhancing tissue and fat by the standard deviation (SD) of background noise. In a similar manner, the synovitis-to-bone marrow and the subcutaneous fat contrast-to-noise (CNR) values at the same anatomic locations were calculated from the STIR images.

In study II, the maximal synovial enhancement rates from DEMRI sequences were calculated from the same anatomic areas as in NC-scintigraphy, but blindly

to NC measurements. To achieve this, a blank anatomic illustration of the carpus with three circular areas was prepared by a nuclear medicine specialist (R.T.). The three areas were selected based on the quantitative results of NC scanning. The purpose of this selection was to investigate whether the NC uptake values in the different areas within the carpus correlate with the MRI measurements. On MRI image data, region of interest (ROI) circles (5–28 mm^2) were placed over the region of maximal synovial enhancement within three pre-selected areas of the carpus. The ROI measurements of the MRI scans were performed by a radiologist (K.P) who was blinded to the NC scintigraphy measurements, clinical data and laboratory results.

In study III, the three different areas were randomly selected by the investigator from different locations of the wrist. However, the area showing visually most intense enhancement was always included in the measurements.

Analysis of the dynamic data was done on a workstation using VIA 2.0 software (Philips Medical Systems MR-technologies Finland, Vantaa, Finland) and it took about 20 minutes per patient. Three curves were obtained, plotting the mean pixel intensity of the ROI circle against the time following gadolinium injection. In most patients, a rapid steep increase in signal intensity was observed after the first post-contrast sequence at 69 s, followed by a slower increase to the maximum level of enhancement.

For quantitative characterization of these curves, the rate of enhancement per second after the first post-contrast sequence (69 seconds) was calculated as follows:

$$\text{E-rate} = (SI_t - SI_0)/\ 69.$$

SI_0 is the signal intensity before the contrast injection, and SI_t is the signal intensity reached after completing the first post-contrast sequence (69 s).

Evaluation of enhancement after the first post-contrast sequence was chosen because a previous study revealed significant correlation (Spearman's $\rho > 0.60$) between the early enhancement rate and the microscopic features of inflammation in the interval of 30 to 120 seconds after the Gd-DTPA injection (maximal correlation at 35 to 55 seconds post-injection) (Ostergaard *et al.* 1998). To compare the results on dynamic MRI and clinical parameters, a single e-rate representing the whole synovial tissue volume would be needed. However, because it was impossible to measure a single e-rate value for the whole synovial tissue volume (12 image slices with multiple different sized areas of enhancing

tissue at different locations), an average enhancement value from the three previously measured ROIs was calculated.

In studies II and III, the semiquantitative scoring of synovial hypertrophy, bone oedema and bone erosions of the wrist joint was done independently by two observers (K.P. and J.V) by reading the STIR images (bone oedema) and static T1-w 3D GRE images obtained before and after contrast enhancement (synovitis and erosions) according to the OMERACT group RAMRIS scoring system (Ostergaard *et al.* 2003b).

Synovitis was scored on a scale of 0–3 at three different locations: Radioulnar joint, radiocarpal joint and intercarpal-carpometacarpal joints (total maximum score 9). A score of 0 is normal, with no enhancement or enhancement up to the thickness of normal synovium, while the scores 1 to 3 (mild, moderate, severe) refer to increments of one third of the presumed maximum volume of enhancing tissue in the synovial compartment. Maximum thickness of enhancing tissue perpendicular to the cortical surface was measured in millimetres to guide the approximation of the presumed maximum volume of the synovial compartments. Carpal bones, distal radius, distal ulna and bases of metacarpals (15 locations) were scored separately for bone oedema (score 0 to 3 by the volume of oedema; 1: 1–33%; 2: 34–66%; 3: 67–100%) and bone erosions (score 0 to 10, based on the proportion of eroded bone compared to ”assessed bone volume”; 0: no erosion; 1: 1–10% of the bone eroded; 2: 11–20%, etc.) The maximum score for bone oedema was 45 and that for bone erosions 150. The metacarpophalangeal joints were not evaluated as they were not completely covered in the image sets.

For the evaluation of bone oedema and erosions, an additional consensus reading was performed (K.P. and J.V) (study II). In study III, the one-year and two-year MRI scans were first scored blinded and without reference to the baseline scans. After independent readings, however, an additional consensus reading was performed (K.P and J.V) with reference to the baseline scans in order to achieve maximum accuracy in the detection of bone erosions and oedema.

In study IV, MRI scoring of lesions resembling erosions and synovitis of the wrist joint were done independently by a radiologist (K.P.) and by a rheumatologist trained in radiology (J.V.) by reading the MRI images according to the OMERACT group RAMRIS score sheet. After initial readings, an additional consensus reading was performed by the readers.

4.3.4 Statistical methods

In study I, qualitative scoring of image sets was evaluated by using the paired nonparametric Wilcoxon signed-rank sum test. The statistical significance of the data from the CNR measurements was tested by using the paired samples *t*-test.

In study II, correlations between MRI, NC scintigraphy and clinical and laboratory assessments were analysed using Spearman's rank correlation coefficient. Intraclass correlation coefficients were calculated to investigate the intra- and interobserver reliability in studies II, III and IV.

In study III, the association between the baseline parameters and the change of erosion scores from baseline to two years were analysed using Spearman's rank correlation coefficient. The baseline variables that were significantly related to erosive progression were then incorporated into a multivariate regression model (forward stepwise). A change in the erosion score of two or more was chosen as the cut-off value. Friedman's test was used to assess the change in the variables over the follow-up. Mann-Whitney's U test was used to explore the variable differences between the groups obtained based on erosive progression and the response to treatment.

In study IV, the independent samples T-test was used to compare the ages of the subjects with erosion- or synovitis-like changes and those without changes.

5 Results

5.1 Image quality of the post-processing water-fat imaging technique for fat suppression at low field (I)

The fat suppression method was successfully applied in all 30 patients. Table 3 shows the distribution of qualitative visual scores between the three techniques. Conspicuity and delineation of enhancing tissue were superior in the fat-suppressed images compared to the non-fat-suppressed images ($P < 0.0001$). This was seen in the whole study group as well as in the three joint subgroups examined separately. The uniformity of fat suppression was evaluated to be more constant or homogeneous in the STIR images compared to the fat-suppressed images, but the difference was not statistically significant. General image quality was assessed to be best in the non-fat-suppressed images, and the difference was statistically significant compared to the fat-suppressed images. There was no significant difference in general image quality between fat-suppressed and STIR images.

The enhancing synovial hypertrophy tissue versus bone marrow and subcutaneous fat CNRs were significantly higher in the fat-suppressed images compared to the non-fat-suppressed images: 44 ± 11 and 44 ± 12; -2 ± 10 and -3 ± 12, respectively ($P < 0.0001$). For comparison, the synovitis-to-bone marrow and subcutaneous fat CNRs of the STIR images were 74 ± 14 and 71 ± 16.

Table 3. Distribution of image quality scores.

Score	Contrast-enhanced T1w 3D GRE images (non-fat suppression)	Contrast-enhanced T1w 3D GRE images with fat suppression	STIR Images
A. General image quality			
1	–	–	–
2	3	3	10
3	4	17	27
4	70	67	53
5	23	13	10
Mean score	4.1	3.9	3.6
B. Conspicuity of synovitis or enhancing synovial hypertrophy			
1	–	–	–
2	7	–	–
3	56	–	7
4	37	37	63
5	–	63	30
Mean score	3.3	4.6	4.2
C. Delineation of synovitis or enhancing synovial hypertrophy			
1	–	–	–
2	3	–	13
3	30	–	63
4	67	23	24
5	–	77	–
Mean score	3.6	4.8	3.1
D. Uniformity of fat suppression			
1		–	–
2		7	3
3		43	17
4		33	73
5		17	7
Mean score		3.6	3.8

A. From 1 (unsatisfactory) to 5 (excellent), B. From 1 (not seen) to 5 (excellent), C. From 1 (blurry) to 5 (sharp), D. From 1 (inadvertent fat suppression) to 5 (excellent)

Note – Numbers are percentages. Mean score values are also presented. General image quality; non-fat suppression vs. fat suppression, $P < 0.05$.; non-fat suppression vs. STIR, $P < 0.05$

Conspicuity of enhancement; fat suppression vs. non-fat suppression, $P < 0.05$

Delineation of enhancing tissue; fat suppression vs. non-fat suppression, $P < 0.05$

P values by paired nonparametric Wilcoxon signed-rank sum test.

A P value of less than 0.05 is considered significant.

5.2 Quantitative MRI and NC scintigraphy in early RA patients (II and III)

5.2.1 Baseline variables and correlations between MRI, NC scintigraphy and clinical parameters (II)

Significant correlations emerged between enhancement rates derived from contrast-enhanced DEMRI and ^{99m}Tc-NC uptake measured from NC scintigraphy (Figure 3). The measures also correlated with synovitis scores and bone oedema scores from static MRI scans, but not with erosion scores, as shown in Table 4. The static MRI scores, maximal and average MRI E-rate, maximal ^{99m}Tc-NC uptake and average ^{99m}Tc-NC uptake of the whole wrist did not correlate with the global disease activity parameters (tender or swollen joint count and HAQ). ESR correlated with the imaging results. Clinical parameters did not correlate with laboratory parameters. Swollen joint count correlated with tender joint count (Spearman's $\rho = 0.72$, $P < 0.01$).

At baseline, marked variation in ^{99m}Tc-NC uptake and E-Rate were detected among the study population [101 to 560 counts/pixel (mean 223) and 0 to 2.1 SI/sec (mean 0.81)] and also among the same wrist in most patients [9 to 156 counts/pixel (mean 66) and 0.01 to 1.51 SI/sec (mean 0.50)].

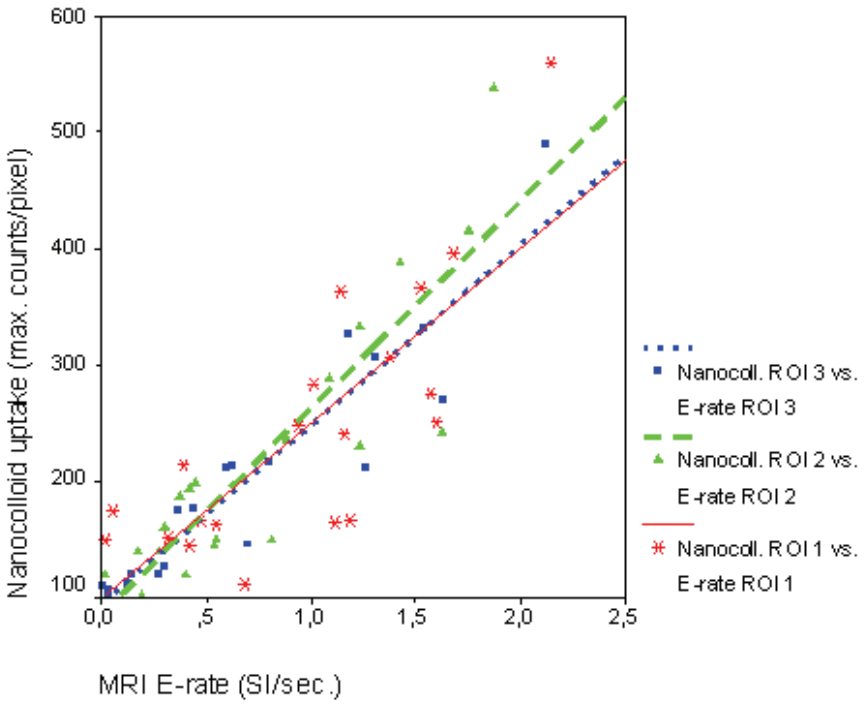

Fig. 3. Scatterplot with linear regression lines between the MRI synovial enhancement rates and quantitative 99mTc-NC uptake in three locations of the wrist joints in 20 early RA patients. Spearman's rank correlation coefficients in ROI 1, ROI 2, and ROI 3 are 0.76, 0.88 and 0.95 (P < 0.01), respectively.

Table 4. Spearman's correlation coefficients between static semiquantitative MRI scores and quantitative results obtained from dynamic MRI and NC scintigraphy (n = 20).

Variable	Synovitis	Bone oedema	Erosions
Maximal MRI E-rate	0.47*	0.67**	0.39
Average MRI E-rate	0.67**	0.76**	0.29
Maximal ^{99m}Tc-NC uptake	0.74**	0.57*	0.29
Average ^{99m}Tc-NC uptake of the whole wrist	0.78**	0.57*	0.16

*P < 0.05, **P < 0.01.

5.2.2 Patient demographics and disease evolution at baseline and follow-up (II and III)

Medication, imaging parameters and clinical measures of inflammation at baseline, one year, and two years are presented in Table 5. In the whole group, the erosion scores progressed during the follow-up. Swollen joint count, tender joint count, HAQ and laboratory parameters improved significantly from baseline to one year.

At baseline, MRI-detectable bone erosions were found in 21 patients (75%). At one year and two years, erosions were found in 22 out of 27 patients (81%) and 20 out of 24 patients (83%), respectively. Four patients had no erosions in their baseline and follow-up scans. Of the patients with erosions at baseline, all but one still had erosions at one-year and two-year follow-ups. At baseline, one year, and two years, MRI detected 64, 88, and 104 erosive bones (out of a total of 420, 405 and 360 wrist bones), respectively.

A persistent response to the treatment (≥ 50% improvement in the tender and swollen joint scores and HAQ, with normal CRP or ESR) was shown by nine patients out of 24 (38%) throughout the two years of follow-up. The median change in the erosion score was 0 (IQR 0, 0) in these patients, compared to 4 (IQR 2, 5) in the patients with an insufficient response ($p = 0.001$) (Figure 4). No significant differences in age, sex or medication were seen between these groups. In the group of responders, only one patient out of nine (11%) presented new erosions. In the group of non-responders, 13 out of 15 patients (87%) presented new/progressive erosions from baseline to one-year follow-up. From one-year to two-year follow-up, nine non-responders out of 15 (60%) had continuing progression of bone damage, while erosive progression had stopped in six non-responders (40%). The patients who presented with erosive progression from one year to two years had higher MRI synovitis scores, oedema scores, ^{99m}Tc-NC uptake and E-rate at the one-year follow-up than the patients without progressive bone damage (Table 6).

Table 5. Data on medication, MRI and NC scintigraphy parameters of the wrist and clinical and laboratory findings at baseline, at one year and two years of follow-up

	Baseline (n = 28)	At one year (n = 27)	At two years (n = 24)	P[1]
DMARD, no (%)[2]	24 (86)	26 (96)	22 (92)	
Single DMARD				
Sulfasalazine, 1.5–3g/day	13	2	2	
Methotrexate, 5–15mg/week	–	2	1	
Hydroxychloroquine, 300mg/day	1	2	1	
Intramuscular gold	1	2	2	
Combination DMARD*	9	18	16	
Predisolone 7–10mg/day, no (%)[2]	15 (54)	9 (33)	7 (29)	
MRI data[3]				
Erosion score	2 (0, 3)	2 (1, 6)	3 (2, 9)	0.001
Synovitis score	5.5 (2.5, 6.5)	3.5 (2, 6.5)	3 (2, 6)	0.148
Oedema score	1.5 (0, 4)	0 (0, 3)	0.5 (0, 2)	0.203
E-rate^{max}	1.12 (0.54, 1.59)	0.65 (0.37, 0.95)	0.61 (0.29, 1.25)	0.468
E-rate^{average}	0.71 (0.36, 1.21)	0.44 (0.26, 0.73)	0.40 (0.19, 0.88)	0.503
NC scintigraphy data[3]				
^{99m}Tc-NC uptake^{max}	244 (163, 356)	173 (155, 264)	177 (147, 296)	0.377
^{99m}Tc-NC uptake^{average}	154 (122, 229)	131 (119, 172)	131 (116, 176)	0.446
Clinical and laboratory data[3]				
Swollen joint count	8 (4, 14)	2 (0, 6)	2 (0, 5)	0.001
Tender joint count	13 (4, 20)	2.5 (0, 6)	2 (1, 4)	0.001
HAQ	0.63 (0.28, 0.97)	0.38 (0, 0.63)	0.25 (0, 0.88)	0.035
CRP (mg/l)	15 (0, 28)	0 (0, 7)	0 (0, 6)	0.001
ESR	25 (14, 54)	8 (5, 15)	7 (2, 17)	0.001

[1]Significance is from the Friedman test. Data are [2] number of patients, with percentage in brackets and [3]median, with interquartile range in brackets. *Methotrexate combined with one or more other DMARDs.
MRI = magnetic resonance imaging; NC = nanocolloid; DMARD = disease-modifying drugs;
E-rate = enhancement rate; HAQ = Health Assessment Questionnaire; CRP = C-reactive protein,
ESR = Erythrocyte sedimentation rate

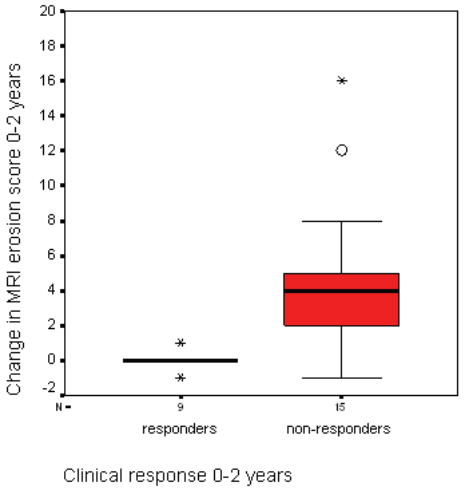

Fig. 4. A boxplot figure showing the erosion progression scores of patients with a persistent clinical response (n = 9) and those with an inadequate clinical response (n = 15) during the two-year follow-up.

Table 6. One-year follow-up parameters of the clinical non-responders (n = 15), divided based on the progression of erosions during the following year.

One-year parameters	Progression of MRI erosion score from 1 to 2 years		P[1]
	No (n = 6)	Yes (n = 9)	
MRI data			
Erosion score	2 (0.5, 6.5)	6 (3.5, 7)	0.272
Synovitis score	3.5 (1.75, 3.5)	6.5 (5.75, 8.5)	0.036
Edema score	0 (0, 1.5)	5 (1, 8.5)	0.026
E-rate^{max}	0.59 (0.31, 0.88)	0.94 (0.78, 1.67)	0.050
E-rate^{average}	0.39 (0.17, 0.47)	0.78 (0.70, 1.33)	0.001
NC scintigraphy data			
^{99m}Tc-NC uptake^{max}	158 (149, 202)	269 (210, 359)	0.012
^{99m}Tc-NC uptake^{average}	121 (110, 131)	191 (135, 235)	0.012
Clinical and laboratory data			
Swollen joint count	2 (1, 5)	5 (0.5, 7.5)	0.328
Tender joint count	5 (1, 17)	5 (0.5, 9)	0.529
HAQ	0.13 (0, 0.88)	0.5 (0.38, 0.63)	0.388
CRP (mg/l)	4 (0, 6)	5 (0, 28)	0.529
ESR	8 (2, 13)	8 (6, 18)	0.689

Data are median, with interquartile range in brackets.

[1]Significance is from the Mann-Whitney test.

5.2.3 Ability of the baseline measures to predict bone damage (III)

Spearman's rank correlation matrix showed that erosive development on MRI correlated with the baseline MRI bone oedema and MRI synovitis score, ESR, CRP, E-rate^{average}, and ^{99m}Tc-NC uptake^{average}, as shown in Table 7. Age, sex, medication (presence of DMARD or prednisone at baseline), swollen or tender joint count, HAQ or RF at baseline did not correlate with the change in the bone erosion score from baseline to two years. Bone marrow oedema was the only baseline variable that showed predictive value for the progression of erosions from baseline to the two-year follow-up when using a multivariate regression model [odds ratio (OR) 4.2, 95% confidence interval (CI) 1.3–13.8].

Table 7. Baseline parameters related to the change in MRI erosion score from baseline to two years.

Variable	ρ	P
Oedema score	0.67	0.001
Synovitis score	0.57	0.004
E-rate^{average}	0.47	0.023
^{99m}Tc-NC uptake^{average}	0.45	0.028
CRP (mg/l)	0.48	0.020
ESR	0.56	0.004

ρ = Spearman's correlation coefficients.

5.3 Lesions resembling erosions and synovitis in bilateral wrist MRI of asymptomatic subjects (IV)

On MRI of both wrists of asymptomatic volunteers, lesions resembling erosions were detected in 14 [45% (95% CI: 27 to 64%)] out of 31 subjects (in 18 of the 62 wrist scans). Erosive-like lesion was usually an incidental finding present in only one wrist (in 10 subjects; 6 dominant vs. 4 non-dominant wrists). In 4 subjects, lesions were present in both wrists.

Altogether 24 of the evaluated 930 wrist bones showed erosion-like lesions (3%). No more than two lesions per wrist were detected. All lesions were small (21 were grade 1 and 3 grade 2; scale 0–10). Maximum diameter of the lesions ranged from 1.5 to 6.8mm (mean 3.3mm) Changes were most often found in the lunate (5 of 62 bones), followed by the scaphoid, trapezium, trapezoid and triquetrum (three erosion-like lesions in each). Two lesions were found in the distal ulna and capitate, one lesion in first metacarpal (MC) base, second MC base

and pisiforme. Eleven of the 24 (46%) lesions were located in the weight-bearing column of the wrist, eight of the 24 (33%) in the thumb axis, and five of the 24 (21%) in the ulnar column. Most lesions (54%) were located on the volar side of the carpus and adjacent to the ligament insertions. Third, fourth and fifth MC base, hamate and distal radius showed no lesions. Of the 24 erosion-like lesions, 14 were found in the dominant wrist and 10 in the non-dominant wrist. The individuals with lesions were older than those with no lesions; mean age 55 (standard deviation [SD] 6.8) years vs. 43 (SD 7.7) years ($p < 0.001$).

Plain radiographs were normal except in the case of one person who had an erosion-like change in the pisiforme not documented on MRI.

Intravenous administration of contrast media was used in the first ten subjects. Synovitis-like mild to moderate GDTPA-enhancement in the synovial compartments of the wrist joint was seen in six of them. Of these six subjects, five had enhancement in both wrists, and one in one wrist. Two wrists presented signs of grade 1 synovial enhancement (scale 0–9), seven wrists grade 2 synovial enhancement and two wrists grade 3 synovial enhancement.

5.4 Reliability of the MRI and NC scintigraphy assessments (II, III, and IV)

MRI scorings by using the OMERACT system in studies II, III and IV were done independently and blindly by a radiologist (K.P.) and a rheumatologist trained in musculoskeletal radiology (J.V.). Intraobserver variability of the e-rate (K.P.) and ^{99m}Tc-NC uptake (R.T.) measurements was evaluated in study II by remeasurements of 10 randomly picked scans. Inter- and intrareader variability of the readings is presented in Table 8. Intraclass correlations between readers were acceptable in scoring synovitis and bone oedema. Somewhat poorer reliability was achieved when scoring erosions from patients (II, III) or erosion-like defects from volunteers (IV).

Table 8. Reliability of MRI readings and NC measurements. Reliability is presented as single-measure fixed-effect intraclass correlation coefficients.

Variable	N	Interobserver	Intraobserver
Study II and III			
Synovitis score	28[1], 27[2], 24[3]	0.87 (0.74–0.94)[1], 0.93 (0.85–0.97)[2], 0.82 (0.63, 0.92)[3]	
Bone oedema score	28[1], 27[2], 24[3]	0.93 (0.85–0.97)[1], 0.86 (0.71–0.93)[2], 0.89 (0.76, 0.95)[3]	
Erosion score	28[1], 27[2], 24[3]	0.91 (0.82–0.96)[1], 0.71 (0.45–0.86)[2], 0.84 (0.66, 0.93)[3]	
E-rate	10		0.92 (0.84–0.96)
^{99m}Tc-NC uptake	10		0.99 (0.98–1.00)
Study IV			
Erosion-like lesions	62[4]	0.71 (0.53–0.83)	

[1] Baseline, [2]1-year follow up, [3]2-year follow-up, [4] 62 wrists, 31 patients (bilateral examination).

6 Discussion

The purpose of this study was to evaluate the value of 0.23T low-field MRI and NC scintigraphy in assessing joint pathology associated with RA.

First, the feasibility and image quality of a single-scan phase difference-based post-processing fat suppression method in the imaging of arthritic joints was evaluated. The method was combined with contrast enhanced T1-w gradient echo imaging to assess the conspicuity of contrast enhancing synovial hypertrophy in the joints of 30 RA patients.

Secondly, the value of quantitative and semiquantitative measures, derived from MRI and NC scintigraphy, in assessing local disease activity of the wrist joint of 28 early RA patients was evaluated.

Furthermore, the value of these measures to predict further erosive development during two years of follow-up was evaluated.

Finally, the prevalence of findings resembling erosions and synovitis was explored in the MRI study of 31 healthy persons.

6.1 Fat suppression at low field

Fat suppression methods are frequently used in clinical imaging to improve the visualization of pathology from surrounding fat. When imaging rheumatoid joints, the use of i.v. contrast medium is often mandatory to depict, quantify and differentiate the enhancing inflamed synovial tissue from non-enhancing surrounding tissues (e.g. ligaments, synovial fluid, subcutaneous and bone marrow fat) (Ostergaard *et al.* 2003b).

Distinction of contrast-enhanced tissue from fat is difficult in non-fat-suppressed images, since both produce bright signal intensity on T1w-images. This is not a substantial problem at high field, since clinically robust frequency-selective presaturation techniques (Fatsat, Chemsat, CHESS) are easily available. However, due to lower frequency shift between fat and water, these methods are practically impossible to apply at low field. A seldom used alternative method for fat suppression that can be employed at low field is the phase-contrast method, first described by Dixon (Dixon 1984) and further developed by many investigators (Glover & Schneider 1991, Pohjonen 1993, Szumowski *et al.* 1994, Zhang *et al.* 1996, Wang *et al.* 1998). The single-scan post-processing water-fat imaging method for fat suppression available in the open configuration 0.23T

MRI scanner located at Oulu University Hospital is based on a modification of this method (Pohjonen 1993).

The clinical value of this method has not been previously assessed. In this study, we wanted to explore whether this technique can help in the detection of contrast-enhancing synovial pathology in the arthritic joints of symptomatic RA patients. This method was successfully combined with contrast-enhanced T1w gradient echo imaging of the arthritic joints. It was qualitatively assessed by two observers to improve the conspicuity and delineation of enhancing synovial hypertrophy when compared to non-fat-suppressed images acquired from the same single scan data set.

As expected, the contrast-to-noise (CNR) measurements demonstrated significantly higher enhancing tissue-to-fat CNRs in the fat suppressed images compared to non-fat-suppressed images.

The major advantage of this method is that along with the standard non-fat-suppressed images, also fat-suppressed and, if desired, water-suppressed images are available in the same image data information. This method is also independent of field strength, and contrary to chemical-shift-selective fat saturation techniques, it does not require additional radiofrequency saturation pulse or special field shimming. Compared to STIR, imaging time is considerably shorter and contrast enhanced imaging can be combined. However, two major problems were encountered in our study: the need of manual post-processing and the inability to achieve uniform fat suppression in some of the image slices. The inhomogeneity of fat suppression was seen especially in some of the outermost image slices in the periphery of the imaged region. This was probably due to irretrievable phase errors caused by the field inhomogeneities. However, the method was considered beneficial especially in the imaging of contrast-enhanced wrist joints where the small amount of enhancing tissue was difficult to identify from the surrounding bone marrow and subcutaneous fat in non-fat-suppressed images. This method thus seems to be useful when combined with contrast-enhanced imaging.

Pääkkö *et al.* found this method useful with a 0.23T scanner in the detection of contrast-enhanced breast lesions. The lesion conspicuity was evaluated to be similar in post-processed fat-suppressed images when compared to spectral fat-suppressed images obtained with a 1.5T scanner (Pääkkö *et al.* 2005). We have also found this technique reliable in the detection of experimental cartilage lesions at 0.23T when compared to spectral fat saturation technique at 1.5T (Palosaari *et al.* 2003).

Because of the great amount of manual post-processing, which is time-consuming and can also cause operator-dependent errors, the method is seldom used in clinical practice, and future development of more automated applications is needed to make this method clinically more practical. This method was not used in studies II and III due to the problems mentioned above. However, the OMERACT scoring system does not necessitate fat suppression for the scoring of synovitis. According to the OMERACT system, simultaneous comparison between standard T1w (non-fat-suppressed) pre- and post-contrast images enables the detection and grading of enhancing synovitis from surrounding bone marrow fat and subcutaneous fat (Ostergaard *et al.* 2003b).

6.2 Dynamic and static MRI in the evaluation of joint inflammation

DEMRI is an established tool for quantifying synovial vascularity in RA joints. Rapid early enhancement derived from DEMRI has been found to correlate to histological grade, increased vascularity and microscopic features consistent with inflammation in arthritic joints (König *et al.* 1990, Tamai *et al.* 1994, Gaffney *et al.* 1995, Ostergaard *et al.* 1998, Gaffney *et al.* 1998).

In accordance with a previous report (Huang *et al.* 2000), we noticed significant correlations between enhancement rates derived from DEMRI and semiquantitative synovitis scores derived from static MR images. The increased vascularity and capillary permeability associated with rapid enhancement thus seem to relate to the amount or volume of the hypertrophied synovial tissue. Interestingly, e-rates also correlated with bone oedema scores. This may indicate that together with high inflammatory activity in the synovial tissue, there is often a simultaneous, ongoing inflammatory reaction in the bone marrow. However, it must be taken into account that the histological reference of the bone marrow oedema seen in early RA is still unknown, since bone biopsies from early RA patients are difficult to justify ethically.

To determine MRI enhancement rates, implementation of a rapid pulse sequence, manual placement of ROI circles on areas of most intense gadolinium enhancement and calculation of time-dependent enhancement curves by software is required. Although this method relies greatly on the skill of the observer in selecting the appropriate tissue and site for the analysis, a high degree of reproducibility was found, with intrareader intraclass correlation coefficient of 0.9. E-rate measurements were done by only one reader, and greater measurement variability would probably have been detected between two readers. However,

similar good reproducibility of this method has been reported previously (interreader and intrareader variability ranging from 9 to 15%) (Ostergaard *et al.* 1996b, Huang *et al.* 2000). The reproducibility of the method is also dependent on the injection rate and on the patient's cardiovascular status. In present study, a standard dose of 15ml of contrast medium (Magnevist 469mg/ml, Schering AG, Berlin, Germany) was injected manually, followed by a saline flush. The injection was performed manually, because no power injector was available in the 0.23T MRI unit. This weakens the reproducibility of the method. However, the injection was usually given by the author, whenever possible.

Typically, in most previous studies utilizing DEMRI in the evaluation of synovitis, a single or a few preselected image slices are imaged, since the addition of multiple image slices will result in increased time between acquisitions (König *et al.* 1990, Tamai *et al.* 1994, Ostergaard *et al.* 1998). This may cause difficulty in finding a sufficient amount of enhancing synovium for the enhancement measurements, especially in smaller joints, such as the wrist (Ostergaard *et al.* 1996b). Therefore, despite the disadvantage of a relatively long acquisition time (69 s/sequence), we preferred selecting multiple (12) continuous 2mm thick coronal image slices to cover most of the wrist joint volume. Based on the previous data, this time interval was considered to be sufficient to still detect early enhancement (Ostergaard *et al.* 1998, Huang *et al.* 2000). However, more accurate data on the early enhancement dynamics would have been obtained if only one or two image slices had been imaged (imaging time 6 sec/slice). The benefit of choosing multiple image slices was the ability to measure enhancement rates from different locations of the wrist joint, which decreases measurement error if the measurements are done from only one location. Furthermore, with this approach, marked variability in the enhancement rates between different locations of the wrists was detected. Since no histological references were obtained, the significance of this phenomenon remains speculative. Some of the variability is probably explained by partial volume effects and a long acquisition time, but regional inflammatory heterogeneity, as previously reported in arthritic knee joints (Lindblad & Hedfors 1985, Ostergaard *et al.* 1996b, Ostergaard *et al.* 1998), is a more probable explanation. Nevertheless, development of faster techniques that permit sampling of the entire joint in a shorter acquisition time is needed to improve the reliability of the method (Verstraete *et al.* 1996).

According to the results of this study, DEMRI can in a few minutes (scan time about six minutes, post-processing analysis about five to ten minutes) and with minimal additional costs add reliable information about local synovial

inflammation to the information about soft tissue and bone changes provided by conventional contrast-enhanced imaging of the RA joint.

6.3 NC scintigraphy in the evaluation of joint inflammation

NC scintigraphy is commonly used for screening of inflammatory joints based on visual analysis of whole body scans (Vorne *et al.* 1989, Liberatore *et al.* 1992, Adams *et al.* 2001). However, more detailed and objective information of local joint inflammation by quantifying the ^{99m}Tc-nanocolloid uptake can be obtained. Therefore, the development and validation of quantification methods for measuring the uptake of the radiopharmaceutical compound was one goal of this study.

To our knowledge, this is the first study exploring the value of NC scintigraphy in the quantification of wrist joint inflammation of RA patients. The NC uptake in inflamed synovium was compared to a well-documented measure of increased vascularity, enhancement rate derived from dynamic MR scans. To ensure comparable imaging information, the NC scintigraphy and MRI examinations were performed on the same day. Measurements of ^{99m}Tc-NC uptake from three different locations in the wrist joints were found to correlate to DEMRI enhancement rates derived from the same locations. This finding indicates similar performances of these methods to detect increased capillary permeability reflecting the degree of local inflammation. Similarly to DEMRI measurements, marked variability in ^{99m}Tc-NC uptake reflecting regional inflammatory heterogeneity could be detected in different locations of the wrist. Even though we had no histological reference, these methods can probably pinpoint the sites with the highest inflammatory activity within the wrist of early RA patients. Significant correlations between quantitative results obtained from NC scintigraphy and static semiquantitative MRI scores of synovitis and bone oedema further support the concept that these measures are linked to local disease activity.

Quantitative NC scintigraphy was found to be a feasible method for detecting the degree of synovial membrane inflammation at the local joint level, even though it required manual processing on a workstation. The filtering, rescaling and measurements of 99mTc-nanocolloid uptake of the wrist joint took 10 to 15 minutes by an experienced nuclear medicine specialist. The most obvious advantage of this method compared to MRI is the ability to acquire data from other joints as well in the same setting. Eight-image data collections were

acquired in 90 minutes to cover all of the major joints. Disadvantages include the use of a radioactive compound, which exposes patients to a small amount of radiation, poor anatomic resolution with inability to differentiate between soft tissue, and bone marrow inflammation.

6.4 Correlation of MRI and NC scintigraphy with clinical and laboratory findings at baseline

Multiple reasons can be postulated to explain the absence of correlation between imaging and clinical evaluation in our study. Typically used global clinical parameters, such as the number of tender and swollen joints and HAQ, are difficult to use as reference standards of inflammation, since they are greatly dependent on patients' subjective symptoms and the clinician's judgement. Clinically positive findings are likely to correspond to a phlogistic process, whereas a clinically negative result is not an absolute proof of the absence of such a process. Furthermore, it is problematic to compare the imaging assessments of a single joint area to the clinical evaluation of multiple joints. Thus, more detailed clinical assessment of the degree of inflammation of the symptomatic wrist joint would have enabled more accurate statistic comparison between clinical evaluation and imaging parameters.

In addition, our study suffered from a relatively long time interval between clinical evaluation and imaging at baseline due to our limited imaging capacity (range 0–11 weeks, median 4 weeks), and medication was usually started before the imaging examinations. The non-existing correlation between the clinical and imaging data at baseline must thus be interpreted cautiously.

A previous report found significant correlations between DEMRI and several clinical global disease activity measures (the number of swollen and tender joints, the Ritchie index, Disease Activity Score, HAQ, CRP, ESR, $\alpha 2$ globulins) (Cimmino *et al.* 2003). However, some other papers address the discrepancy between clinical evaluation and MRI. Gaffney *et al.*, who studied rheumatoid knee joints, noted no correlation between DEMRI and clinical assessment or laboratory parameters (Gaffney *et al.* 1995). When comparing dynamic MRI of the rheumatoid wrist with clinical parameters, Huang *et al.* found a weak but significant correlation with the pain score, but not with the other clinical parameters (Huang *et al.* 2000). These results are in accordance with ours, and this further addresses the difficulty of comparing increased vascularity of a single

joint area detected by DEMRI and NC scintigraphy to the global clinical measures.

In our study, the MRI and NC scintigraphy parameters correlated with ESR. This may reflect systemic disease activity. A weaker correlation emerged between CRP and the average ^{99m}Tc-NC uptake and between CRP and the wrist MRI synovitis and bone oedema scores. However, no correlation was found between CRP and MRI E-rates. In the literature, there are also conflicting reports concerning the relationship between MRI-detectable joint inflammation and the laboratory parameters of inflammation. In an early RA study of 42 patients, MRI scores of the wrist correlated with CRP and ESR (McQueen *et al.* 1998). In some other papers, no correlation was found between the laboratory parameters and MRI (Gaffney *et al.* 1995, Ostergaard *et al.* 1996b, Huang *et al.* 2000).

6.5 The value of MRI and NC scintigraphy in the follow-up of early RA patients

Baseline imaging parameters of inflammation (bone oedema score, synovitis score, e-rate, ^{99m}Tc-NC uptake) were found to associate with erosive development during the two-year follow-up. Previous longitudinal studies have also demonstrated the relationship between MRI-detectable synovial inflammation, bone oedema, and subsequent MRI-detectable bone damage (Ostergaard *et al.* 1999, Conaghan *et al.* 2003b, Quinn *et al.* 2005). Our results support the existing data on the importance of MRI in disease monitoring and the prognostication of erosive disease together with the contribution of quantitative NC scintigraphy, a method not previously documented in the follow-up of early RA.

The most powerful baseline variable with a significant association with the change in the erosion score at two years was bone marrow oedema. Furthermore, in the multivariate regression model, it was the only baseline variable that predicted erosive progression. The small size of the study population probably explains why the other significantly associated baseline variables had no predictive value in the regression model. However, it should be noted that bone marrow oedema is a non-specific, reversible finding that is frequently seen in trauma, tumours, osteoarthritis and rheumatoid arthritis. In RA, bone oedema has been interpreted as a pre-erosive lesion, and it has been reported to associate with a six-fold risk for erosion occurrence on MRI at the same site one and six years later (McQueen *et al.* 1999, McQueen *et al.* 2003). Our results of the site-specific

analysis are similar, but show an even greater risk for erosive development if bone oedema is present at baseline.

The clinical parameters (the number of swollen and painful joints and HAQ) improved during the follow-up, while bone damage in the wrist joint proceeded. Previous longitudinal studies have also shown the discrepancy between improvement in clinical measures of disease activity and bone damage detected by MRI or radiographs (Mulherin *et al.* 1996, Jevtic *et al.* 1997, Ostergaard *et al.* 1999, McQueen *et al.* 1999, Klarlund *et al.* 2000a, McQueen *et al.* 2001). Thus, conventional DMARD treatment suppresses disease activity as detected by clinical and laboratory parameters, but seems to have less impact on the progression of erosions, at least in some of the patients. It has been postulated that the processes underlying joint inflammation may differ from those resulting in erosion and articular damage (Mulherin *et al.* 1996). Scott *et al.* summarized data from a number of studies and showed that radiographically detected bone damage and clinical outcome assessed by HAQ are not related in the earliest phases of RA. Significant correlations are found 5–8 years after disease onset, and they increase further in late disease (Scott *et al.* 2000). Long-term MRI follow-up studies are few, but one study of early RA patients found that baseline MRI parameters (bone oedema score, total MR score) of the dominant wrist had predictive value on functional outcome at six years after disease onset (Benton *et al.* 2004).

During the two years of follow-up, nine patients out of 24 (38%) showed a persistent response to the treatment (≥ 50% improvement in the tender and swollen joint scores and HAQ, with normal CRP or ESR levels). Only one of these patients presented with new erosions. Thus, persistent erosive progression seems unlikely in patients with persistent clinical response. The significance of this finding is greatly influenced by the small number of subjects in this subgroup. A previous two-year follow-up study of 187 established RA patients (mean disease duration of 7 yrs) with clinical remission at entry showed that clinically relevant erosive progression in hand and feet radiographs can be detected in 7% of patients with ongoing persistent remission (Molenaar *et al.* 2004).

MRI and NC scintigraphy may be especially useful in patients with insufficient clinical response. The wide range of erosion progression scores among these patients in our study reflects varying tendency in the erosiveness of the disease, ranging from persistent non-erosive to persistent erosive disease. In these cases, evaluation of local disease activity by quantitative imaging methods may be useful for predicting future erosiveness. During follow-up, bone marrow oedema with thick and intensively enhancing synovitis in MRI or intense

^{99m}Tc-NC uptake in scintigraphy seem to imply later erosive development (Table 6).

One major weakness of this study was the fact that the MRI imaging protocol differs partly from the OMERACT recommendations (pre- and post-contrast T1w images in coronal and axial plane). At the start of the study, the OMERACT MRI scoring criteria had not yet been published. At baseline, we had post-contrast images only in one plane (coronal), which made it difficult to evaluate the accurate amount of the hypertrophied synovial tissue. Thus, at follow-up, the baseline axial sequence (pre-contrast T2w FSE) was replaced by an axial post-contrast T1-w GRE sequence. This may have had an impact on the results in terms of more accurate grading of synovitis at follow-up when compared to baseline images. In addition, erosions were more easily depicted from axial T1w images when compared to baseline axial T2w FSE images. This may have resulted in improved erosion detection in the follow-up scans. However, two readers with blinded readings and an additional consensus reading with reference to the baseline images were used to achieve as accurate scoring of erosions as possible.

This study represents clinical treatment practice from the late 1990s in a regional secondary clinic in a university hospital serving a population of 270,000 inhabitants. Thus, our clinics admit patients with the whole disease spectrum from mild to severe RA. At baseline, one third of the patients were treated with some DMARD combination, including methotrexate, which is a rather conservative approach compared to the modern aggressive treatment strategies. The treatment was guided by clinical parameters, and at the end of the two-year follow-up, two thirds of the patients were on a combination. Furthermore, the imaging findings were available to the treating rheumatologists during the follow-up, which may have modified their treating decisions.

According to our results, more intensive treatment with e.g. biological agents should be considered if high inflammatory activity can be documented as a form of bone oedema and/or high NC uptake in patients on DMARDs without a clinically sufficient response to the treatment. However, these findings must be interpreted cautiously, because no attempt to standardize DMARD therapy was made in this observational study, which was not designed to study any specific treatment. A previous report of 20 poor-prognosis early RA patients showed increased rates of clinical remission and a lower rate of new MRI-detectable erosions after one year in 10 patients treated with methotrexate combined with anti-TNFα agent infliximab, when compared to 10 patients treated with

methotrexate only (Quinn *et al.* 2005). Further case-controlled studies with more patients are needed to explore this topic more thoroughly.

In conclusion, MRI and NC scintigraphy may help to identify the patients with persistent erosive disease from patients with persistent non-erosive disease in the follow-up of early RA.

6.6 MRI findings resembling erosions and synovitis in asymptomatic subjects

In the MRI study of both wrists (IV), small bony lesions resembling erosions were found in 14 out of 31 healthy volunteers (45%, 95% CI: 27 to 64%). Altogether 24 of the 930 wrist bones (15 bones of each wrist) showed erosion-like lesions (3%), detected by using OMERACT criteria. A similar number of changes resembling erosions was found in a previously published MRI study of 28 healthy individuals, in which 2.2% of the evaluated MCP joint bones and 1.7% of the evaluated wrist bones showed small erosion-like changes, as evaluated by OMERACT definitions (Ejbjerg *et al.* 2004).

Rather than true specific erosions, some of these lesions are more likely to represent subchondral juxtaarticular or degenerative cysts, which have been reported to be common in a previous cadaver study (Schrank *et al.* 2003). In this study, 280 formalin-fixed cadaver wrists with a mean age 80.3 years (range 40 to 101 years) were radiographed. 87 wrists showed 1 to 3 radiolucent cyst-like foci. Of these 87 wrists 50 specimens underwent MRI imaging and further histological examination (37 were excluded because of severe degenerative changes). In MRI, 27 wrists showed 48 intraosseous ganglion cysts and 7 degenerative cysts, which were proved by histopathology. The prevalence of ganglion cyst was thus 10%. However, only the wrists with radiolucent foci were imaged by MRI, so the true prevalence is probably higher.

In a recently published high-field MRI study of 30 asymptomatic volunteers (mean age 31 years, range 22–49 years), 24 bright osseous lesions were identified in 14 subjects (47%, 95% CI 29–65%) by two musculoskeletal radiologists (Robertson *et al.* 2006). Among the 24 osseous lesions, erosions, intraosseous ganglia, subchondral cysts and five regions of bone marrow oedema were identified at consensus. The readers were not able to reach agreement entirely as to whether these lesions were erosions, cysts or intraosseous ganglia. Fewer lesions were found in our study, probably because the lack of fat-suppressed sequences prevented us from scoring bone oedema and non-scoring of

intraosseous cysts as an erosion, if suspected. Better spatial resolution achieved with the high-field scanner used in this study may also explain why fewer lesions were detected in our study.

According to the results of study IV, the lesions resembling erosions were always small and few in number; i.e., no more than two erosive-like changes per wrist could be detected. Furthermore, these lesions were more often found in older subjects. This should be kept in mind when interpreting MRI scans of patients with joint pain without clinical signs of inflammation. A single small erosion-like lesion in a wrist joint seems to be a highly non-specific finding. Again, multiple erosive-like changes should be taken to imply inflammatory joint disease.

Administration of i.v. contrast medium was used in the first 10 subjects to evaluate synovitis. Synovitis-like mild to moderate GDTPA-enhancement in the synovial compartments of the wrist joint was seen in six of them. Of these six subjects, five had enhancement in both wrists, and one in one wrist. This finding is in accordance with previous reports. Patrik *et al.* found contrast enhancement in radiocarpal joints in 8 [44%] out of 18 healthy subjects (Partik *et al.* 2002). Ejberg et al, who used the OMERACT criteria, detected mild synovitis-like changes in the wrist joints of 6 (21%) out of 28 healthy subjects (Ejbjerg *et al.* 2004).

One dose of intravenous contrast media was used to image both wrists. This led to delayed post-contrast imaging of the non-dominant wrist (about 12 minutes after contrast injection). In the rheumatoid knee, diffusion of the contrast media from the hypertrophied enhancing synovial tissue to the joint fluid has been reported to become significantly visible in MRI from about 11 minutes after contrast injection (Ostergaard & Klarlund 2001). However, diffusion of the contrast media to the joint fluid was not considered a substantial problem in our study, since joint effusion was not an expected occurrence in volunteers who had been clinically assessed to be symptom-free before imaging.

In conclusion, small bony defects resembling erosions and mild to moderate enhancement in wrist joint compartments can be detected in about half of normal volunteers; these lesions are thus not necessarily related to inflammatory joint disorders.

6.7 Future aspects and recommendations

Compared to the traditional closed-bore high-field scanners, the benefits of open configuration MRI scanners are lower price and increased comfort to claustrophobic patients. Open configuration also enables image-guided interventions and therapy. Recent technological advances have also allowed the construction of open configuration scanners that operate in high magnetic fields (up to 1T). More sophisticated imaging methods, e.g. selective presaturation techniques for fat suppression, are available in the newer open configuration scanners as compared to the older generation scanner that was used in this study.

One major drawback of low-field scanners has been the inability to obtain suitable fat suppression techniques for contrast-enhanced imaging. The single-scan phase-contrast method offers a promising and reliable tool to overcome this problem without any substantial increase in imaging time. However, the need for operator-dependent post-processing manoeuvres decreases the clinical value of this method.

Future technical development is needed to make the phase-contrast method more automatic. A modified three-point Dixon "sandwich" technique, a close relative of the phase-contrast method, has been reported to produce reliable fat suppression at low field without manual post-processing in the evaluation of knee joint pathology and in contrast-enhanced examinations of the spine (Bredella *et al.* 2001, Huegli *et al.* 2004). In the latest software version available to Oulu University Hospital's 0.23T scanner, there is an automated modified multiple echo three-point Dixon fat suppression method that can be combined with contrast-enhanced imaging. (Personal information from Philips Medical Systems MR Finland). However, since no experience of this method exists, the feasibility and reliability of this technique remains to be explored.

MRI is the only imaging modality that can detect both inflammatory lesions (synovitis, bone oedema) and erosions in RA. However, despite its inability to detect synovitis and bone oedema, conventional radiography remain the primary imaging method of erosive damage thanks to its superior availability and lower cost when compared to MRI. During the time from the start of this study, numerous cross-sectional studies have been published to address the value of MRI in the detection of inflammation and bone damage in RA. However, few long-term longitudinal studies exist to assess the value of MRI or NC scintigraphy in monitoring therapy response and in predicting structural and functional outcome. Our plan is to image further the small cohort of early RA

patients in this study with MRI and NC scintigraphy at eight years after disease onset to evaluate whether initial and follow-up imaging parameters derived from these methods have value in predicting joint damage and functional outcome at the stage of established disease.

In conclusion, even though there are technical limitations associated with low field, clinically useful information about the degree of local disease activity that is further associated with the future erosive development in early RA patients can be obtained with a 0.23T open-configuration scanner. NC scintigraphy gives similar information as MRI about the local inflammatory activity of the wrist joint, with the benefit of imaging multiple joints at the same session but with inferior anatomic resolution and inability to depict or differentiate bone damage. MRI and NC scintigraphy can be recommended especially if sustained clinical response to treatment is not achieved, as these methods may help to differentiate the patients with persistent erosive disease from those with symptomatic non-erosive disease.

7 Summary and conclusions

1. The phase difference-based fat suppression method can be successfully employed at low field in the imaging of contrast-enhanced arthritic joints, it improves the conspicuity and delineation of contrast-enhancing synovitis, but the method is considered time-consuming due to manual post-processing of images. Further development is needed to make this method clinically more useful.
2. ^{99m}Tc-NC uptake can be reliably measured from specific regions of the inflamed joint, and the degree of the uptake is strongly associated with enhancement rates measured from the same regions in dynamic MRI. Furthermore, these measures associate with the semiquantitative estimations of the volume of synovial hypertrophy and bone oedema and with laboratory markers of inflammation. Clinically useful quantitative information about the inflammatory load of the wrist joint in early RA can thus be obtained with these imaging methods.
3. High local inflammatory activity, assessed by MRI and NC scintigraphy at inclusion, is closely related to progression of wrist joint erosions on MRI during the first two years of RA. Thus early RA patients with intense ^{99m}Tc-NC uptake in scintigraphy, rapid and intense enhancement of contrast media in dynamic MRI or bone oedema and thick synovial hypertrophy in static MRI are at risk of developing further bone damage. Furthermore, at one-year follow-up, in the subgroup of patients without sustained clinical response, these methods seem to distinguish the patients with persistent erosive disease from the patients with persistent non-erosive disease, when evaluated one year later. This may be useful in clinical decision-making to target more effective therapy at the non-responders with high inflammatory activity on MRI and NC scintigraphy.
4. In the MRI of the wrist joint, small lesions resembling erosions and mild synovitis-like contrast enhancement can be found in about half of the normal volunteers. These signs are thus not always related to arthritis, and must always be interpreted with reference to the clinical picture.

References

Adams BK, Al Attia HM, Khadim RA & Al Haider ZY (2001) 99Tc(m) nanocolloid scintigraphy: a reliable way to detect active joint disease in patients with peripheral joint pain. Nucl Med Commun 22: 315–318.

Ahn CB, Lee SY, Nalcioglu O & Cho ZH (1986) Spectroscopic imaging by quadrature modulated echo time shifting. Magn Reson Imaging 4: 110–111.

Alamanos Y & Drosos AA (2005) Epidemiology of adult rheumatoid arthritis. Autoimmun Rev 4: 130–136.

Alamanos Y, Voulgari PV & Drosos AA (2004) Epidemiology of rheumatic diseases in Greece. J Rheumatol 31: 1669–1670.

Alasaarela E, Suramo I, Tervonen O, Lahde S, Takalo R & Hakala M (1998) Evaluation of humeral head erosions in rheumatoid arthritis: a comparison of ultrasonography, magnetic resonance imaging, computed tomography and plain radiography. Br J Rheumatol 37: 1152–1156.

Althoff CE, Appel H, Rudwaleit M, Sieper J, Eshed I, Hamm B & Hermann KG (2007) Whole-body MRI as a new screening tool for detecting axial and peripheral manifestations of spondyloarthritis. Ann Rheum Dis 66: 983–985.

American College of Rheumatology Subcommittee on Rheumatoid Arthritis Guidelines (2002) Guidelines for the management of rheumatoid arthritis: 2002 Update. Arthritis Rheum 46: 328–346.

Appel H, Hermann KG, Althoff CE, Rudwaleit M & Sieper J (2007) Whole-body magnetic resonance imaging evaluation of widespread inflammatory lesions in a patient with ankylosing spondylitis before and after 1 year of treatment with infliximab. J Rheumatol 34: 2497–2498.

Argyropoulou MI, Glatzouni A, Voulgari PV, Xydis VG, Nikas SN, Efremidis SC & Drosos AA (2005) Magnetic resonance imaging quantification of hand synovitis in patients with rheumatoid arthritis treated with infliximab. Joint Bone Spine 72: 557–561.

Arnett FC, Edworthy SM, Bloch DA, McShane DJ, Fries JF, Cooper NS, Healey LA, Kaplan SR, Liang MH & Luthra HS (1988) The American Rheumatism Association 1987 revised criteria for the classification of rheumatoid arthritis. Arthritis Rheum 31: 315–324.

Arzu GE, Aras G, Kucuk O, Atay G, Tutak I, Ataman S, Soylu A & Ibis E (2003) Comparison of Tc-99m HIG and three-phase Tc-99m MDP bone scintigraphy for evaluating the efficacy of Yttrium-90 silicate radionuclide synovectomy. Clin Nucl Med 28: 277–285.

Atlas SW, Grossman RI, Hackney DB, Goldberg HI, Bilaniuk LT & Zimmerman RA (1988) STIR MR imaging of the orbit. AJR Am J Roentgenol 151: 1025–1030.

Backhaus M, Burmester GR, Sandrock D, Loreck D, Hess D, Scholz A, Blind S, Hamm B & Bollow M (2002) Prospective two year follow up study comparing novel and conventional imaging procedures in patients with arthritic finger joints. Ann Rheum Dis 61: 895–904.

Backhaus M, Kamradt T, Sandrock D, Loreck D, Fritz J, Wolf KJ, Raber H, Hamm B, Burmester GR & Bollow M (1999) Arthritis of the finger joints: a comprehensive approach comparing conventional radiography, scintigraphy, ultrasound, and contrast-enhanced magnetic resonance imaging. Arthritis Rheum 42: 1232–1245.

Ballara S, Taylor PC, Reusch P, Marme D, Feldmann M, Maini RN & Paleolog EM (2001) Raised serum vascular endothelial growth factor levels are associated with destructive change in inflammatory arthritis. Arthritis Rheum 44: 2055–2064.

Balzer T (2003) Contrast agents for magnetic resonanace imaging. In: Reimer P, Parizel PM & Stichnoth F-A (eds) Clinical MR Imaging. Berlin, Germany, Springer: 53–63.

Barrera P, Oyen WJ, Boerman OC & van Riel PL (2003) Scintigraphic detection of tumour necrosis factor in patients with rheumatoid arthritis. Ann Rheum Dis 62: 825–828.

Bathon JM, Martin RW, Fleischmann RM, Tesser JR, Schiff MH, Keystone EC, Genovese MC, Wasko MC, Moreland LW, Weaver AL, Markenson J & Finck BK (2000) A comparison of etanercept and methotrexate in patients with early rheumatoid arthritis. N Engl J Med 343: 1586–1593.

Baudouin CJ, Bryant DJ & Young IR (1992) Fat suppression in magnetic resonance imaging at low field strength using binomial pulse sequences. Br J Radiol 65: 132–136.

Becker W, Emmrich F, Horneff G, Burmester G, Seiler F, Schwarz A, Kalden J & Wolf F (1990) Imaging rheumatoid arthritis specifically with technetium 99m CD4-specific (T-helper lymphocytes) antibodies. Eur J Nucl Med 17: 156–159.

Beckers C, Jeukens X, Ribbens C, Andre B, Marcelis S, Leclercq P, Kaiser MJ, Foidart J, Hustinx R & Malaise MG (2006) (18)F-FDG PET imaging of rheumatoid knee synovitis correlates with dynamic magnetic resonance and sonographic assessments as well as with the serum level of metalloproteinase-3. Eur J Nucl Med Mol Imaging 33: 275–280.

Beckers C, Ribbens C, Andre B, Marcelis S, Kaye O, Mathy L, Kaiser MJ, Hustinx R, Foidart J & Malaise MG (2004) Assessment of disease activity in rheumatoid arthritis with (18)F-FDG PET. J Nucl Med 45: 956–964.

Beltran J, Caudill JL, Herman LA, Kantor SM, Hudson PN, Noto AM & Baran AS (1987) Rheumatoid arthritis: MR imaging manifestations. Radiology 165: 153–157.

Benton N, Stewart N, Crabbe J, Robinson E, Yeoman S & McQueen FM (2004) MRI of the wrist in early rheumatoid arthritis can be used to predict functional outcome at 6 years. Ann Rheum Dis 63: 555–561.

Berna L, Torres G, Diez C, Estorch M, Martinez-Duncker D & Carrio I (1992) Technetium-99m human polyclonal immunoglobulin G studies and conventional bone scans to detect active joint inflammation in chronic rheumatoid arthritis. Eur J Nucl Med 19: 173–176.

Bird P, Ejbjerg B, Lassere M, Ostergaard M, McQueen F, Peterfy C, Haavardsholm E, O'Connor P, Genant H, Edmonds J, Emery P & Conaghan PG (2007) A multireader reliability study comparing conventional high-field magnetic resonance imaging with extremity low-field MRI in rheumatoid arthritis. J Rheumatol 34: 854–856.

Bird P, Lassere M, Shnier R & Edmonds J (2003) Computerized measurement of magnetic resonance imaging erosion volumes in patients with rheumatoid arthritis: a comparison with existing magnetic resonance imaging scoring systems and standard clinical outcome measures. Arthritis Rheum 48: 614–624.

Bleeker-Rovers CP, Boerman OC, Rennen HJ, Corstens FH & Oyen WJ (2004) Radiolabeled compounds in diagnosis of infectious and inflammatory disease. Curr Pharm Des 10: 2935–2950.

Boerman OC, Dams ET, Oyen WJ, Corstens FH & Storm G (2001) Radiopharmaceuticals for scintigraphic imaging of infection and inflammation. Inflamm Res 50: 55–64.

Bredella MA, Losasso C, Moelleken SC, Huegli RW, Genant HK & Tirman PF (2001) Three-point Dixon chemical-shift imaging for evaluating articular cartilage defects in the knee joint on a low-field-strength open magnet. AJR Am J Roentgenol 177: 1371–1375.

Breedveld FC, Emery P, Keystone E, Patel K, Furst DE, Kalden JR, St Clair EW, Weisman M, Smolen J, Lipsky PE & Maini RN (2004) Infliximab in active early rheumatoid arthritis. Ann Rheum Dis 63: 149–155.

Brower AC (1990) Use of the radiograph to measure the course of rheumatoid arthritis. The gold standard versus fool's gold. Arthritis Rheum 33: 316–324.

Bukhari M, Lunt M, Harrison BJ, Scott DG, Symmons DP & Silman AJ (2002) Rheumatoid factor is the major predictor of increasing severity of radiographic erosions in rheumatoid arthritis: results from the Norfolk Arthritis Register Study, a large inception cohort. Arthritis Rheum 46: 906–912.

Buscombe JR, Lui D, Ensing G, de JR & Ell PJ (1990) 99mTc-human immunoglobulin (HIG)--first results of a new agent for the localization of infection and inflammation. Eur J Nucl Med 16: 649–655.

Bydder GM & Young IR (1985) Clinical use of the partial saturation and saturation recovery sequences in MR imaging. J Comput Assist Tomogr 9: 1020–1032.

Carmona L, Villaverde V, Hernandez-Garcia C, Ballina J, Gabriel R & Laffon A (2002) The prevalence of rheumatoid arthritis in the general population of Spain. Rheumatology (Oxford) 41: 88–95.

Chapman PT, Jamar F, Keelan ET, Peters AM & Haskard DO (1996) Use of a radiolabeled monoclonal antibody against E-selectin for imaging of endothelial activation in rheumatoid arthritis. Arthritis Rheum 39: 1371–1375.

Chianelli M, D'Alessandria C, Conti F, Priori R, Valesini G, Annovazzi A & Signore A (2006) New radiopharmaceuticals for imaging rheumatoid arthritis. Q J Nucl Med Mol Imaging 50: 217–225.

Cimmino MA, Innocenti S, Livrone F, Magnaguagno F, Silvestri E & Garlaschi G (2003) Dynamic gadolinium-enhanced magnetic resonance imaging of the wrist in patients with rheumatoid arthritis can discriminate active from inactive disease. Arthritis Rheum 48: 1207–1213.

Cimmino MA, Parodi M, Innocenti S, Succio G, Banderali S, Silvestri E & Garlaschi G (2005) Dynamic magnetic resonance of the wrist in psoriatic arthritis reveals imaging patterns similar to those of rheumatoid arthritis. Arthritis Res Ther 7: R725–R731.

Cindas A, Gokce-Kustal Y, Kirth PO & Caner B (2001) Scintigraphic evaluation of synovial inflammation in rheumatoid arthritis with (99m)technetium-labelled human polyclonal immunoglobulin G. Rheumatol Int 20: 71–77.

Conaghan P, Edmonds J, Emery P, Genant H, Gibbon W, Klarlund M, Lassere M, McGonagle D, McQueen F, O'Connor P, Peterfy C, Shnier R, Stewart N & Ostergaard M (2001) Magnetic resonance imaging in rheumatoid arthritis: summary of OMERACT activities, current status, and plans. J Rheumatol 28: 1158–1162.

Conaghan P, Lassere M, Ostergaard M, Peterfy C, McQueen F, O'Connor P, Bird P, Ejbjerg B, Klarlund M, Shnier R, Genant H, Emery P & Edmonds J (2003a) OMERACT Rheumatoid Arthritis Magnetic Resonance Imaging Studies. Exercise 4: an international multicenter longitudinal study using the RA-MRI Score. J Rheumatol 30: 1376–1379.

Conaghan PG, Ejbjerg B, Lassere M, Bird P, Peterfy C, Emery P, McQueen F, Haavardsholm E, O'Connor P, Edmonds J, Genant H & Ostergaard M (2007) A multicenter reliability study of extremity-magnetic resonance imaging in the longitudinal evaluation of rheumatoid arthritis. J Rheumatol 34: 857–858.

Conaghan PG, McQueen FM, Peterfy CG, Lassere MN, Ejbjerg B, Bird P, O'Connor PJ, Haavardsholm E, Edmonds JP, Emery P, Genant HK & Ostergaard M (2005) The evidence for magnetic resonance imaging as an outcome measure in proof-of-concept rheumatoid arthritis studies. J Rheumatol 32: 2465–2469.

Conaghan PG, O'Connor P, McGonagle D, Astin P, Wakefield RJ, Gibbon WW, Quinn M, Karim Z, Green MJ, Proudman S, Isaacs J & Emery P (2003b) Elucidation of the relationship between synovitis and bone damage: a randomized magnetic resonance imaging study of individual joints in patients with early rheumatoid arthritis. Arthritis Rheum 48: 64–71.

de Bois MH, Arndt JW, Speyer I, Pauwels EK & Breedveld FC (1996) Technetium-99m labelled human immunoglobulin scintigraphy predicts rheumatoid arthritis in patients with arthralgia. Scand J Rheumatol 25: 155–158.

de Bois MH, Arndt JW, Tak PP, Kluin PM, van d, V, Pauwels EK & Breedveld FC (1993) 99Tcm-labelled polyclonal human immunoglobulin G scintigraphy before and after intra-articular knee injection of triamcinolone hexacetonide in patients with rheumatoid arthritis. Nucl Med Commun 14: 883–887.

de Bois MH, Arndt JW, van d, V, Pauwels EK & Breedveld FC (1994) Joint scintigraphy for quantification of synovitis with 99mTc-labelled human immunoglobulin G compared to late phase scintigraphy with 99mTc-labelled diphosphonate. Br J Rheumatol 33: 67–73.

de Bois MH, Arndt JW, van d, V, van der Lubbe PA, Westedt ML, Pauwels EK & Breedveld FC (1992) 99mTc human immunoglobulin scintigraphy--a reliable method to detect joint activity in rheumatoid arthritis. J Rheumatol 19: 1371–1376.

de Bois MH, Pauwels EK & Breedveld FC (1995a) New agents for scintigraphy in rheumatoid arthritis. Eur J Nucl Med 22: 1339–1346.

de Bois MH, Tak PP, Arndt JW, Kluin PM, Pauwels EK & Breedveld FC (1995b) Joint scintigraphy for quantification of synovitis with 99mTc-labelled human immunoglobulin G compared to histological examination. Clin Exp Rheumatol 13: 155–159.

De Schrijver M, Streule K, Senekowitsch R & Fridrich R (1987) Scintigraphy of inflammation with nanometer-sized colloidal tracers. Nucl Med Commun 8: 895–908.

DeLand FH, Kim EE, Primus FJ, Casper S & Goldenberg DM (1979) In vivo radioimmunodetection of neoplasms. Compr Ther 5: 31–36.

Devauchelle P, V, Saraux A, Berthelot JM, Alapetite S, Jousse S, Chales G, Thorel JB, Hoang S, Nouy-Trolle I, Martin A, Chiocchia G, Youinou P & Le GP (2004) Ability of foot radiographs to predict rheumatoid arthritis in patients with early arthritis. J Rheumatol 31: 66–70.

Disler DG, McCauley TR, Kelman CG, Fuchs MD, Ratner LM, Wirth CR & Hospodar PP (1996) Fat-suppressed three-dimensional spoiled gradient-echo MR imaging of hyaline cartilage defects in the knee: comparison with standard MR imaging and arthroscopy. AJR Am J Roentgenol 167: 127–132.

Dixon WG & Symmons DP (2005) Does early rheumatoid arthritis exist? Best Pract Res Clin Rheumatol 19: 37–53.

Dixon WT (1984) Simple proton spectroscopic imaging. Radiology 153: 189–194.

Dohn UM, Ejbjerg BJ, Court-Payen, Hasselquist M, Narvestad E, Szkudlarek M, Moller JM, Thomsen HS & Ostergaard M (2006) Are bone erosions detected by magnetic resonance imaging and ultrasonography true erosions? A comparison with computed tomography in rheumatoid arthritis metacarpophalangeal joints. Arthritis Res Ther 8: R110.

Dohn UM, Ejbjerg BJ, Hasselquist M, Narvestad E, Court-Payen, Szkudlarek M, Moller J, Thomsen HS & Ostergaard M (2007) Rheumatoid arthritis bone erosion volumes on CT and MRI: reliability and correlations with erosion scores on CT, MRI and radiography. Ann Rheum Dis 66: 1388–1392.

Drossaers-Bakker KW, Zwinderman AH, Vlieland TP, van ZD, Vos K, Breedveld FC & Hazes JM (2002) Long-term outcome in rheumatoid arthritis: a simple algorithm of baseline parameters can predict radiographic damage, disability, and disease course at 12-year followup. Arthritis Rheum 47: 383–390.

Edwards J (1994) Rheumatoid arthritis. Synovium. In: Klippel JH, Diepe PA (eds) Rheumatology. Mosby-Year Book Europe Limited, London, United Kingdom: 3.7.1.–3.7.8.

Egsmose C, Lund B, Borg G, Pettersson H, Berg E, Brodin U & Trang L (1995) Patients with rheumatoid arthritis benefit from early 2nd line therapy: 5 year followup of a prospective double blind placebo controlled study. J Rheumatol 22: 2208–2213.

Ejbjerg B, Narvestad E, Rostrup E, Szkudlarek M, Jacobsen S, Thomsen HS & Ostergaard M (2004) Magnetic resonance imaging of wrist and finger joints in healthy subjects occasionally shows changes resembling erosions and synovitis as seen in rheumatoid arthritis. Arthritis Rheum 50: 1097–1106.

Ejbjerg BJ, Narvestad E, Jacobsen S, Thomsen HS & Ostergaard M (2005a) Optimised, low cost, low field dedicated extremity MRI is highly specific and sensitive for synovitis and bone erosions in rheumatoid arthritis wrist and finger joints: comparison with conventional high field MRI and radiography. Ann Rheum Dis 64: 1280–1287.

Ejbjerg BJ, Vestergaard A, Jacobsen S, Thomsen HS & Ostergaard M (2005b) The smallest detectable difference and sensitivity to change of magnetic resonance imaging and radiographic scoring of structural joint damage in rheumatoid arthritis finger, wrist, and toe joints: a comparison of the OMERACT rheumatoid arthritis magnetic resonance imaging score applied to different joint combinations and the Sharp/van der Heijde radiographic score. Arthritis Rheum 52: 2300–2306.

Firestein GS (1994). Rheumatoid arthritis. Rheumatoid synovitis and pannus. In: Klippel JH, Diepe PA, eds. Rheumatology. Mosby-Year Book Europe Limited, London, United Kingdom. 3.12.1–30

Firestein GS (1999) Starving the synovium: angiogenesis and inflammation in rheumatoid arthritis. J Clin Invest 103: 3–4.

Firestein GS (2003) Evolving concepts of rheumatoid arthritis. Nature 423: 356–361.

Fischman AJ, Fucello AJ, Pellegrino-Gensey JL, Geltofsky J, Yarmush ML, Rubin RH & Strauss HW (1992) Effect of carbohydrate modification on the localization of human polyclonal IgG at focal sites of bacterial infection. J Nucl Med 33: 1378–1382.

Fischman AJ, Rubin RH, White JA, Locke E, Wilkinson RA, Nedelman M, Callahan RJ, Khaw BA & Strauss HW (1990) Localization of Fc and Fab fragments of nonspecific polyclonal IgG at focal sites of inflammation. J Nucl Med 31: 1199–1205.

Fleury HJ, Pinson P, Faure M, Masquelier B & Dupon M (2003) HIV-1 transmission during scintigraphy. Lancet 362: 210.

Fries JF, Spitz P, Kraines RG & Holman HR (1980) Measurement of patient outcome in arthritis. Arthritis Rheum 23: 137–145.

Gaal J, Mezes A, Siro B, Varga J, Galuska L, Janoky G, Garai I, Bajnok L & Suranyi P (2002) 99m Tc-HMPAO labelled leukocyte scintigraphy in patients with rheumatoid arthritis: a comparison with disease activity. Nucl Med Commun 23: 39–46.

Gaffney K, Cookson J, Blades S, Coumbe A & Blake D (1998) Quantitative assessment of the rheumatoid synovial microvascular bed by gadolinium-DTPA enhanced magnetic resonance imaging. Ann Rheum Dis 57: 152–157.

Gaffney K, Cookson J, Blake D, Coumbe A & Blades S (1995) Quantification of rheumatoid synovitis by magnetic resonance imaging. Arthritis Rheum 38: 1610–1617.

Genovese MC, Bathon JM, Martin RW, Fleischmann RM, Tesser JR, Schiff MH, Keystone EC, Wasko MC, Moreland LW, Weaver AL, Markenson J, Cannon GW, Spencer-Green G & Finck BK (2002) Etanercept versus methotrexate in patients with early rheumatoid arthritis: two-year radiographic and clinical outcomes. Arthritis Rheum 46: 1443–1450.

Gerli R & Goodson NJ (2005) Cardiovascular involvement in rheumatoid arthritis. Lupus 14: 679–682.

Glover GH & Schneider E (1991) Three-point Dixon technique for true water/fat decomposition with B0 inhomogeneity correction. Magn Reson Med 18: 371–383.

Gnanasegaran G, Croasdale J & Buscombe JR (2005) Nuclear medicine imaging of infection and inflammation 4: 127–137

Goldbach-Mansky R, Woodburn J, Yao L & Lipsky PE (2003) Magnetic resonance imaging in the evaluation of bone damage in rheumatoid arthritis: a more precise image or just a more expensive one? Arthritis Rheum 48: 585–589.

Goodson NJ, Wiles NJ, Lunt M, Barrett EM, Silman AJ & Symmons DP (2002) Mortality in early inflammatory polyarthritis: cardiovascular mortality is increased in seropositive patients. Arthritis Rheum 46: 2010–2019.

Gordon DA & Hastings DE (2006). Rheumatoid arthritis. Clinical features: Early, progressive and late disease. In: Klippel JH, Diepe PA, eds. Rheumatology. Mosby-Year Book Europe Limited, London, United Kingdom: 3.4.1–14

Goronzy JJ, Matteson EL, Fulbright JW, Warrington KJ, Chang-Miller A, Hunder GG, Mason TG, Nelson AM, Valente RM, Crowson CS, Erlich HA, Reynolds RL, Swee RG, O'Fallon WM & Weyand CM (2004) Prognostic markers of radiographic progression in early rheumatoid arthritis. Arthritis Rheum 50: 43–54.

Goupille P, Roulot B, Akoka S, Avimadje AM, Garaud P, Naccache L, Le PA & Valat JP (2001) Magnetic resonance imaging: a valuable method for the detection of synovial inflammation in rheumatoid arthritis. J Rheumatol 28: 35–40.

Grassi W, Filippucci E, Farina A & Cervini C (2000) Sonographic imaging of tendons. Arthritis Rheum 43: 969–976.

Green M, Marzo-Ortega H, McGonagle D, Wakefield R, Proudman S, Conaghan P, Gooi J & Emery P (1999) Persistence of mild, early inflammatory arthritis: the importance of disease duration, rheumatoid factor, and the shared epitope. Arthritis Rheum 42: 2184–2188.

Haase A, Frahm J, Hanicke W & Matthaei D (1985) 1H NMR chemical shift selective (CHESS) imaging. Phys Med Biol 30: 341–344.

Haavardsholm EA, Ostergaard M, Ejbjerg BJ, Kvan NP, Uhlig TA, Lilleas FG & Kvien TK (2005) Reliability and sensitivity to change of the OMERACT rheumatoid arthritis magnetic resonance imaging score in a multireader, longitudinal setting. Arthritis Rheum 52: 3860–3867.

Hakala M, Pöllanen R & Nieminen P (1993) The ARA 1987 revised criteria select patients with clinical rheumatoid arthritis from a population based cohort of subjects with chronic rheumatic diseases registered for drug reimbursement. J Rheumatol 20: 1674–1678.

Harned EM, Mitchell DG, Burk DL, Jr., Vinitski S & Rifkin MD (1990) Bone marrow findings on magnetic resonance images of the knee: accentuation by fat suppression. Magn Reson Imaging 8: 27–31.

Harrison BJ, Symmons DP, Barrett EM & Silman AJ (1998) The performance of the 1987 ARA classification criteria for rheumatoid arthritis in a population based cohort of patients with early inflammatory polyarthritis. American Rheumatism Association. J Rheumatol 25: 2324–2330.

Hirohata S, Miura Y, Tomita T, Yoshikawa H, Ochi T & Chiorazzi N (2006) Enhanced expression of mRNA for nuclear factor kappaB1 (p50) in CD34+ cells of the bone marrow in rheumatoid arthritis. Arthritis Res Ther 8: R54.

Hirohata S, Yanagida T, Nagai T, Sawada T, Nakamura H, Yoshino S, Tomita T & Ochi T (2001) Induction of fibroblast-like cells from CD34(+) progenitor cells of the bone marrow in rheumatoid arthritis. J Leukoc Biol 70: 413–421.

Huang J, Stewart N, Crabbe J, Robinson E, McLean L, Yeoman S, Tan PL & McQueen FM (2000) A 1-year follow-up study of dynamic magnetic resonance imaging in early rheumatoid arthritis reveals synovitis to be increased in shared epitope-positive patients and predictive of erosions at 1 year. Rheumatology (Oxford) 39: 407–416.

Huegli RW, Tirman PF, Bonel HM, Staedele H, Zaim S, Grigorian M & Genant HK (2004) Use of the modified three-point Dixon technique in obtaining T1-weighted contrast-enhanced fat-saturated images on an open magnet. Eur Radiol 14: 1781–1786.

Huh YM, Suh JS, Jeong EK, Lee SK, Lee JS, Choi BW & Kim DK (1999) Role of the inflamed synovial volume of the wrist in defining remission of rheumatoid arthritis with gadolinium-enhanced 3D-SPGR MR imaging. J Magn Reson Imaging 10: 202–208.

Iagnocco A, Filippucci E, Perella C, Ceccarelli F, Cassara E, Alessandri C, Sabatini E, Grassi W & Valesini G (2007a) Clinical and Ultrasonographic Monitoring of Response to Adalimumab Treatment in Rheumatoid Arthritis. J Rheumatol.

Iagnocco A, Perella C, Naredo E, Meenagh G, Ceccarelli F, Tripodo E, Basili S & Valesini G (2007b) Etanercept in the treatment of rheumatoid arthritis: clinical follow-up over one year by ultrasonography. Clin Rheumatol.

Imhof H, Nobauer-Huhmann IM, Gahleitner A, Kainberger F, Krestan C, Sulzbacher I & Trattnig S (2002) Pathophysiology and imaging in inflammatory and blastomatous synovial diseases. Skeletal Radiol 31: 313–333.

Jamar F, Chapman PT, Manicourt DH, Glass DM, Haskard DO & Peters AM (1997) A comparison between 111In-anti-E-selectin mAb and 99Tcm-labelled human non-specific immunoglobulin in radionuclide imaging of rheumatoid arthritis. Br J Radiol 70: 473–481.

Jamar F, Houssiau FA, Devogelaer JP, Chapman PT, Haskard DO, Beaujean V, Beckers C, Manicourt DH & Peters AM (2002) Scintigraphy using a technetium 99m-labelled anti-E-selectin Fab fragment in rheumatoid arthritis. Rheumatology (Oxford) 41: 53–61.

Jamar F, Manicourt DH, Leners N, Vanden BM & Beckers C (1995) Evaluation of disease activity in rheumatoid arthritis and other arthritides using 99mtechnetium labeled nonspecific human immunoglobulin. J Rheumatol 22: 850–854.

Jevtic V, Watt I, Rozman B, Kos-Golja M, Praprotnik S, Logar D, Presetnik M, Demsar F, Jarh O, Campion G & Musikic P (1997) Contrast enhanced Gd-DTPA magnetic resonance imaging in the evaluation of rheumatoid arthritis during a clinical trial with DMARDs. A prospective two-year follow-up study on hand joints in 31 patients. Clin Exp Rheumatol 15: 151–156.

Jimenez-Boj E, Nobauer-Huhmann I, Hanslik-Schnabel B, Dorotka R, Wanivenhaus AH, Kainberger F, Trattnig S, Axmann R, Tsuji W, Hermann S, Smolen J & Schett G (2007) Bone erosions and bone marrow edema as defined by magnetic resonance imaging reflect true bone marrow inflammation in rheumatoid arthritis. Arthritis Rheum 56: 1118–1124.

Jorgensen C, Couret I, Bologna C, Rossi M & Sany J (1995) Radiolabelled lymphocyte migration in rheumatoid synovitis. Ann Rheum Dis 54: 39–44.

Jorgensen C, Cyteval C, Anaya JM, Baron MP, Lamarque JL & Sany J (1993) Sensitivity of magnetic resonance imaging of the wrist in very early rheumatoid arthritis. Clin Exp Rheumatol 11: 163–168.

Joseph PM (1985) A spin echo chemical shift MR imaging technique. J Comput Assist Tomogr 9: 651–658.

Joshua F, Lassere M, Bruyn GA, Szkudlarek M, Naredo E, Schmidt WA, Balint P, Filippucci E, Backhaus M, Iagnocco A, Scheel AK, Kane D, Grassi W, Conaghan PG, Wakefield RJ & D'Agostino MA (2007) Summary findings of a systematic review of the ultrasound assessment of synovitis. J Rheumatol 34: 839–847.

Juweid M, Strauss HW, Yaoita H, Rubin RH & Fischman AJ (1992) Accumulation of immunoglobulin G at focal sites of inflammation. Eur J Nucl Med 19: 159–165.

Kaipiainen-Seppänen O, Aho K, Isomaki H & Laakso M (1996) Incidence of rheumatoid arthritis in Finland during 1980-1990. Ann Rheum Dis 55: 608–611.

Kim EE, DeLand FH, Casper S, Corgan RL, Primus FJ & Goldenberg DM (1980) Radioimmunodetection of colorectal cancer. Cancer 45: 1243–1247.

Kinne RW, Becker W, Schwab J, Horneff G, Schwarz A, Kalden JR, Emmrich F, Burmester GR & Wolf F (1993) Comparison of 99Tcm-labelled specific murine anti-CD4 monoclonal antibodies and nonspecific human immunoglobulin for imaging inflamed joints in rheumatoid arthritis. Nucl Med Commun 14: 667–675.

Klarlund M, Ostergaard M, Gideon P, Sorensen K, Jensen KE & Lorenzen I (1999) Wrist and finger joint MR imaging in rheumatoid arthritis. Acta Radiol 40: 400–409.

Klarlund M, Ostergaard M, Jensen KE, Madsen JL, Skjodt H & Lorenzen I (2000a) Magnetic resonance imaging, radiography, and scintigraphy of the finger joints: one year follow up of patients with early arthritis. The TIRA Group. Ann Rheum Dis 59: 521–528.

Klarlund M, Ostergaard M, Rostrup E, Skjodt H & Lorenzen I (2000b) Dynamic magnetic resonance imaging of the metacarpophalangeal joints in rheumatoid arthritis, early unclassified polyarthritis, and healthy controls. Scand J Rheumatol 29: 108–115.

Klett R, Grau K, Puille M, Matter HP, Lange U, Steiner D & Bauer R (2000) Comparison of HIG scintigraphy and bloodpool scintigraphy using HDP in arthritic joint disease. Nuklearmedizin 39: 33–37.

König H, Sieper J & Wolf KJ (1990) Rheumatoid arthritis: evaluation of hypervascular and fibrous pannus with dynamic MR imaging enhanced with Gd-DTPA. Radiology 176: 473–477.

König H, Sieper J & Wolf KJ (1990) Rheumatoid arthritis: evaluation of hypervascular and fibrous pannus with dynamic MR imaging enhanced with Gd-DTPA. Radiology 176: 473–477.

Korpela M, Laasonen L, Hannonen P, Kautiainen H, Leirisalo-Repo M, Hakala M, Paimela L, Blafield H, Puolakka K & Möttönen T (2004) Retardation of joint damage in patients with early rheumatoid arthritis by initial aggressive treatment with disease-modifying antirheumatic drugs: five-year experience from the FIN-RACo study. Arthritis Rheum 50: 2072–2081.

Koski JM, Saarakkala S, Helle M, Hakulinen U, Heikkinen JO, Hermunen H, Balint P, Bruyn GA, Filippucci E, Grassi W, Iagnocco A, Luosujarvi R, Manger B, De ME, Naredo E, Scheel AK, Schmidt WA, Soini I, Szkudlarek M, Terslev L, Uson J, Vuoristo S & Ziswiler HR (2006) Assessing the intra- and inter-reader reliability of dynamic ultrasound images in power Doppler ultrasonography. Ann Rheum Dis.

Krinsky G, Rofsky NM & Weinreb JC (1996) Nonspecificity of short inversion time inversion recovery (STIR) as a technique of fat suppression: pitfalls in image interpretation. AJR Am J Roentgenol 166: 523–526.

Kroot EJ, de Jong BA, Van Leeuwen MA, Swinkels H, van den Hoogen FH, van't HM, van de Putte LB, van Rijswijk MH, van Venrooij WJ & van Riel PL (2000) The prognostic value of anti-cyclic citrullinated peptide antibody in patients with recent-onset rheumatoid arthritis. Arthritis Rheum 43: 1831–1835.

Landewe R (2007) Predictive markers in rapidly progressing rheumatoid arthritis. J Rheumatol Suppl 80: 8–15.

Landewe RB, Boers M, Verhoeven AC, Westhovens R, van de Laar MA, Markusse HM, van Denderen JC, Westedt ML, Peeters AJ, Dijkmans BA, Jacobs P, Boonen A, van der Heijde DM & van der LS (2002) COBRA combination therapy in patients with early rheumatoid arthritis: long-term structural benefits of a brief intervention. Arthritis Rheum 46: 347–356.

Lange JM, Boucher CA, Hollak CE, Wiltink EH, Reiss P, van Royen EA, Roos M, Danner SA & Goudsmit J (1990) Failure of zidovudine prophylaxis after accidental exposure to HIV-1. N Engl J Med 322: 1375–1377.

Lard LR, Visser H, Speyer I, vander Horst-Bruinsma IE, Zwinderman AH, Breedveld FC & Hazes JM (2001) Early versus delayed treatment in patients with recent-onset rheumatoid arthritis: comparison of two cohorts who received different treatment strategies. Am J Med 111: 446–451.

Larikka MJ, Ahonen AK, Junila JA, Niemelä O, Hämäläinen MM & Syrjalä HP (2001) Extended combined 99mTc-white blood cell and bone imaging improves the diagnostic accuracy in the detection of hip replacement infections. Eur J Nucl Med 28: 288–293.

Larsen A, Dale K & Eek M (1977) Radiographic evaluation of rheumatoid arthritis and related conditions by standard reference films. Acta Radiol Diagn (Stockh) 18: 481–491.

Lassere M, McQueen F, Ostergaard M, Conaghan P, Shnier R, Peterfy C, Klarlund M, Bird P, O'Connor P, Stewart N, Emery P, Genant H & Edmonds J (2003) OMERACT Rheumatoid Arthritis Magnetic Resonance Imaging Studies. Exercise 3: an international multicenter reliability study using the RA-MRI Score. J Rheumatol 30: 1366–1375.

Lassere MN & Bird P (2001) Measurements of rheumatoid arthritis disease activity and damage using magnetic resonance imaging. Truth and discrimination: does MRI make the grade? J Rheumatol 28: 1151–1157.

Lee DM & Weinblatt ME (2001) Rheumatoid arthritis. Lancet 358: 903–911.

Liberatore M, Clemente M, Iurilli AP, Zorzin L, Marini M, Di RE & Colella AC (1992) Scintigraphic evaluation of disease activity in rheumatoid arthritis: a comparison of technetium-99m human non-specific immunoglobulins, leucocytes and albumin nanocolloids. Eur J Nucl Med 19: 853–857.

Liberatore M, Iurilli AP, Ponzo F, Prosperi D, Santini C, Baiocchi P, Rizzo L, Speziale F, Fiorani P & Colella AC (1998) Clinical usefulness of technetium-99m-HMPAO-labeled leukocyte scan in prosthetic vascular graft infection. J Nucl Med 39: 875–879.

Lindblad S & Hedfors E (1985) Intraarticular variation in synovitis. Local macroscopic and microscopic signs of inflammatory activity are significantly correlated. Arthritis Rheum 28: 977–986.

Lindegaard H, Vallo J, Horslev-Petersen K, Junker P & Ostergaard M (2001) Low field dedicated magnetic resonance imaging in untreated rheumatoid arthritis of recent onset. Ann Rheum Dis 60: 770–776.

Love C, Din AS, Tomas MB, Kalapparambath TP & Palestro CJ (2003) Radionuclide bone imaging: an illustrative review. Radiographics 23: 341–358.

Machold KP, Stamm TA, Eberl GJ, Nell VK, Dunky A, Uffmann M & Smolen JS (2002) Very recent onset arthritis--clinical, laboratory, and radiological findings during the first year of disease. J Rheumatol 29: 2278–2287.

Marcus C, Thakur ML, Huynh TV, Louie JS, Leibling M, Minami C & Diggles L (1994) Imaging rheumatic joint diseases with anti-T lymphocyte antibody OKT-3. Nucl Med Commun 15: 824–830.

Martins FP, Gutfilen B, de Souza SA, de Azevedo MN, Cardoso LR, Fraga R & da Fonseca LM (2008) Monitoring rheumatoid arthritis synovitis with 99mTc-anti-CD3. Br J Radiol 81: 25–29.

McGonagle D, Conaghan PG, O'Connor P, Gibbon W, Green M, Wakefield R, Ridgway J & Emery P (1999a) The relationship between synovitis and bone changes in early untreated rheumatoid arthritis: a controlled magnetic resonance imaging study. Arthritis Rheum 42: 1706–1711.

McGonagle D, Gibbon W, O'Connor P, Green M, Pease C, Ridgway J & Emery P (1999b) An anatomical explanation for good-prognosis rheumatoid arthritis. Lancet 353: 123–124.

McQueen F, Ostergaard M, Peterfy C, Lassere M, Ejbjerg B, Bird P, O'Connor P, Genant H, Shnier R, Emery P, Edmonds J & Conaghan P (2005) Pitfalls in scoring MR images of rheumatoid arthritis wrist and metacarpophalangeal joints. Ann Rheum Dis 64 Suppl 1: i48–i55.

McQueen FM, Benton N, Crabbe J, Robinson E, Yeoman S, McLean L & Stewart N (2001) What is the fate of erosions in early rheumatoid arthritis? Tracking individual lesions using x rays and magnetic resonance imaging over the first two years of disease. Ann Rheum Dis 60: 859–868.

McQueen FM, Benton N, Perry D, Crabbe J, Robinson E, Yeoman S, McLean L & Stewart N (2003) Bone edema scored on magnetic resonance imaging scans of the dominant carpus at presentation predicts radiographic joint damage of the hands and feet six years later in patients with rheumatoid arthritis. Arthritis Rheum 48: 1814–1827.

McQueen FM, Gao A, Ostergaard M, King A, Shalley G, Robinson E, Doyle A, Clark B & Dalbeth N (2007) High grade MRI bone oedema is common within the surgical field in rheumatoid arthritis patients undergoing joint replacement and is associated with osteitis in subchondral bone. Ann Rheum Dis.

McQueen FM & Ostergaard M (2007) Established rheumatoid arthritis - new imaging modalities. Best Pract Res Clin Rheumatol 21: 841–856.

McQueen FM, Stewart N, Crabbe J, Robinson E, Yeoman S, Tan PL & McLean L (1998) Magnetic resonance imaging of the wrist in early rheumatoid arthritis reveals a high prevalence of erosions at four months after symptom onset. Ann Rheum Dis 57: 350–356.

McQueen FM, Stewart N, Crabbe J, Robinson E, Yeoman S, Tan PL & McLean L (1999) Magnetic resonance imaging of the wrist in early rheumatoid arthritis reveals progression of erosions despite clinical improvement. Ann Rheum Dis 58: 156–163.

Molenaar ET, Voskuyl AE, Dinant HJ, Bezemer PD, Boers M & Dijkmans BA (2004) Progression of radiologic damage in patients with rheumatoid arthritis in clinical remission. Arthritis Rheum 50: 36–42.

Möttönen T, Hannonen P, Leirisalo-Repo M, Nissilä M, Kautiainen H, Korpela M, Laasonen L, Julkunen H, Luukkainen R, Vuori K, Paimela L, Blafield H, Hakala M, Ilva K, Yli-Kerttula U, Puolakka K, Järvinen P, Hakola M, Piirainen H, Ahonen J, Palvimäki I, Forsberg S, Koota K & Friman C (1999) Comparison of combination therapy with single-drug therapy in early rheumatoid arthritis: a randomised trial. FIN-RACo trial group. Lancet 353: 1568–1573.

Möttönen T, Paimela L, Leirisalo-Repo M, Kautiainen H, Ilonen J & Hannonen P (1998) Only high disease activity and positive rheumatoid factor indicate poor prognosis in patients with early rheumatoid arthritis treated with "sawtooth" strategy. Ann Rheum Dis 57: 533–539.

Möttönen TT (1988) Prediction of erosiveness and rate of development of new erosions in early rheumatoid arthritis. Ann Rheum Dis 47: 648–653.

Möttönen TT, Hannonen P, Toivanen J, Rekonen A & Oka M (1988) Value of joint scintigraphy in the prediction of erosiveness in early rheumatoid arthritis. Ann Rheum Dis 47: 183–189.

Mulherin D, Fitzgerald O & Bresnihan B (1996) Clinical improvement and radiological deterioration in rheumatoid arthritis: evidence that the pathogenesis of synovial inflammation and articular erosion may differ. Br J Rheumatol 35: 1263–1268.

Myllykangas-Luosujarvi R, Aho K, Kautiainen H & Isomäki H (1995) Shortening of life span and causes of excess mortality in a population-based series of subjects with rheumatoid arthritis. Clin Exp Rheumatol 13: 149–153.

Nakahara N, Uetani M, Hayashi K, Kawahara Y, Matsumoto T & Oda J (1996) Gadolinium-enhanced MR imaging of the wrist in rheumatoid arthritis: value of fat suppression pulse sequences. Skeletal Radiol 25: 639–647.

Newman JS, Laing TJ, McCarthy CJ & Adler RS (1996) Power Doppler sonography of synovitis: assessment of therapeutic response--preliminary observations. Radiology 198: 582–584.

Nitz W (2003). Artifacts in magnetic resonance imaging. In: Reimer P, Parizel PM & Stichnoth F-A (eds) Clinical MR Imaging. Berlin, Germany, Springer: 45–52.

Ojala R (2002). MR-guided interventions at 0.23T. PhD. thesis. Acta Univ. Oul. D 62. Oulu University Press. Oulu.

Ostendorf B, Peters R, Dann P, Becker A, Scherer A, Wedekind F, Friemann J, Schulitz KP, Modder U & Schneider M (2001) Magnetic resonance imaging and miniarthroscopy of metacarpophalangeal joints: sensitive detection of morphologic changes in rheumatoid arthritis. Arthritis Rheum 44: 2492–2502.

Ostergaard M, Duer A, Moller U & Ejbjerg B (2004) Magnetic resonance imaging of peripheral joints in rheumatic diseases. Best Pract Res Clin Rheumatol 18: 861–879.

Ostergaard M, Duer A, Nielsen H, Johansen JS, Narvestad E, Ejbjerg BJ, Baslund B, Moller JM, Thomsen HS & Petersen J (2005a) Magnetic resonance imaging for accelerated assessment of drug effect and prediction of subsequent radiographic progression in rheumatoid arthritis: a study of patients receiving combined anakinra and methotrexate treatment. Ann Rheum Dis 64: 1503–1506.

Ostergaard M, Edmonds J, McQueen F, Peterfy C, Lassere M, Ejbjerg B, Bird P, Emery P, Genant H & Conaghan P (2005b) An introduction to the EULAR-OMERACT rheumatoid arthritis MRI reference image atlas. Ann Rheum Dis 64 Suppl 1: i3–i7.

Ostergaard M, Ejbjerg B & Szkudlarek M (2005c) Imaging in early rheumatoid arthritis: roles of magnetic resonance imaging, ultrasonography, conventional radiography and computed tomography. Best Pract Res Clin Rheumatol 19: 91–116.

Ostergaard M, Gideon P, Sorensen K, Hansen M, Stoltenberg M, Henriksen O & Lorenzen I (1995) Scoring of synovial membrane hypertrophy and bone erosions by MR imaging in clinically active and inactive rheumatoid arthritis of the wrist. Scand J Rheumatol 24: 212–218.

Ostergaard M, Hansen M, Stoltenberg M, Gideon P, Klarlund M, Jensen KE & Lorenzen I (1999) Magnetic resonance imaging-determined synovial membrane volume as a marker of disease activity and a predictor of progressive joint destruction in the wrists of patients with rheumatoid arthritis. Arthritis Rheum 42: 918–929.

Ostergaard M, Hansen M, Stoltenberg M, Jensen KE, Szkudlarek M, Pedersen-Zbinden B & Lorenzen I (2003a) New radiographic bone erosions in the wrists of patients with rheumatoid arthritis are detectable with magnetic resonance imaging a median of two years earlier. Arthritis Rheum 48: 2128–2131.

Ostergaard M, Hansen M, Stoltenberg M & Lorenzen I (1996a) Quantitative assessment of the synovial membrane in the rheumatoid wrist: an easily obtained MRI score reflects the synovial volume. Br J Rheumatol 35: 965–971.

Ostergaard M & Klarlund M (2001) Importance of timing of post-contrast MRI in rheumatoid arthritis: what happens during the first 60 minutes after IV gadolinium-DTPA? Ann Rheum Dis 60: 1050–1054.

Ostergaard M, Klarlund M, Lassere M, Conaghan P, Peterfy C, McQueen F, O'Connor P, Shnier R, Stewart N, McGonagle D, Emery P, Genant H & Edmonds J (2001) Interreader agreement in the assessment of magnetic resonance images of rheumatoid arthritis wrist and finger joints--an international multicenter study. J Rheumatol 28: 1143–1150.

Ostergaard M, McQueen FM, Bird P, Ejbjerg B, Lassere MN, Peterfy CG, O'Connor PJ, Haavardsholm E, Shnier R, Genant HK, Emery P, Edmonds JP & Conaghan PG (2005d) Magnetic resonance imaging in rheumatoid arthritis advances and research priorities. J Rheumatol 32: 2462–2464.

Ostergaard M, Peterfy C, Conaghan P, McQueen F, Bird P, Ejbjerg B, Shnier R, O'Connor P, Klarlund M, Emery P, Genant H, Lassere M & Edmonds J (2003b) OMERACT Rheumatoid Arthritis Magnetic Resonance Imaging Studies. Core set of MRI acquisitions, joint pathology definitions, and the OMERACT RA-MRI scoring system. J Rheumatol 30: 1385–1386.

Ostergaard M, Stoltenberg M, Henriksen O & Lorenzen I (1996b) Quantitative assessment of synovial inflammation by dynamic gadolinium-enhanced magnetic resonance imaging. A study of the effect of intra-articular methylprednisolone on the rate of early synovial enhancement. Br J Rheumatol 35: 50–59.

Ostergaard M, Stoltenberg M, Lovgreen-Nielsen P, Volck B, Jensen CH & Lorenzen I (1997) Magnetic resonance imaging-determined synovial membrane and joint effusion volumes in rheumatoid arthritis and osteoarthritis: comparison with the macroscopic and microscopic appearance of the synovium. Arthritis Rheum 40: 1856–1867.

Ostergaard M, Stoltenberg M, Lovgreen-Nielsen P, Volck B, Sonne-Holm S & Lorenzen I (1998) Quantification of synovistis by MRI: correlation between dynamic and static gadolinium-enhanced magnetic resonance imaging and microscopic and macroscopic signs of synovial inflammation. Magn Reson Imaging 16: 743–754.

Ostergaard M & Szkudlarek M (2001) Magnetic resonance imaging of soft tissue changes in rheumatoid arthritis wrist joints. Semin Musculoskelet Radiol 5: 257–274.

Ostergaard M & Szkudlarek M (2003) Imaging in rheumatoid arthritis--why MRI and ultrasonography can no longer be ignored. Scand J Rheumatol 32: 63–73.

Pääkkö E, Reinikainen H, Lindholm EL & Rissanen T (2005) Low-field versus high-field MRI in diagnosing breast disorders. Eur Radiol 15: 1361–1368.

Palmer WE, Rosenthal DI, Schoenberg OI, Fischman AJ, Simon LS, Rubin RH & Polisson RP (1995) Quantification of inflammation in the wrist with gadolinium-enhanced MR imaging and PET with 2-[F-18]-fluoro-2-deoxy-D-glucose. Radiology 196: 647–655.

Palosaari K, Ojala R, Blanco-Sequeiros R & Tervonen O (2003) Fat suppression gradient-echo magnetic resonance imaging of experimental articular cartilage lesions: comparison between phase-contrast method at 0.23T and chemical shift selective method at 1.5T. J Magn Reson Imaging 18: 225–231.

Paltiel Z (1985) Separate water and lipids images obtained by a single scan. In: Proceedings of the 4th annual scientific meeting of the Society of Magnetic Resonance of Medicine. Society of Magnetic Resonance in Medicine. New York: 172–173.

Partik B, Rand T, Pretterklieber ML, Voracek M, Hoermann M & Helbich TH (2002) Patterns of gadopentetate-enhanced MR imaging of radiocarpal joints of healthy subjects. AJR Am J Roentgenol 179: 193–197.

Patrick JL, Haacke EM & Hahn JE (1985). Water/fat separation and chemical shift articact correction using a single scan. In: Proceedings of the 4th annual scientific meeting of the Society of Magnetic Resonance of Medicine. New York, Society of Magnetic Resonance in Medicine: 174–175.

Perry D, Stewart N, Benton N, Robinson E, Yeoman S, Crabbe J & McQueen F (2005) Detection of erosions in the rheumatoid hand; a comparative study of multidetector computerized tomography versus magnetic resonance scanning. J Rheumatol 32: 256–267.

Peterfy CG (2001) Magnetic resonance imaging in rheumatoid arthritis: current status and future directions. J Rheumatol 28: 1134–1142.

Peterfy CG (2004) MRI of the wrist in early rheumatoid arthritis. Ann Rheum Dis 63: 473–477.

Peterfy CG, Roberts T & Genant HK (1998) Dedicated extremity MR imaging: An emerging technology. Magn Reson Imaging Clin N Am 6: 849–870.

Peters AM (1994) The utility of [99mTc]HMPAO-leukocytes for imaging infection. Semin Nucl Med 24: 110–127.

Pierre-Jerome C, Bekkelund SI, Husby G, Mellgren SI & Torbergsen T (1996) Bilateral fast MR imaging of the rheumatoid wrist. Clin Rheumatol 15: 42–46.

Pohjonen JA (1993). Methods for reduction of phase shift artifacts in gradient echo magnetic resonance imaging. Helsinki, Acta Polytechnica Scandinavica: 1–95.

Pons F, Sanmarti R, Herranz R, Collado A, Piera C, Vidal-Sicart S, Munoz-Gomez J & Setoain J (1996) Scintigraphic evaluation of the severity of inflammation of the joints with 99TCm-HIG in rheumatoid arthritis. Nucl Med Commun 17: 523–528.

Quinn MA, Conaghan PG, O'Connor PJ, Karim Z, Greenstein A, Brown A, Brown C, Fraser A, Jarret S & Emery P (2005) Very early treatment with infliximab in addition to methotrexate in early, poor-prognosis rheumatoid arthritis reduces magnetic resonance imaging evidence of synovitis and damage, with sustained benefit after infliximab withdrawal: results from a twelve-month randomized, double-blind, placebo-controlled trial. Arthritis Rheum 52: 27–35.

Quinn SF, Sheley RC, Demlow TA & Szumowski J (1995) Rotator cuff tendon tears: evaluation with fat-suppressed MR imaging with arthroscopic correlation in 100 patients. Radiology 195: 497–500.

Raza K, Buckley CE, Salmon M & Buckley CD (2006) Treating very early rheumatoid arthritis. Best Pract Res Clin Rheumatol 20: 849–863.

Reece RJ, Kraan MC, Radjenovic A, Veale DJ, O'Connor PJ, Ridgway JP, Gibbon WW, Breedveld FC, Tak PP & Emery P (2002) Comparative assessment of leflunomide and methotrexate for the treatment of rheumatoid arthritis, by dynamic enhanced magnetic resonance imaging. Arthritis Rheum 46: 366–372.

Reimer P, Parizel PM, Stichnoth F-A (Eds) (2003) Clinical MR Imaging. 2nd Edition. Spiringer-Verlag, Berlin Heidelberg New York.

Reiser MF, Bongartz GP, Erlemann R, Schneider M, Pauly T, Sittek H & Peters PE (1989) Gadolinium-DTPA in rheumatoid arthritis and related diseases: first results with dynamic magnetic resonance imaging. Skeletal Radiol 18: 591–597.

Reiser MF & Naegele M (1993) Inflammatory joint disease: static and dynamic gadolinium-enhanced MR imaging. J Magn Reson Imaging 3: 307–310.

Rennen HJ, Boerman OC, Oyen WJ & Corstens FH (2001) Imaging infection/inflammation in the new millennium. Eur J Nucl Med 28: 241–252.

Robertson PL, Page PJ & McColl GJ (2006) Inflammatory arthritis-like and other MR findings in wrists of asymptomatic subjects. Skeletal Radiol 35: 754–764.

Roivainen A, Parkkola R, Yli-Kerttula T, Lehikoinen P, Viljanen T, Mottonen T, Nuutila P & Minn H (2003) Use of positron emission tomography with methyl-11C-choline and 2-18F-fluoro-2-deoxy-D-glucose in comparison with magnetic resonance imaging for the assessment of inflammatory proliferation of synovium. Arthritis Rheum 48: 3077–3084.

Rominger MB, Bernreuter WK, Kenney PJ, Morgan SL, Blackburn WD & Alarcon GS (1993) MR imaging of the hands in early rheumatoid arthritis: preliminary results. Radiographics 13: 37–46.

Sahin M, Bernay I, Basoglu T & Canturk F (1999) Comparison of Tc-99m MDP, Tc-99m HSA and Tc-99m HIG uptake in rheumatoid arthritis and its variants. Ann Nucl Med 13: 389–395.

Saraux A, Berthelot JM, Chales G, Le HC, Thorel JB, Hoang S, Valls I, Devauchelle V, Martin A, Baron D, Pennec Y, Botton E, Mary JY, Le GP & Youinou P (2001) Ability of the American College of Rheumatology 1987 criteria to predict rheumatoid arthritis in patients with early arthritis and classification of these patients two years later. Arthritis Rheum 44: 2485–2491.

Savnik A, Malmskov H, Thomsen HS, Bretlau T, Graff LB, Nielsen H, nneskiold-Samsoe B, Boesen J & Bliddal H (2001) MRI of the arthritic small joints: comparison of extremity MRI (0.2 T) vs high-field MRI (1.5 T). Eur Radiol 11: 1030–1038.

Savnik A, Malmskov H, Thomsen HS, Graff LB, Nielsen H, nneskiold-Samsoe B, Boesen J & Bliddal H (2002) MRI of the wrist and finger joints in inflammatory joint diseases at 1-year interval: MRI features to predict bone erosions. Eur Radiol 12: 1203–1210.

Schrank C, Meirer R, Stabler A, Nerlich A, Reiser M & Putz R (2003) Morphology and topography of intraosseous ganglion cysts in the carpus: an anatomic, histopathologic, and magnetic resonance imaging correlation study. J Hand Surg [Am] 28: 52–61.

Scott DL (2002) The diagnosis and prognosis of early arthritis: rationale for new prognostic criteria. Arthritis Rheum 46: 286–290.

Scott DL, Pugner K, Kaarela K, Doyle DV, Woolf A, Holmes J & Hieke K (2000) The links between joint damage and disability in rheumatoid arthritis. Rheumatology (Oxford) 39: 122–132.

Senna ER, De Barros AL, Silva EO, Costa IF, Pereira LV, Ciconelli RM & Ferraz MB (2004) Prevalence of rheumatic diseases in Brazil: a study using the COPCORD approach. J Rheumatol 31: 594–597.

Sharp JT, Young DY, Bluhm GB, Brook A, Brower AC, Corbett M, Decker JL, Genant HK, Gofton JP, Goodman N & . (1985) How many joints in the hands and wrists should be included in a score of radiologic abnormalities used to assess rheumatoid arthritis? Arthritis Rheum 28: 1326–1335.

Smith RC, Lange RC & McCarthy SM (1991) Chemical shift artifact: dependence on shape and orientation of the lipid-water interface. Radiology 181: 225–229.

Sokka T, Kankainen A & Hannonen P (2000) Scores for functional disability in patients with rheumatoid arthritis are correlated at higher levels with pain scores than with radiographic scores. Arthritis Rheum 43: 386–389.

Starck SA & Carlsson S (1997) Digital filtering of bone scans: an ROC study. Nucl Med Commun 18: 98–104.

Stenger AA, Van Leeuwen MA, Houtman PM, Bruyn GA, Speerstra F, Barendsen BC, Velthuysen E & van Rijswijk MH (1998) Early effective suppression of inflammation in rheumatoid arthritis reduces radiographic progression. Br J Rheumatol 37: 1157–1163.

Strunk J, Klingenberger P, Strube K, Bachmann G, Muller-Ladner U & Kluge A (2006) Three-dimensional Doppler sonographic vascular imaging in regions with increased MR enhancement in inflamed wrists of patients with rheumatoid arthritis. Joint Bone Spine.

Swen WA, Jacobs JW, Hubach PC, Klasens JH, Algra PR & Bijlsma JW (2000) Comparison of sonography and magnetic resonance imaging for the diagnosis of partial tears of finger extensor tendons in rheumatoid arthritis. Rheumatology (Oxford) 39: 55–62.

Symmons DP, Hazes JM & Silman AJ (2003) Cases of early inflammatory polyarthritis should not be classified as having rheumatoid arthritis. J Rheumatol 30: 902–904.

Szkudlarek M, Klarlund M, Narvestad E, Court-Payen, Strandberg C, Jensen KE, Thomsen HS & Ostergaard M (2006) Ultrasonography of the metacarpophalangeal and proximal interphalangeal joints in rheumatoid arthritis: a comparison with magnetic resonance imaging, conventional radiography and clinical examination. Arthritis Res Ther 8: R52.

Szkudlarek M, Narvestad E, Klarlund M, Court-Payen, Thomsen HS & Ostergaard M (2004) Ultrasonography of the metatarsophalangeal joints in rheumatoid arthritis: comparison with magnetic resonance imaging, conventional radiography, and clinical examination. Arthritis Rheum 50: 2103–2112.

Szumowski J, Coshow WR, Li F & Quinn SF (1994) Phase unwrapping in the three-point Dixon method for fat suppression MR imaging. Radiology 192: 555–561.

Tamai K, Yamato M, Yamaguchi T & Ohno W (1994) Dynamic magnetic resonance imaging for the evaluation of synovitis in patients with rheumatoid arthritis. Arthritis Rheum 37: 1151–1157.

Tamai M, Kawakami A, Uetani M, Takao S, Tanaka F, Fujikawa K, Aramaki T, Nakamura H, Iwanaga N, Izumi Y, Arima K, Aratake K, Kamachi M, Huang M, Origuchi T, Ida H, Aoyagi K & Eguchi K (2007) Bone edema determined by magnetic resonance imaging reflects severe disease status in patients with early-stage rheumatoid arthritis. J Rheumatol 34: 2154–2157.

Tan AL, Tanner SF, Conaghan PG, Radjenovic A, O'Connor P, Brown AK, Emery P & McGonagle D (2003) Role of metacarpophalangeal joint anatomic factors in the distribution of synovitis and bone erosion in early rheumatoid arthritis. Arthritis Rheum 48: 1214–1222.

Tanaka N, Sakahashi H, Ishii S, Sato E, Hirose K & Ishima T (2005) Synovial membrane enhancement and bone erosion by magnetic resonance imaging for prediction of radiologic progression in patients with early rheumatoid arthritis. Rheumatol Int 25: 103–107.

Taouli B, Zaim S, Peterfy CG, Lynch JA, Stork A, Guermazi A, Fan B, Fye KH & Genant HK (2004) Rheumatoid arthritis of the hand and wrist: comparison of three imaging techniques. AJR Am J Roentgenol 182: 937–943.

Tonolli-Serabian I, Poet JL, Dufour M, Carasset S, Mattei JP & Roux H (1996) Magnetic resonance imaging of the wrist in rheumatoid arthritis: comparison with other inflammatory joint diseases and control subjects. Clin Rheumatol 15: 137–142.

Tsai JC & Zlatkin MB (1990) Magnetic resonance imaging of the shoulder. Radiol Clin North Am 28: 279–291.

van der Heijde DM (1995) Joint erosions and patients with early rheumatoid arthritis. Br J Rheumatol 34 Suppl 2: 74–78.

van der Heijde DM, Van Leeuwen MA, van Riel PL & van de Putte LB (1995) Radiographic progression on radiographs of hands and feet during the first 3 years of rheumatoid arthritis measured according to Sharp's method (van der Heijde modification). J Rheumatol 22: 1792–1796.

van der Horst-Bruinsma IE, Speyer I, Visser H, Breedveld FC & Hazes JM (1998) Diagnosis and course of early-onset arthritis: results of a special early arthritis clinic compared to routine patient care. Br J Rheumatol 37: 1084–1088.

van der Laken CJ, Voskuyl AE, Roos JC, Stigter van WM, de Groot ER, Wolbink G, Dijkmans BA & Aarden LA (2007) Imaging and serum analysis of immune complex formation of radiolabelled infliximab and anti-infliximab in responders and non-responders to therapy for rheumatoid arthritis. Ann Rheum Dis 66: 253–256.

Verstraete KL, Van der Woude HJ, Hogendoorn PC, De-Deene Y, Kunnen M & Bloem JL (1996) Dynamic contrast-enhanced MR imaging of musculoskeletal tumors: basic principles and clinical applications. J Magn Reson Imaging 6: 311–321.

Visser H, le CS, Vos K, Breedveld FC & Hazes JM (2002) How to diagnose rheumatoid arthritis early: a prediction model for persistent (erosive) arthritis. Arthritis Rheum 46: 357–365.

Vorne M, Lantto T, Paakkinen S, Salo S & Soini I (1989) Clinical comparison of 99Tcm-HMPAO labelled leucocytes and 99Tcm-nanocolloid in the detection of inflammation. Acta Radiol 30: 633–637.

Wakefield RJ, Gibbon WW, Conaghan PG, O'Connor P, McGonagle D, Pease C, Green MJ, Veale DJ, Isaacs JD & Emery P (2000) The value of sonography in the detection of bone erosions in patients with rheumatoid arthritis: a comparison with conventional radiography. Arthritis Rheum 43: 2762–2770.

Walther M, Harms H, Krenn V, Radke S, Faehndrich TP & Gohlke F (2001) Correlation of power Doppler sonography with vascularity of the synovial tissue of the knee joint in patients with osteoarthritis and rheumatoid arthritis. Arthritis Rheum 44: 331–338.

Wang Y, Li D, Haacke EM & Brown JJ (1998) A three-point Dixon method for water and fat separation using 2D and 3D gradient-echo techniques. J Magn Reson Imaging 8: 703–710.

Warchol O, Konig B, Dworak E, Kohn H, Dunky A & Mostbeck A (1998) [Value of inflammation and bone scintigraphy in differential diagnosis of painful affections of small joints]. Acta Med Austriaca 25: 7–12.

Watt I (1997) Basic differential diagnosis of arthritis. Eur Radiol 7: 344–351.

Wheeler JG, Slack NF, Duncan A, Palmer M & Harvey RF (1990) 99Tcm-nanocolloid imaging in inflammatory bowel disease. Nucl Med Commun 11: 127–133.

Wolfe F & Sharp JT (1998) Radiographic outcome of recent-onset rheumatoid arthritis: a 19-year study of radiographic progression. Arthritis Rheum 41: 1571–1582.

Yoshimitsu K, Varma DG & Jackson EF (1995) Unsuppressed fat in the right anterior diaphragmatic region on fat-suppressed T2-weighted fast spin-echo MR images. J Magn Reson Imaging 5: 145–149.

Zhang W, Goldhaber DM & Kramer DM (1996) Separation of water and fat MR images in a single scan at .35 T using "sandwich" echoes. J Magn Reson Imaging 6: 909–917.

Original publications

I Palosaari K & Tervonen O (2002) Post-processing water-fat imaging technique for fat suppression in a low-field MR imaging system, evaluation in patients with rheumatoid arthritis. MAGMA 15: 1–9.

II Palosaari K, Vuotila J, Takalo R, Jartti A, Niemelä R, Haapea M, Tervonen O & Hakala M (2004) Contrast-enhanced dynamic and static MRI correlates with quantitative 99Tcm-labelled nanocolloid scintigraphy. Study of early rheumatoid arthritis patients. Rheumatology 43: 1364–1373.

III Palosaari K, Vuotila J, Takalo R, Jartti A, Niemelä RK, Karjalainen A, Haapea M, Soini I, Tervonen O & Hakala M (2006) Bone edema predicts erosive progression on wrist MRI in early RA. A two-year observational MRI and NC scintigraphy study. Rheumatology 45: 1542–1548.

IV Palosaari K, Vuotila J, Soini I, Kaarela K, Kautiainen H & Hakala M (2008) Changes resembling erosions in bilateral wrist MRI of healthy subjects. Manuscript.

Original publications are not included in the electronic version of the dissertation.

964. Rysä, Jaana (2008) Gene expression profiling in experimental models of cardiac load

965. Ikäheimo, Pekka (2008) Suomalaisen aikuisen astma – kysely- ja rekisteritutkimus vuonna 2000

966. Junttila, Juhani (2008) Characteristics of subjects with Brugada syndrome type electrocardiogram

967. Huilaja, Laura (2008) Collagen XVII and pathomechanisms of junctional epidermolysis bullosa and gestational pemphigoid

968. Heikka, Helena (2008) Sosiaali- ja terveysjohtajan työn sisältö ja kompetenssit

969. Juntti, Hanna (2008) Association of respiratory syncytial virus infection with asthma and atopic allergy

970. Winqvist, Satu (2008) Alcohol misuse in relation to traumatic brain injury. The Northern Finland 1966 birth cohort study

971. Makkonen, Saara (2008) Teknillisestä apulaisesta laboratoriohoitajaksi. Turun laboratoriohoitajakoulutuksen kehitys vuosina 1955–1990

972. Liljeroos, Mari (2008) Toll-like receptor 2 (TLR2) and TLR4 signaling in the innate response against bacterial components

973. Vierimaa, Outi (2008) Multiple Endocrine Neoplasia Type 1 (MEN1) and Pituitary Adenoma Predisposition (PAP) in Northern Finland

974. Muhonen, Virpi (2008) Bone–Biomaterial Interface. The effects of surface modified NiTi shape memory alloy on bone cells and tissue

975. Oikarinen, Arja (2008) Kainuulaisten miesten terveyskäyttäytyminen — kulttuurinen näkökulma

976. Kantojärvi, Liisa (2008) Personality disorders in the Northern Finland 1966 Birth Cohort Study

977. Valkealahti, Maarit (2008) The effects of bisphosphonates and COX-2 inhibitors on the bone remodelling unit

978. Hiiri, Anne (2008) Community-wide Oral Health Promotion in the Pitkäranta District of Russian Karelia – a case study

979. Koivunen, Kirsi (2008) Alaraajojen valtimonkovettumistautia sairastavien terveyteen liittyvä elämänlaatu sekä hoitomenetelmien kustannukset

Book orders:
OULU UNIVERSITY PRESS
P.O. Box 8200, FI-90014
University of Oulu, Finland

Distributed by
OULU UNIVERSITY LIBRARY
P.O. Box 7500, FI-90014
University of Oulu, Finland

UNIVERSITY OF OULU P.O. Box 7500 FI-90014 UNIVERSITY OF OULU FINLAND

ACTA UNIVERSITATIS OULUENSIS

ISBN 978-951-42-8861-6 (Paperback)
ISBN 978-951-42-8862-3 (PDF)
ISSN 0355-3221 (Print)
ISSN 1796-2234 (Online)